ENGINEERING SOLUTIONS TO THE CHARACTERISATION OF CLINICAL DISORDERS OF UPPER EYELID MOVEMENT

A thesis submitted in partial fulfilment for the degree of Doctor of Philosophy

Felix H.W. Mak

Department of Mechanical Engineering

University College London

Torrington Place, London WC1E 7JE

United Kingdom

May, 2017

ABSTRACT

This project is about improving functioning in patients with ptosis associated with poor levator palpebrae superioris (LPS) function. LPS is a highly specialised muscle responsible for raising the eyelid. Defective LPS may cause the eyelid to droop uncontrollably, thereby covering the visual axis and affecting vision. The current method of correction relies heavily on the experience of the surgeon. Rarely, the implanted materials are at risk of exposure, infection, rejection. More commonly, the ability to completely shut the eyelids is impaired, leading to the danger of corneal exposure that can lead to severe pain and sight-threatening complications. Many patients will require repeat surgeries for correction in the future. One reason for such mechanical failure includes the lack of understanding of the mechanical characteristics of the muscle involved in blinking, and the current surgical suspension material used in replacing it. This lack of a scientific basis means that ptosis is a major challenge in ophthalmic surgery. The aim of this work will include analysing and characterising LPS and blinking dynamics, in the hope of improving future clinical procedures and perhaps provide insights on surgical materials.

Two separate approaches are running in parallel to investigate blinking dynamics: to define the mechanical characteristics and properties of the muscles involved in blinking, a new apparatus was designed and constructed to measure the force in eyelid closure, particularly the maximum force of contraction and natural force of closure. On another aspect, a high-speed camera was used at Moorfields Eye Hospital to record and analyse blinking in 32 patients with ptosis, thyroid eye disease and Blepharospasm. The collected and analysed data are used to investigate how eye blinking dynamics in diseased patients are different from healthy individuals and to attempt to separate them from controls using a modelling system. In addition, the blinking dynamics of dermatochalasis patients before and after blepharoplasty surgery were also compared with healthy individuals using high-speed camera and later advanced statistical analysis.

IMPACT STATEMENT

Upper eyelid disorders such as blepharoptosis, thyroid eye disease, blepharospasm and dermatochalasis can lead to complex secondary clinical abnormalities and cause a major functional visual impact. It has tremendous impact on the person's social life leading to psychosocial distress. Furthermore, many human interactions are communicated through eye contacts, physical abnormalities of the upper eyelids can be, and were associated with increased level of social anxiety and avoidance compared to general population norms. In these conditions, fundamental blink dynamics such as force of eyelid closure/ opening, palpebral aperture, duration and the velocities were evidently altered, but to yet have been fully examined by researchers.

This study investigates the blinking kinematics of above mentioned conditions using minimally invasive techniques to offer insights on improving clinical diagnosis and perhaps future developments in surgical materials, methods or interventions. Not only can the data and the mathematical model generated in this study be used as a base line or reference in clinical settings, when compared to controls, it allow the clinicians to track and monitor the progress of the diseases, thus advise the best course of treatment to aid recovery, improving the quality of life of these patients. Furthermore, this study have developed an apparatus and method to measure eye blinking forces of various types of eyelid closure, including the weight of the upper eyelid, spontaneous and forced closure. Using the mathematical model generated in this study and the data collected from healthy and diseased individuals, subsequent analysis will enable investigation of force in blinking and its correlations to pathogenesis. This has resulted in a UK patent being filed.

ACKNOWLEDGEMENTS

I would like to take this opportunity to show my gratitude to those who have assisted me in a myriad of ways. This work is also supported by UCL IMPACT studentship and Moorfields Eye Hospital NHS Foundation trust.

I would first like to express my sincere thanks to my primary supervisor Professor Mohan Edirisinghe for his influence on way of life and scientific approach in my professional development. I was very fortunate to be entrusted and given the opportunities to carry out the research under his supervision.

Within the University, profound gratitude goes to Professor Anthony Harker, who has been a truly dedicated collaborator. I am particularly indebted to Anthony for his constant support and his input throughout the project. His insightful ideas and comments helped me drive this project forward and widened my research from various perspectives. I am deeply grateful for my mentor, Dr. Kyung-Ah J. Kwon for continue support and guidance during the first year of my PhD, to assist my scientific understanding and development. I would like to express my gratitude to UCL Mechanical engineering workshop staff, especially Mr Peter Kelly – chapter 8 would not be possible without their help in manufacturing my designs, providing advice and continued modifications.

I would also like to thank my secondary supervisor and consultant ophthalmologist Mr. Daniel Ezra of the Moorfields Eye Hospital (London, UK) also, consultant Mr. Geoff Rose and Dr. Fabiola Murta for their valuable time conducting meetings, providing samples, organising test days with patients, and their professional advices. I will not forget the help I received from the Moorfields Eye Hospital staff and patients who agreed to participate in this report; whose permissions have been obtained. I wish to thank the Engineering and Physical Sciences research Council (EPSRC) UK for providing the computing system and high-speed camera used in this work.

Finally, I would like to thank my family, albeit I understand any amount of gratitude shown to them is woefully inadequate. To my late father Frankie Kwai-To Mak, who has always encouraged me in my studies. To my brother Rick H.S. Mak, thank you for your support and guidance. And finally, my mother Allie C.C. Fung who provided a constant, unconditional love and support, and has made untold number of sacrifices for my entire education. Hence, great appreciation and enormous thanks are due to her. I am blessed to have them in my life.

PUBLICATIONS, PATENT AND CONFERENCE PRESENTATIONS

1. Mak F.H.W., Harker A., Edirisinghe M., Murta F., Ezra D., "Effects of Blepharoplasty Surgery on Dermatochalasis Patients: Blink Dynamic Comparisons Between Pre-operation, Post-operation and Age Matched Controls Using a High Speed Camera", ***in preparation***.

2. Mak F.H.W. "Utilizing High-Speed Camera in Blink Dynamic Analysis and Characterization of Various Ophthalmic Conditions", Oral presentation at the **Annual Conference on Engineering and Applied Science**, Kyoto, Japan. November 2016

3. Mak F.H.W., Harker A., Kwon K.A., Edirisinghe M., Rose G., Murta F., Ezra D., "Characterising Upper Eyelid Movement Disorders Using Blink Dynamic Analysis" 2016, ***in preparation***.

4. Mak F.H.W., Harker A., Kwon K.A., Edirisinghe M., Rose G., Murta F., Ezra D., "Analysis of Blink Dynamics in Patients with Blepharoptosis", ***Journal of the Royal Society Interface*** 2016, 13 (116).

5. Mak F.H.W., Harker A., Rose G., Murta F., Ezra D., Edirisinghe M., "Apparatus and Method for Measuring a Force Produced by an Eyelid", May 2017. **U.K. Patent Application No. 1707418.8**.

6. Mak F.H.W. "Investigation of Blinking Dynamics in Diseased Patients Using High Speed Camera Images", Oral presentation at the **University College London Annual Mechanical Engineering PhD Conference**, London, UK. June 2015.

7. Mak F.H.W. “Investigation of Blinking Dynamics in Diseased Patients Using High Speed Camera Images”, Poster presentation at the **University College London Annual Mechanical Engineering PhD Conference**, London, UK. June 2015.

8. Mak F.H.W. “A New Apparatus and Method to Measure Eye Blinking Force”, Oral presentation at the **University College London Annual Mechanical Engineering PhD Conference**, London, UK. July 2014.

9. Mak F.H.W. “A New Apparatus and Method to Measure Eye Blinking Force”, Poster presentation at the **University College London Annual Mechanical Engineering PhD Conference**, London, UK. July 2014.

TABLE OF CONTENT

LIST OF FIGURES

LIST OF TABLES

LIST OF APPENDICES

LIST OF EQUATIONS

ABBREVIATIONS

ACh – Acetylcholine

AL – Anterior layer(s)

ALO – Apraxia of lid opening

BEB – Benign essential blepharospasm

BOTOX – Botulinum A toxin

CAD – Computer-Aided-Design

DFG – Digital force gauge

EMG – Electromyograph(y)

EOG – Electrooculuograph(y)

FPS – Frames per second

GUER – Graves' upper eyelid retraction

IR-OG – Infrared-oculuography

LA – Levator aponeurosis

LDA – Linear discriminant analysis

LF – Levator function

LPS – Levator palpebrae superioris

MM – Muller's muscle

MEH – Moorfields Eye Hospital

MRD – Marginal reflex distance

MSA – Multiple system atrophy

NHS – National Health Service

OOM - orbicularis oculi muscle

PA – Palpebral aperture

PET – Positron emission tomography

PF – Palpebral fissure

PL – Posterior layer(s)

PSP - Progressive supranuclear palsy

PTFE – Polytetrafluoroethylene

Ptosis - Blepharoptosis

RMSD – Root mean square deviation

SEM – Standard error of the mean

SMFAT – Submuscular fibroadipose tissue

TED - Thyroid eye disease

WL - Whitnall's ligament

CHAPTER 1: INTRODUCTION

1.1 Background

The word blepharoptosis is directly translated to: eyelid (bleph), and falling (ptosis). Ptosis is commonly understood as the droopy eyelid syndrome. It can be congenital or acquired, and it is characterised by abnormal lowering of the upper eyelid. Affected individuals find it difficult to impossible to raise their eyelid without exercising their accessory muscles on the forehead, or even with maximum effort (without the help of hands), they fail to maintain open eyes. Some patients may have moderate drooping of the upper lid and manage to see with their heads tilted backwards. However, in severe ptosis the visual axis may be obscured by the eyelid, causing functional blindness.

This disease could cause by a variety of underlying conditions, such as defects in the aponeurosis, Muller's muscle (MM) or could due to neuromuscular problems. Levator palpebrae superioris (LPS) is a highly specialised muscle responsible for raising the upper eyelid. In many cases, defective or weakened LPS will induce ptosis, causing life-altering deficits in both function and appearance. There is currently no pharmacological cure for ptosis and very few studies on the blinking dynamics, therefore the lack of understanding of the mechanical characteristics of the defect muscles involved in blinking leaves ptosis a challenging disease to cure and remedies are restricted to surgical intervention.

Amongst various ptosis treatments, internal brow suspension surgery is most common to treat patients with poor or absent LPS muscle function. Such treatment involves an exogenous

material surgically inserted under the brow. Various synthetic materials have been used such as silicone rod (Carter, et al., 1996; Lee, et al., 2009; Leone Jr, et al., 1981; Rowan, et al., 1977), monofilament polypropylene (Chow, et al., 2011; Manners, et al., 1994), braided polyamide (Saunders, et al., 1991; Kook, et al., 2004; Katowitz, 1979), polyester mesh (Sharma, et al., 2003; Mehta, et al., 2004; Hintschich, et al., 1995; Downes, et al., 1989) and expanded polytetrafluoroethylene (ePTFE) strips (Steinkogler, et al., 1993; Ruban, et al., 1996), as well as biological autogenous fascia lata (Takahashi, et al., 2010; Crawford, 1977; Flanagan, et al., 1981). The selection of materials is based on the individual's need of different mechanical properties they possess – for example, their shape (rod or band), elastic modulus, tensile strength or work of fracture.

Whichever the chosen material, it is attached to the frontalis muscle and the upper eyelid margin, tightened and then adjusted to the desirable height (Dutton, 1989; Fox, 1980; Edmonson, et al., 2005). Such surgeries can improve the quality and field of vision where part of the eye was previously obstructed by the drooping eyelid, it will also restore the normal appearance of the lid and improve symmetry. However, patients undergoing ptosis surgeries are at risk of bruising and swelling, sore eyelids, poor contour/ symmetry of the upper eyelid, over- or under-correction, and in worst cases wound infection and granuloma formation. The materials inserted for internal brow suspension are also at risk of exposure and rejection. These materials may cause the eyelids to be incompletely shut, causing the danger of corneal exposure that can lead to severe pain and sight-threatening complications. Some patients will require repeat surgeries for correction in the future, inducing further complications and leaving ptosis a difficult condition to be effectively managed.

Although ophthalmic plastic and reconstructive surgeries in the eyelid have been successfully performed for decades, there have been very few studies on the underlying problems such as the mechanics and the dynamics of an eye blink, especially as to how much force the eyelid can exert is poorly understood. One study (Frueh, et al., 1990) described how the force generated by LPS could play a role in the etiology of ptosis: they measured levator force generation, both by actively contracting and passively stretching the LPS by using a force transducer that attached to the upper eyelid lashes to measure the maximum lid excursion during up gaze and classified that as the levator force. They measured 187 patients diagnosed with different forms of ptosis and found that when combined with clinical evaluation (history, observation, palpebral aperture measurement, eyelid excursion test etc.), diagnosis was correct at 97.9%, compared with the traditional method of eyelid excursion (78.1% success rate). They concluded that the strength of the LPS influences the development of ptosis (Frueh, et al., 1996). However, the patient pool of this study was relatively small and the tools and devices used in this study were quite primitive, therefore the accuracy and validity could be questionable.

An even more primitive study of active levator force generation was carried out in 1980. A suture was placed through the upper eyelid of the subject and attached to a spring scale. The subject would then look up and the scale be read to determine the force generated (Madroszkiewicz, 1980). Although the subject had local anaesthetic injection prior the testing, this method was overly invasive leading to a lack of subject participation.

In the early 1950s, a device was introduced to measure the force of forced eye closure, using a hand-pumped cylinder connected to a pair of speculums (Jacobs, 1954). It was considered that the force of the orbicularis oculi muscle (OOM) contributed to the development of

various ophthalmic disorders. For a number of technical reasons, such as a defect in the instrument; the position and tilt of the instrument held relative to the volunteers; variable insertion of the instrument to the palpebral fissure; the shear in the piston's movements, the author found that the range was too wide to establish a norm. Despite the negative aspect of the findings, this study introduced a new idea to further develop such device to improve measurements of this kind. Even though there is much room for improvement, not much study has been undertaken to advance the technique in measuring forces acting on blinking in relation to ptosis and other clinical conditions.

The force of blinking could tell us whether the eyes are in a healthy state, and the dynamics of blinking such as the palpebral aperture (PA), the rate of the upper lid movements, blink duration and even frequency may also provide valuable information.

Clinical conditions like focal cranial dystonia form a group of neurological diseases characterised by painful and uncontrolled muscular spasms around head, neck and face. In particular, BEB is a type of focal cranial dystonia characterised by forcible closure of the eyelids, excessive irregular blinking and eyelid twitching. Much like ptosis, BEB patients usually have normal eyes. The visual disturbance is due solely to the forced closure of the eyelids. Although it is not life threatening, BEB has impact beyond the physical symptoms and pain/ discomfort. It also has significant impact on the person's social life due to how they move and their abnormal facial posture.

Studies have shown that blinking dynamics were changed in these BEB patients. A group (Bentivoglio *et al.,* 2006) in Italy has assessed the blink rate at rest, during conversation and reading in 50 patients with blepharospasm and compared it against 150 healthy subjects. It was found that the majority of patients with blepharospasm had higher blink rate at rest than

during conversation, whereas it is completely opposite for the controls. Moreover, when they combined the *resting blink rate greater than 27* and the *resting blink rate>conversation blink rate* pattern, they were able to accurately discriminate blepharospasm patients and the controls (Bentivoglio, et al., 2006). This suggests that specific features of blink rate can be associated with blepharospasm, and that the analysis of blink rate may be valuable for the diagnosis of blepharospasm in early stages.

There have been many different methods to measure blinking dynamics and eyelid movement. The magnetic search coil technique, which is based on magnetic induction, was described by Robinson (Robinson, 1963). This method was amongst the most popular eye saccades monitoring systems for humans and animals (Mcelligott, et al., 1979; Reulen, et al., 1982; Optican, et al., 1982; Remmel, 1984; Sprenger, et al., 2008). This system was also used to measure eyelid movement in spontaneous blinks (Abell, et al., 1998). In off-line analysis, covariation of amplitude, peak velocity and duration can be determined (Stava, et al., 1994).

This methodology of the magnetic search coil technique is based on Faraday's law of induction in electromagnetism. A search coil can be embedded into contact lenses which are fitted on the subject's eyes. By measuring the values of polarity and amplitude of the electric current generated during eye movements, the position of the eye can be calculated with direction and angular displacement. This electrical current is generated by alternating magnetic fields placed around the eyes. Electromagnetic search coil techniques have been extensively researched and improved tremendously through decades of modifications and modern digital advances. It is now possible to integrate stimuli such as air puff, flashes of light and tones within the device to evoke reflex blinks (Delgao-Garcia, et al., 2003). The eyelid responses can then be recorded quantitatively.

Other methods of detecting blinking dynamics will be discussed in later chapters (Chapter 2.4).

1.2 Aim and objectives

This project stemmed from a proposal to improve function in patients with ptosis associated with poor LPS function. The solution for ptosis had remained unchanged since the 1950s and is confined to internal suspension of the eyelid to the brow (brow suspension technique). There have been no studies that define the mechanical characteristics of the system nor the material used. This lack of scientific basis means that ptosis is a major challenge in ophthalmic surgery as the procedure carries inherent risks of material exposure, rejection of foreign material and granuloma formation. The eyelid is often left in an open position after surgery, resulting in corneal exposure that can lead to severe pain and even sight-threatening complications.

Although a vast amount of studies have been carried out on the topic of blinking (majority in the field of visual neuroscience and behavioural sciences), mechanical characterisation of blinking that connects the dynamics of an eye blink to clinical conditions have not been done before. This project aims to define these dynamics of blinking in relation to ptosis and similar conditions from an engineering perspective.

The objectives of the work include:

- Recruit ptosis patients and healthy volunteers to participate in this study
- Measure blink dynamics in patients with ptosis and healthy volunteers with minimum invasive techniques
- Analyse data and characterise ptosis

- Discriminate ptosis patients from healthy controls and generate a statistical model
- Characterise upper eyelid disorders by analysing blink dynamics
- Recruit patients of thyroid eye disease (TED), BEB and primary ptosis
- Generate a model to discriminate the different diseases and the group of healthy controls
- Explore aging related upper eyelid conditions
- Recruit dermatochalasis patients
- Characterise dermatochalasis and analyse data before and after corrective surgery
- Design and build an instrument prototype to measure blinking force
- Recruiting volunteers to carry out preliminary testing of the device
- Measure voluntary eye blinking forces at resting state

Outline of the thesis

The thesis consists of eight chapters covering the background of this research, addressing the methods and means to achieve the final aim. It concludes and provides the recommendations for future work. The contents of each chapter are described as follows.

Chapter 1 **Introduction** to this work with an emphasis to bring the reader up to date with the current research topic. This chapter also introduces the different research methods used by various groups; the aims and objectives of this project.

Chapter 2 **Literature review** of the human eyelid anatomy, ocular musculoskeletal system and mechanics of blinking, including the muscle structure, characteristics and neurological systems. Various ophthalmic conditions will be covered as well as current understanding of blinking dynamics with an extension to the method and various technologies used.

Chapter 3 **Experimental details** including how we have recruited/ selected our subjects, experimental set-up and methods chosen for capturing blinking and offline analysis of the blinking dynamics used in this project.

Chapter 4 **Characterising blinking dynamics in patients suffering from ptosis** and how they are different from healthy individuals. A model was generated to distinguish ptosis patients in the data.

Chapter 5 **Investigation of blinking kinematics in various upper eyelid disorders** and the application of statistical discrimination analysis to separate the disorders from each other and from healthy subjects.

Chapter 6 **Comparitive study of blinking dynamics between pre-operate and post-operate dermatochalasis patients** undergoing blepharoplasty surgery. The data were also compared to healthy individuals.

Chapter 7 **Investigating force** in blinking in blink dynamic analysis. Construction of the blink force measurement device and the development of the procedures and preliminary testing of the device.

Chapter 8 **Conclusions** of the research and the **recommendations** for further research.

CHAPTER 2: LITERATURE REVIEW

2.1 Human upper eyelid function and anatomy

Our upper eyelids serve important functions for the protection of our eyes including the prevention of excess light entry, harmful external contact and also maintaining a constant moisture level for the cornea and the conjunctiva by blinking.

The ocular anatomy is complex in which the muscles are arranged specifically for its purpose. There are 3 major muscles involved in blinking; the LPS, which is responsible for active lifting of the eyelid; the Muller's muscle (MM), which assists the LPS to a certain extent and contributes a few millimetres in upper eyelid elevation; and lastly the OOM, a striated muscle primarily accountable for active closing force. There are also passive lid closure forces produced by the stretching of ligaments and tendons of the eyelid (Skarf, 2005). The frontalis muscle on the forehead acts as an accessory muscle to help retract the lid and brow in extreme up gaze.

The LPS is an extraocular muscle that receives its innervation from the superior division of the oculomotor (third cranial) nerve fibres, suitable for fatigue-resistant tonic activity (Porter, et al., 1988). The LPS originates from the annulus of Zinn, a tendinous ring attaching the lesser wings of the sphenoid bone. The sphenoid bone is one of the seven bones that form the orbit. The LPS courses anteriorly along the superior aspect of the orbit and passes through a suspensory ligament called the Whitnall's ligament (WL). Posterior to the WL, the LPS gradually broadens and becomes the levator aponeurosis (LA), which then attaches anteriorly to the lower surface of the superior tarsal plate. Before the LA inserts into the superior tarsal

plate, is divided into anterior (AL) and posterior layers (PL). In fact, only the PL reaches the tarsus and subcutaneous tissues while the AL reflects superiorly above the tarsus to become contiguous with the orbital septum (figure 1). Such configuration contributes to the formation of the upper eyelid crease and represents the interface where the OOM attaches to the tarsus due to bunched fibres of PL penetrating through OOM to fuse with the subcutaneous tissues. Posterior to the PL lies the MM. This sympathetically innervated muscle supports LA during active eyelid opening and originates from the distal end of the LPS near Whitnall's ligament and inserts onto the upper margin of the tarsus (Kakizaki, et al., 2005). The MM also plays a role in adjusting the width of the palpebral fissure (PF). In Horner's syndrome, where the sympathetic nervous system is damaged may result in the inhibition this muscle, leading to partial ptosis.

OOM is the primary muscle responsible for closing the eyelid and much of the facial expressions. OOM is innervated unilaterally by the facial (seventh cranial) nerve. It is a concentric, striated muscle originating from the medial palpebral ligament and is divided into three parts covering the complete orbital opening. The innermost part is the pretarsal portion of the OOM which is situated anterior to the upper and lower tarsal plates. It inserts onto the medial and lateral canthal tendons. The outer part is the preseptal OOM. It is fused to the lateral palpebral raphe and the medial palpebral ligament. The preseptal and pretarsal portions of the muscle are primarily responsible for lowering the eyelids, such as in sleep or blinking, whereas the orbital portion is active in forced closure. The anatomical positioning and attachments of the preseptal muscles of the OOM pull and expand the lacrimal sac (Older, 2003), thereby filling the canaliculi and lacrimal sac with tears at the opening phase of a blink. Finally the outermost part, the orbital portion, forms a complete ellipse between the lateral

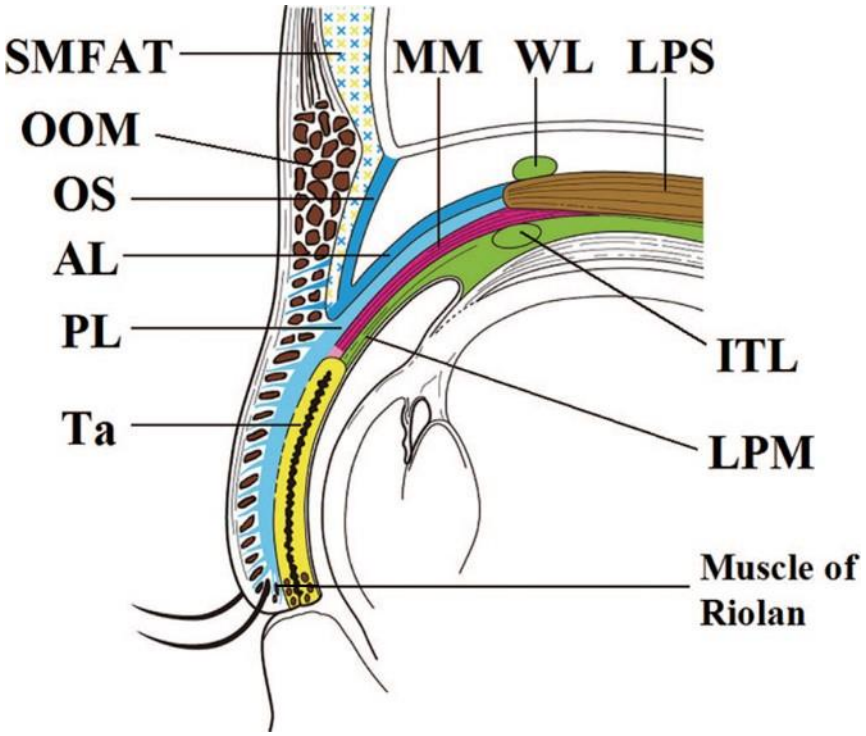

Figure 1.| Sagittal cross sectional view of the upper eyelid. Whitnall's ligament (WL) is located on the levator palpebrae superioris muscle, and at a slightly distal site, the LPS muscle attaches to the LA, under which is located the intermuscular transverse ligament (ITL). The LA is constituted by the anterior and posterior layers; the anterior layer (AL) continues to the orbital septum (OS) and the submuscular fibroadipose tissue (SMFAT), while the posterior layer (PL) extends more distally on the anterior aspect of the tarsus (Ta) and attaches to its inferior one-third. More distally, it distributes densely in the eyelid margin. The PL also pierces the opening of the orbicularis oculi muscle (OOM) and reaches to the subcutaneous tissue. Under the PL, locates the smooth muscle MM. This muscle is innervated by the sympathetic nervous system. Between the MM and the conjunctival epithelium, the lamina propria mucosae (LPM) of conjunctiva is located, which superiorly continues to the ITL *(Kakizaki, et al., 2009)*.

palpebral raphe and the medial palpebral ligament, overlying the orbital rim and the cheek and participates primarily in forceful eyelid closure.

During a blink, the OOM contacts, thereby lowering the eyelid. The LPS is synchronously inhibited to allow such eyelid movement. This pair of muscles works antagonistically and shows reciprocal innervation in healthy individuals. An EMG recording demonstrates this clearly (figure 2). However, disturbance of this close LPS-OOM relationship may result in eyelid movement disorders such as blepharospasm. Aramideh *et al.* have described clinical findings of a few patients with unusual LPS-OOM co-activation. The patients were unable to reopen the eyes after voluntary closure of the eyelids. In one case, the EMG findings revealed normal tonic activities of LPS muscles, and all three portions (pretarsal, preseptal and orbital) of the OOM remained quiescent while in the eyelid opening state. LPS-OOM reciprocal action appears to be normal during spontaneous blink. On command to close the eyes, LPS was inhibited and OOM contraction followed as expected. However, on the command to open the eyes, OOM activity persisted and could not be voluntarily inhibited even though LPS muscle showed periods of tonic activities. This LPS discharge did not overcome the persistent OOM activation and therefore the eyes could not be opened, despite maximum effort of the patient (marked frontalis muscle contraction and eyebrows raised above the orbital rim). Such motor persistences of OOM were found to be restricted to predominantly the pretarsal portion of the muscle; orbital portion to a lesser degree and preseptal portion was inhibited normally. Another case showed involuntary drooping of the eyelids leading to complete closure and over-inhibition of the LPS muscles with no evidence of OOM activity (Aramideh, et al., 1995). This also describes apraxia of eyelid opening. From these cases, it should be noted that the excessive OOM activation (like blepharospasm) does not generate the same result as the excessive LPS inhibition (apraxia of eyelid opening), but both may coincide in the same patient.

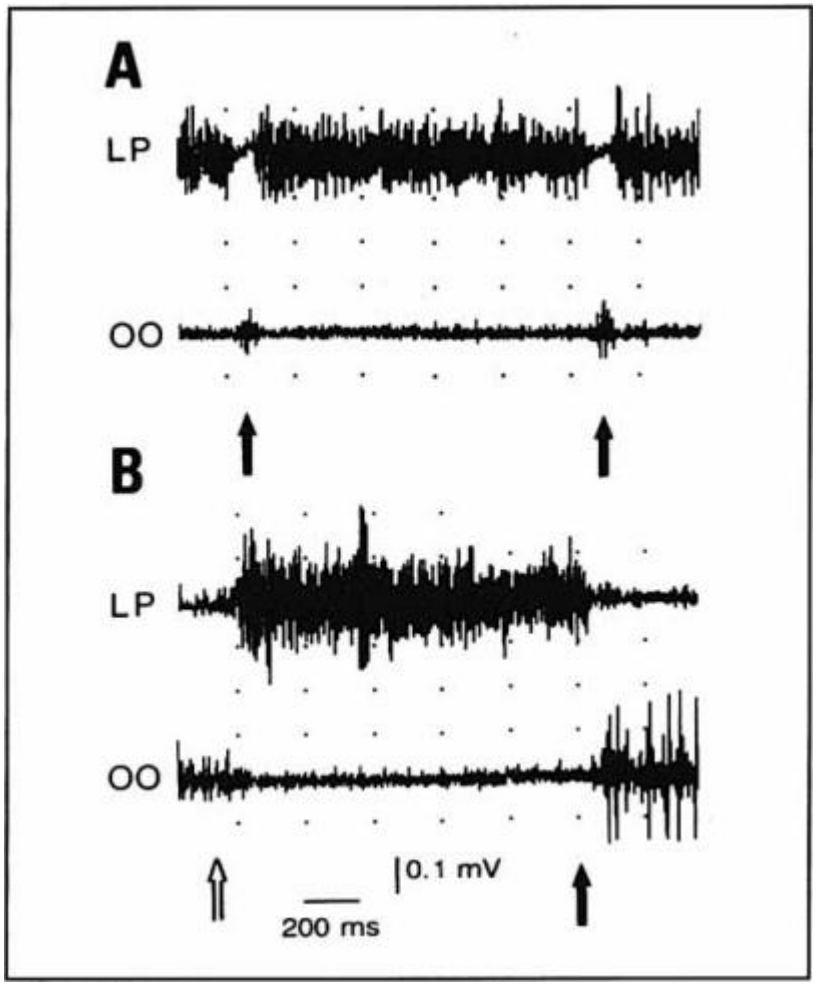

Figure 2.| EMG recordings of the reciprocal innervations of levator palpebrae (LP) superioris and orbicularis oculi (OO) muscles in control subjects *(Aramideh, et al., 1995)*. (A) The solid arrows indicate the onset of two spontaneous blinks. Suppression of LP can be seen clearly. Whereas (B) reveals the activities of those muscles upon closure on command. The open arrow represents the opening and the solid arrow represents the closure of the eyelid. This EMG demonstrates the reciprocal actions of the LP and OO muscles during a blink and how LP is inhibited when OO is active, *vice versa*.

2.1.1 Human blinks

Human blinks are tightly coordinated and controlled by the reciprocal activity of two highly specialised muscles: LPS and OOM. To initiate a blink, the LPS relaxes in order for the eyelid to drop due to gravity and the elasticity of the tendons and ligaments, the OOM then contracts to achieve a full closure. This combination of active transient burst of OOM and passive lid closing force rapidly lowers the upper eyelid. When the OOM signal terminates, the tonic LPS activity starts again, thereby lifting the eyelid (Kakizaki, et al., 2009). There are not many muscles responsible for the blinking action, therefore if some malfunction (myopathy), or their nervous system become damaged (neuropathy), or other problems such as neuromuscular and mechanical complications develop, various disorders might occur.

Smooth lid movement during blinking requires coordination of the LPS and the OOM motor neurons of the brainstem cranial motor nuclei. They are located in the caudal central sub-nucleus of the ocular motor nerve and the subdivision of the facial nucleus, respectively. To maintain the eyelids in the open state, LPS is tonically active and the OOM is silent (Evinger, et al., 1984; Evinger, et al., 1991; Fuchs, et al., 1992). However, magnetic search coil technique and EMG studies showed increased LPS activities during upward lid movements that accompany upward saccadic eye movements as well as the upward phase of a blink. In contrary, the downward lid movement produced by the downward saccadic eye movements is solely the result of the passive downward forces and relaxation of the LPS (Evinger, et al., 1991); different from the expected activation of OOM during closing phase of the blink.

The blinking action also serves to facilitate lubrication of the surface of the globe. The contraction of the OOM (including the preseptal muscles) compresses the canaliculi and

lacrimal sac thus driving the tears into the nose. Then the separation of the eyelids creates a vacuum effect, drawing the tears onto the ocular surface and at the same time pulling the next bolus of tears into the canalicular system. This lacrimal pump theory was discussed in detail in Jones's model of capillary action (Jones, 1961). In this case, if OOM malfunctions, it will affect the tear drainage system and may reduce the tear flow over the surface of the cornea and could lead to dry eye syndrome.

2.1.2 Blink types

There are different types of blinks and each has its own characteristics. Spontaneous blinks are brief bilateral repetitive eye closures that occur unconsciously and periodically without any obvious external stimuli (Karson, 1983); voluntary blinks are similar to spontaneous blinks but are triggered internally and intentionally; whereas reflexive blinks were defined as rapid eye closures that initiated via the reflex arc in the neural pathway so that the sensory neurons do not pass directly through the brain but synapse in the spinal cord. This type of blink acts to protect the eye from noxious situations that could be triggered by auditory (e.g. sudden loud noise), visual (e.g. strong light), trigeminal and external stimuli (Peshori, et al., 2001).

In this work, we focus on voluntary blinks as these can be controlled and are similar to spontaneous blinks. There are also no significant differences in maximum velocity between spontaneous, reflexive and voluntary blinks, (Guitton, et al., 1991) especially during the

closing phase where the acceleration and deceleration were approximately the same (figure 3).

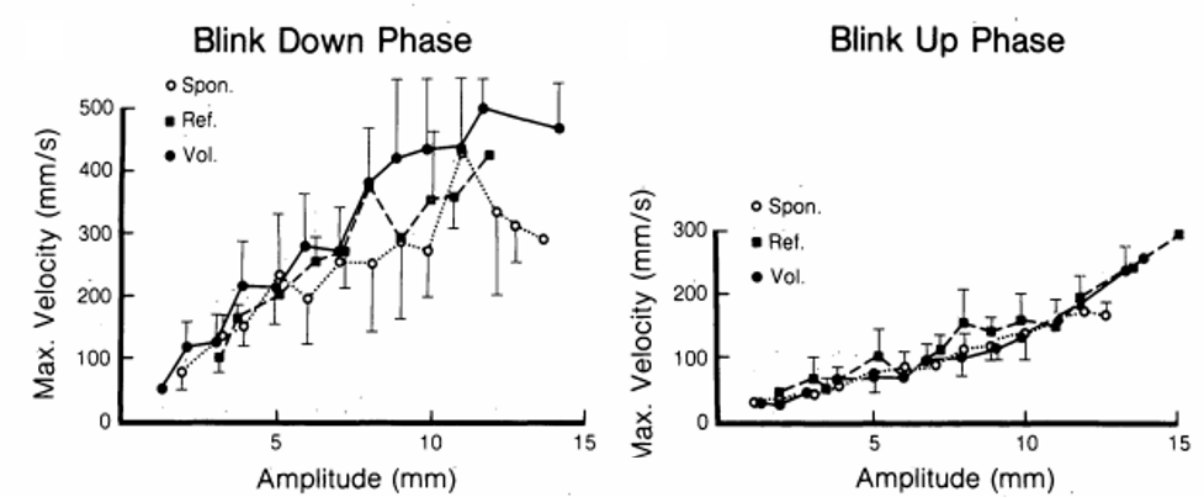

Figure 3.| Relationship between maximum velocity and amplitude in various types of human blinks. Spontaneous blinks (Spon.), reflexive blinks (Ref.) and voluntary blinks (Vol.) measured by mounting a miniature coil of wire directly on the eyelid and subjecting the search coil to a vertically directed alternating magnetic field. The results were found to be similar, with no significant differences when compared its maximum (Max.) velocity against the respective amplitude in the down phase (left panel), and up phase (right panel) of a blink. Vertical bars on each point show one standard deviation (Guitton, et al., 1991).

2. 2 Ethnic variation in ocular structure

There is ethnic variability in facial structure, especially between Western and Oriental Asian faces, the dominant features of the Asian face being a significantly wider intercanthal distance and a narrower vertical PA as well as a wider facial contour compared to Caucasian subjects (Le, et al., 2002). These differences in facial structures are reflected in varied muscle

attachments and, combined with a narrower PA, this might affect the blink mechanics and dynamics that were measured in these studies, especially in single eyelid Asians.

A study by Le *et al.* in 2002 took a number of direct linear projective measurements of the facial features of 180 oriental Asian adults including Singaporean, Thai and Vietnamese comparing to a larger control group of Caucasians. Horizontal measurements such as intercanthal width and PF length was measured but no significant differences were found between oriental Asians groups. However, PF length were greater in Caucasians in all cases and intercanthal width was significantly greater only in the Chinese and Vietnamese subgroups. It is smaller in Thai subjects compared to Caucasians (Le, et al., 2002).

When looking at the muscle attachments, histopathologic studies showed that the location of orbital septum fusion to the LA was essential in forming the upper eyelid crease and in Asians, this happens below the superior tarsal border, whereas in Caucasians it is above. Asians also appear to have a higher ratio of subcutaneous and suborbicularis fat compared to Caucasian eyelids. A pretarsal fat pad and a preaponeurotic fat pad that descends anteriorly to the tarsal plate are more prominent in Asians (Saonanin, 2014), and can cause a puffy appearance. This appears to be unique to the Asian single eyelid morphology. The combined effect of the above mentioned upper eyelid anatomy may cause the absent or lower crease in Asians (Jeong, et al., 1999). However, there are great variations of the configuration of the crease in the upper eyelids even amongst Asians, such as Chinese, Koreans, and Japanese (Han, et al., 1992; Liu, et al., 1986; Onizuka, et al., 1984). However, a direct comparison between these studies is difficult due to various methods that were employed.

2.3 Ophthalmic conditions involved in this project

Blink dynamics such as blink rate, amplitude, duration and peak speed varies significantly between healthy and unhealthy eyes (Bologna, et al., 2009; Choi, et al., 2003; Choi, et al., 2007; Korošec, et al., 2006). Involuntary blink rate was found to be higher at rest than in conversation in blepharospasm patients, whereas it's completely opposite for controls. The study suggested that analysis of specific features of the blink rate can be helpful in diagnosis of blepharospasm in early stages (Bentivoglio, et al., 2006). Similarly, voluntary blinking, as well as spontaneous and reflex blinking were studied in healthy individuals and compared to patients with progressive supranuclear palsy. Bologna et al. measured various blinking kinematics in patients and found that peak blink velocity have decreased across all three types of blinking. Not only that opening and closing phases were attenuated, the acceleration of the upper eyelid was also affected during the opening phase of the blink. In spontaneous and reflex blinking, patients with the condition also exhibit a prolonged pause between the closing and opening phases (Bologna, et al., 2009). These studies provided support for the use of blink dynamics in clinical diagnosis.

This section of the thesis will cover the various ophthalmic conditions that are involved in this work, which we have attempted to separate from controls using the differences in eyelid dynamics between each disorders.

2.3.1 Blepharoptosis

Ptosis is also known as blepharoptosis or the droopy eyelid syndrome. It translates as *the fallen eyelid* from Greek and this is an abnormal condition where the upper eyelid droops

down involuntarily (figure 4) and depending on its severity, may cover the visual axis and cause functional blindness.

PF is the distance between the margins of the top and the bottom eyelids. This usually varies between 9-12 mm (Sudhakar, 2009) and the average differs in different ethnicities, especially Asian oriental in origin are significantly less. For healthy adults, the upper eyelid margin is 0.5-2 mm below the superior corneal limbus. Ptosis can be categorised into different severities based on the amount of lowering of the upper eyelid. It may be minimal, moderate or severe (table 1), covering the pupil entirely, but it is better defined by the marginal reflex distance (MRD). This is the distance between the central corneal light reflex and upper eyelid margin at primary gaze. MRD is usually measured to 4-5 mm in healthy subjects or less than 2 mm or an asymmetry of more than 2 mm between eyes. With these parameters, a typical ptosis patient exhibits a contraction of the superior visual field to 30° or less. PF measurement often over- or under-estimates the severity due to the inclusion of lower lid margin. Patients often complaint of ocular discomfort, frontal tension headache due to increase effort to maintain upper lid open (due to attempt to elevate the eyelids by elevating the eyebrows), or the head might be tilted back to see under the lid. It also gives a sleepy or tired appearance and affects the patient's daily living. Children with untreated ptosis that obstruct the pupil may suffer interference with normal development of vision and develop amblyopia.

Figure 4.| Patient from Moorfields Eye Hospital displaying bilateral ptosis with a more severe right side, blocking the visual axis.

Ptosis can arise from a variety of underlying problems, such as i) myogenic, where there is a defect or fatigue in the retractor muscles (LPS and MM), or by the impairment of the neurotransmission at the neuromuscular junction (neuromyopathic) like myasthenia gravis; ii) aponeurotic – defect or detachment of the LA; iii) neurogenic – caused by innervational defects such as 3rd nerve and oculosympathetic palsy (Horner's syndrome); iv) mechanical – gravitational effect of a mass such as inflammation or scarring; v) traumatic – eyelid laceration with LPS transection or contusion injury to the LPS; vi) medication, such as the intramuscular injection of a neurotoxin, botulinum A toxin (botox) to induce local muscle paralysis in small doses. Ptosis can occur bilaterally or unilaterally (or cortical ptosis, a rare manifestation of hemisphere dysfunction), it can also be congenital or acquired and is categorised into isolated and non-isolated based on if it is presented with other conditions. For a detailed breakdown of non-isolated and isolated ptosis in congenital and acquired ptosis, please refer to the review published in the American Journal of Clinical Medicine (Sudhakar, 2009).

With such a large range of factors, treatments are based on causation and must rule out certain diseases during diagnosis. These include Horner's syndrome, 3rd cranial nerve palsy, myasthenia gravis and superior eyelid or orbital malignancy because they would require a different approach to the treatment and could respond differently to medications for example. Although a variety of causes, it generally surrounds the weakening of the LPS muscle, which is responsible for lifting the upper eyelid. LPS function, or levator excursion can be measured by the distance travelled by the upper lid margin from a down to up gaze position.

The amount of elevation can be used to classify the LPS function (table 1). Sudhakar suggested that LPS function should be measured in all cases, as low function may be an early presenting symptoms of a serious underlying disease, and in severe cases may develop amblyopia in pediatric patients without treatments (Sudhakar, 2009). Thus, early diagnosis and appropriate management of ptosis is essential and critical to avoid the consequences as discussed.

Palpebral fissure (mm)		LPS function – Levator elevation (mm)	
MINIMAL	1 – 2	POOR	0 – 5
MODERATE	3 – 4	FAIR	6 – 11
SEVERE	> 4	GOOD	>12

Table 1.|Classifications for droopy eyelid. Information gathered from *(Finsterer, 2003; Sudhakar, 2009)*.

The condition rarely improves over time without treatment, and therefore requires corrective surgery to improve upper part visual field, quality of vision and symmetry of open eyelids. However, transient, acute, unilateral ptosis has been reported previously, between age 7 to 75 years, both male and female. All patients had sudden onset of unilateral ptosis with MRD1 values between 1.5 mm to 3.5 mm with minimal decrease of LPS function but full eyelid motility. The ptosis was completely resolved spontaneously within 4 weeks in all cases without recurrence. Migraine, oculomotor nerve and partial or total palsy, Horner syndrome, orbital inflammatory disease and myasthenia gravis was ruled out in the diagnosis. Furthermore, a common finding amongst all patients is that they all had a presumed upper respiratory tract infection prior or during the transient acute onset of ptosis. Therefore it is speculated that viral infection causing focal inflammation that affects the superior branch of the oculomotor nerve was considered an etiological factor (Arat, et al., 2013). Previous

literature has reported oculomotor or isolated superior division oculomotor palsy secondary to viral infections including norovirus, influenza A, echovirus, varicella zoster and Epstein-Barr virus causing acute, unilateral transient ptosis (Kuki, et al., 2008; Yamashita, et al., 2008; Hertenstein, et al., 1976; Farooqui, et al., 2009; Ishibashi, et al., 1998; Saeki, et al., 2000). In such cases, the isolated ptosis condition resolved in a short period of time without intervention. However other more common types of ptosis will require surgical intervention.

Procedures such as blepharoplasty and frontalis suspension (briefly described in the management of blepharospasm section: 2.3.2b) are the most common treatment for true ptosis with poor levator function. There are numerous studies on the material selection for frontalis suspension and each have their advantages and disadvantages. Autogenous fascia lata harvested from the side of the thigh is sometimes used as the suspension sling material due to its biocompatibility and lasting results. It is predictable and can avoid granuloma formation compared to synthetic materials. However it could cause long and short term complications such as the cosmetic appearance of leg scar which caused minor concern in 38% of patients, early postoperative problems with pain on walking – 67%, limping – 38% and wound pain – 57% (Wheatcroft, et al., 1997). Synthetic materials considered include mersilene mesh (El-Toukhy, et al., 2001), polytetrafluoroethylene (PTFE) (Nakauchi, et al., 2013) and silicone rod (Tabatabaie, et al., 2012). Current solutions for ptosis correction remain unchanged since the 1950s and are confined to internal suspension of the eyelid to the brow. No studies have defined the mechanical characteristics of the system or suspension materials. This lack of a scientific basis means that ptosis is a major challenge in ophthalmic surgery as brow-suspension often leaves the eyelid in an open position, with resulting corneal exposure that can lead to severe pain and sight-threatening complications. Other post

operation side-effects include material exposures, infection or extrusions, lid lag and lagophthalmos have been reported in majorities of the studies.

2.3.2 Benign Essential Blepharospasm

Benign essential blepharospasm (BEB), meaning non-life threatening, uncontrolled muscle contractions of the eyelids of unknown etiology. It is a form of focal dystonia (Marsden, 1976), which is caused by involuntary over-activity of OOM with LPS co-contraction activity (Jinnah, et al., 2011) raising the blink rate considerably. This abnormal inhibitory reflex results in forceful, excessive and prolonged blinks, and frequently, episodes of sustained eyelid closure known as apraxia of lid opening (ALO) (Hallett, 2002). This is a rare condition that is often symmetrical and synchronous in both eyes and affects between 16-133 people per million. It also appears to be more prevalent in females (Defazio, et al., 2002; Defazio, 2007). A large epidemiologic study done in Italy has shed light on a probable cause of BEB. It was discovered that approximately 20% of affected individuals have a first degree related family member that suffers from some sort of dystonia. The study also compared various associated factors, sex and age of onset and suggested that BEB may result from a genetic predisposition combined with some environmental contingency. Coffee drinking also demonstrated a protective effect (Defazio, et al., 2011; Hallett, et al., 2008). However this study was restricted to Italy, it would be interesting to find out just how the rest of the world differ from their results.

The exact cause of BEB is still unclear, some studies found that the gray matter increases bilaterally in the putamen in BEB (Etgen, et al., 2006), but also another study found it to be decreased (Obermann, et al., 2007). With dramatic increased blink rates in BEB patients, it is only logical to relate other conditions that also brought increased blink rate. In conditions that affect the extrapyramidal systems such as dystonia, akathisia, Parkinsonism, Tourette syndrome and tardive dyskinesia, blink rate is altered (Jankovic, et al., 1982). These conditions all showed abnormalities in the neuro-network of the motor system in the brain that causes involuntary movements and reflexes, which is in turn modulated by the basal ganglia in the central nervous system. A report focused on Oppenheim dystonia showed pathology mainly localised in the brainstem (McNaught, et al., 2004). Many studies have investigated the effect of dopamine, a neurotransmitter in the brain, on BEB. Dopamine-blocking agent appears to induce acute dystonia (van Harten, et al., 1999) and a significantly reduced dopamine D_2 receptor binding is demonstrated in BEB patients (Horie, et al., 2009), as well as primary focal dystonia (Naumann, et al., 1998; Perlmutter, et al., 1997). These findings suggest that such decrease in the dopamine receptor may play an important role in the loss of control in the motor circuit in BEB patients. It is unlikely that a single defect in the neuro-network in the brain the primary cause of this disease.

Although normal blink rate is reported in some dystonic patients (Karson, et al., 1984; Deuschl, et al., 1998), a more recent study has found that specific features of blink rate can be associated with BEB (Bentivoglio, et al., 2006). This study analysed the blink rate of 50 patients displaying BEB symptoms and compared it against 150 healthy subjects under 3 conditions: rest, conversation and reading. It was noted that 76% of BEB patients have resting blink rate greater than conversation blink rate, whereas 74% of the control have greater blink rate in conversation than at rest (figure 5). According to their findings, the authors assumed blink

rate of over 27 per minute is associated to BEB and achieved 90% sensitivity with confidence interval of up to 95.7%. These results suggests that the analysis of blink rate can aid diagnosis of BEB in early stages when comparing the blinking rate in conversation and at rest.

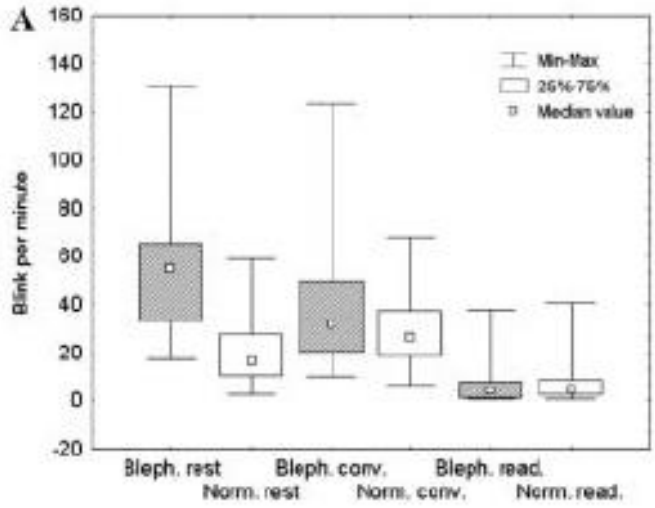

Figure 5.|Median values of blink rate at rest in patients of BEB and in controls in different behavioural settings: rest, conversation, reading *(Bentivoglio, et al., 2006)*.

2.3.2b Diagnosis and the management of blepharospasm

BEB normally occurs in patients from their 5th or 6th decade of life. In early stages of the disease, symptom of increased rate of blinking usually begins with increasing light intensity. Patients usually become more sensitive to air pollution, wind and noise. This progresses to involuntary spasms in both eyes even with movement of the head, mouth with stress. Patients also complain of ocular surface discomfort, facial and brow spasms, and eyelid tic. This condition is often occupationally and socially disabling, patients will find reading, watching TV and driving etc. increasingly difficult. In severe cases, the patient is rendered functionally blind. A grading system was developed (table 2) to help evaluate the condition by score. A family history of dystonia or BEB can also aid in early diagnosis.

The management of BEB can be divided into pharmacotherapy and surgical intervention. Although no pharmacological cure currently exists for BEB, patients presenting early signs of symptoms are usually treated symptomatically. Tinted lenses are advised to reduce amount of light entry for the light sensitive patients, and patients are urged to improve lid hygiene to avoid eye irritation and prescribed artificial tears to alleviate dry eyes. However, the condition frequently progresses despite treatments.

Score Description
Severity
0 None
1 Increased blinking caused only by external stimuli (eg, bright light, wind, movement, or glabellar tap)
2 Mild but spontaneous eyelid fluttering (without actual spasm), definitely noticeable, possibly embarassing, but not functionally incapacitating
3 Moderate, very noticeable spasm of eyelids, mildly incapacitating; slight contraction of other facial muscles
4 Severe incapacitation spasm of eyelids and possibly other facial muscles
Frequency
0 None
1 Slightly increased frequency of blinking (>20/min)
2 Increased blinking rate and eyelid fluttering of <1 s in duration
3 Eyelid spasms lasting >1 s, eyes open >50% of the waking time
4 Functionally "blind" due to persistent blepharospasm >50% of the waking time

Table 2.| Blepharospasm evaluation scale *(Jankovic, et al., 1982)*.

As mentioned above, it is uncertain what is causes BEB, so a definitive pharmacological cure remains a major challenge. In the past, BEB was considered to be a psychiatric rather than a neurologic illness and, therefore, antipsychotic and antidepressant drugs were used. Nowadays, these drugs are used to block dopamine receptors and inhibit catecholamine synthesis or to deplete monoamines that are hyperactive in the brain region; to suppress abnormal involuntary movements. Due to a diverse manifestation of BEB in various diseases, such as ALO associated BEB, BEB in Parkinsonism, BEB in myotonic dystrophy etc. not one drug is suitable or effective in treating BEB. For example, levodopa, a precursor of the neurotransmitter dopamine, is used to treat Parkinson's disease and certain type of dystonia. This drug is occasionally effective to suppress BEB in Parkinsonian patients (Klawans, et al.,

1969; Chakravorty, 1974) but not found to be beneficial to other forms of BEB (Jankovic, et al., 1982).

Currently subcutaneous and intramuscular botox injection to the OOM, corrugator and procerus muscles is the most preferred treatment as it rapidly reduces local spasm (Jost, et al., 2001). Botox is a protein that belongs to the class of neurotoxins. It was first extracted from the bacterium *Clostridium botulinum* and it is extremely potent. It is lethal to humans but can be beneficial cosmetically and medically when used in small quantities. The toxin inhibits neurotransmission at muscular junctions and causes muscle paralysis in two steps. When injected, the botox targets the motor nerve endings and binds with the cholinergic nerve terminal and enters the cell by the process of receptor-mediated endocytosis. Once inside the cell, a part of the toxin is released from the vesicle into the cytoplasm of the nerve terminal, where it begins to cleave the SNARE protein complex responsible for release of acetylcholine (ACh) into the synaptic cleft to relay the action potential that generates muscle contraction, thereby destroying the motor neuron end plate and causing paralysis. The neuro-receptors do regenerate and resume function but it takes several months, therefore BEB patient will require a repeat injection every few (1-5) months.

Various studies investigated the most effective site for injection. Previously pretarsal region of the OOM was the choice of many ophthalmologist (Kowal, 1997), but later it was suggested that injection to the MM is particularly effective (Mackie, 2000). Although it seems very promising, some people are non-responsive to botox and not all injections result in complete cure with no side effects. Botox injection for ALO associated BEB at the central upper eyelid frequently causes ptosis due to diffusion into the LPS (Pariseau, et al., 2013). To reduce the risks of sustaining ptosis, injections to the medial and lateral portion of the pretarsal part of

OOM is usually sufficient to stop spasms. Various forms of botox, incotulinum toxin A and onabotulinum toxin A have also been tested to be used to treat forms of blepharospasm (Chundury, et al., 2013; Saad, et al., 2014).

Surgical therapies can be considered when pharmacological intervention failed to achieve satisfactory results. Many patients that fail to respond to botox are found to have ALO associated with BEB. A clinical study showed 12 patients treated for pure ALO and ALO associated with BEB over the course of 3 years. All of them were treated with botox with very poor results and subsequently underwent surgical procedures like blepharoplasty, limited myectomy, aponeurosis repair and or frontalis suspension. Patients with post-operative botox injections were shown to be very effective (Kerty, et al., 2006). This study highlights the importance of making a correct diagnosis (BEB or ALO associated BEB) early and providing the correct treatment can speed up the surgical therapy. The authors also demonstrated that the surgical and botox combination treatment can be very effective.

Myectomy is a surgical procedure that involves removal of muscles. In the case of BEB, the protractor muscles are pretarsal, preseptal and orbital potion of OOM around the eyelids. Limited myectomy is a partial upper eyelid myectomy that removes less tissues and is generally performed in conjunction with post-operative botox injections. Extended myectomy will include accessory muscles procerus muscle and corrugator supercilii that are mainly responsible for producing facial expression by pulling the skin between eyebrows downward and towards the nose. This method prevents further unwanted eye blinking by removing the responsible muscles. The MM and a stripe of muscle along the margin of the upper eyelid remain untouched to maintain some voluntary blinking actions and protect the

eyelash roots. Myectomy often leaves the patient with dry eyes and lagophthalmos due to the removal of responsible muscles. Chronic lid swelling can also occur.

Blepharoplasty procedures are performed by oculoplastic surgeons or ophthalmologists where some amount of skin, muscle or fat are removed. Frontalis suspension creates a linkage between the frontalis muscle on the forehead and the tarsus of the upper eyelid. This physical linkage uses different sling materials that are biologically compatible. Thus, frontalis muscle can also aid in the eyelid elevation. However, frontalis suspension is not the best solution as lid closure difficulty often leaves the patient with lagophthalmos, corneal exposure, dry eyes and other complications.

2.3.3 Apraxia of lid opening

ALO is the inability to open the eyelids at will following either voluntary (mainly) or involuntary eye closure, however spontaneous blinking is not usually affected. Its exact mechanism is unknown but it is thought to be due to intermittent (Esteban, et al., 1988) or prolonged (Esteban, et al., 1973) inhibition of LPS activity (Aramideh, et al., 1994) and can occur even with the absence of OOM contraction, greatly increases the blink duration and therefore decreases blink rate. There have not been studies defining its blinking dynamics. This condition is not a type of paralysis because the patients can open their eyes following a reflex blink. Ugarte and Teimory described their patient with ALO resulting from involuntary LPS inhibition and persistent pretarsal OOM contraction (Ugarte, et al., 2007). Other uses of accessory muscles or movements such as forceful contraction of the frontalis muscle and backward thrusting of the head are ineffective in opening the eyelids. In that study, the

patient demonstrated normal reflex blinking but failed to open the lids after voluntary closure. Botox injection at pretarsal and preseptal OOM did not improve his condition, suggesting the OOM is not involved actively.

This syndrome is closely related to BEB and often co-exists. Similar to BEB, ALO was apparent in patients with extrapyramidal disorders affecting the basal ganglia (Goldstein, et al., 1965). ALO is also very common in Parkinson's disease but can also occur in isolation as pure ALO. Lesions in various parts of the brain have also implicated ALO development, including non-dominant hemisphere (De Renzi, et al., 1986) and rostral brainstem (Micheli, et al., 1999). Positron emission tomography (PET) was used to measure regional cerebral glucose metabolism in 11 ALO patients and compared against 11 healthy subjects and found significant decrease in bilateral anterior cingulate gyrus and the left supplementary motor area as well as the primary visual cortex (Suzuki, et al., 2003). These results support the idea of glucose hypometabolism in medial frontal cortex of patients with ALO (Smith, et al., 1995).

Treatment for this condition is similar to BEB patients, with botox injection into the pretarsal (because motor persistence of OOM was found to be restricted in this portion of the muscle; see section 2.1) and or the preseptal OOM associated with involuntary OOM contraction causing forceful lid closure. However this treatment is not effective in isolated ALO with involuntary LPS inhibition (Forget, et al., 2002; Jankovic, 2009) but these patients had a response to valproate (Chand, et al., 1994). Levodopa, as for BEB associated in Parkinson's disease, was reported to improve the symptoms of ALO in a patient with progressive ALO resulting from involuntary LPS inhibition (Dewey, et al., 1994) but could not be replicated in later studies (Boghen, 1997). Anticholinergic agent was also reported to improve ALO in isolated ALO patients (Klostermann, et al., 1997). Furthermore, medications such as Sulpiride

(Tsuji, et al., 2002) and Lithium intoxication (Micheli, et al., 1999) have been reported to induce ALO. Studying the pathway that these drugs work in relation to ALO may open more doors to establish what could have caused the condition. Surgical therapy is also similar to BEB patients with myectomy of OOM (Georgescu, et al., 2008) and LPS aponeurosis reinsertion and also frontalis suspension (Kerty, et al., 2006) are proven to be satisfactory.

2.3.3 Thyroid eye disease

Thyroid eye disease (TED) or Graves' Ophthalmopathy is an autoimmune disorder manifesting from Graves' disease. It is typically recognised by proptosis, forward displacement of the globe resulting from excessive ocular tissue remodelling and enlargement of the adipose tissues within the orbit. This can be seen in figure 6, where excessive orbital tissues were formed behind the globe, compressing the optic nerve (Figure 6c) and pushing the globe forward (figure 6a,b). This can be compared to the normal patient in figure 6d. Graves' disease affects approximately 0.5% of the population and affects more women than men (Cooper, 2003). It is usually characterised by hyper thyroid activity, due to an enlarged thyroid and an increased thyroid hormone production. Around 25-50% of patients with Graves' disease will develop TED, of whom only 3-5% will develop a more severe form of TED (Prabhakar, et al., 2003). Patients usually experience symptoms such as a dry and gritty irritation on the eyes, photophobia, excessive tearing, double vision and a pressure sensation behind the eyes. If left untreated, the disease could progress and develop permanent facial disfigurement and sight threatening complications such as exposure keratopathy, compressive optic neuropathy, inflammation, intense pain, diplopia and corneal

ulceration. A study have found that smoking greatly increases the risk of developing TED (odds ratio, 7.7; 95% confidence interval, 4.3 to 13.7). This study also showed that smokers have a higher chance of developing a more severe form of ophthalmopathy (Prummel, et al., 1993) and are less likely to respond well to immunosuppressive therapies (Bartalena, et al., 2000). There appear to be other factors, such as genetic predisposition, affecting the risk rate. For an in depth review on the development of TED, please refer to Bahn's review on Graves' Ophthalmopathy (Bahn, 2010). TED has been reported to develop in patients with normal and low level (5%) of thyroid hormone in their system (Eckstein, et al., 2009), these patients normally have low titres of anti-thyrotropin-receptor antibodies and make diagnosis more difficult. Otherwise, anti-thyrotropin-receptor antibodies are present in practically all TED patients with hyperthyroidism (Khoo, et al., 2000). Further, a study of 52 TED patients has revealed that a reduction in levator excursion was found to be associated with increasing levels of lagophthalmos and eyelid lag (both achieving $p<0.001$). The authors suggested the potential of levator excursion measurement replacing the conventional eyelid lag grading and lagophthalmos as a more accurate indicator to predict these conditions in TED (Lelli, et al., 2010).

Apart from the excessive remodelling and enlargement of the adipose tissues behind the eyeball that give rise to the signature eye protrusion, the upper and lower eyelids also play a significant role. The condition was first described by Robert J. Graves in 1835 in a patient (Graves, 1835), initially thought to be hysterical, whose eyes were apparently so enlarged that she could not shut her eyes completely and slept with wide opened eyes. However, he noted that the eyes assumed a singular appearance and that it may not be of mental issues alone. Later in 1849, Cooper mentioned John Dalrymple's explanation of the eye changes when discussing a patient with exophthalmos and goiter. The severe exophthalmos denuded the

protection of the upper eyelid by a constant and powerful spasm of the LPS, which drew the eyelids upward and backward that the sclera above the cornea was visible (Cooper, 1849).

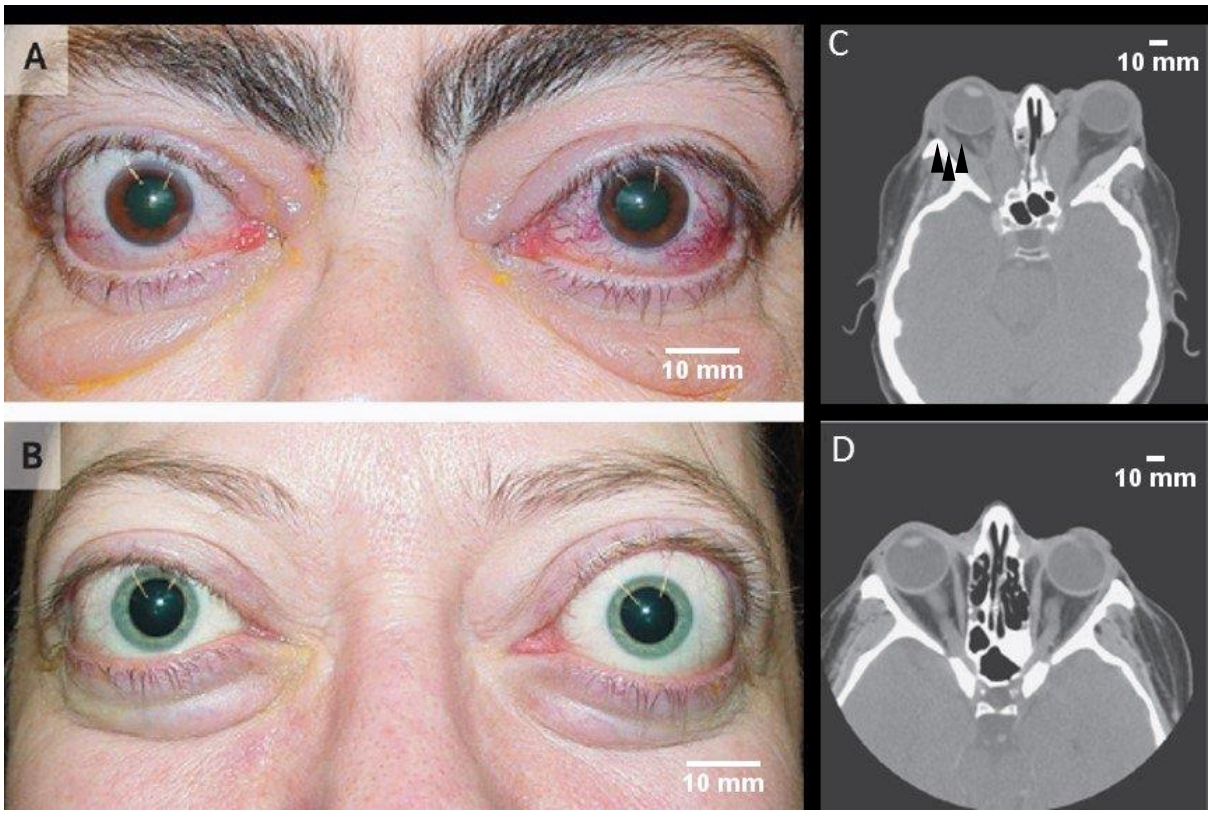

Figure 6.| Patients with TED and computed tomographic scan of a TED patients and a normal subject. A&B) Women with excess proptosis, moderate eyelid edema, and erythema of the periorbital tissues and conjunctivae, as well as eyelid retraction. Proptosis and eyelid edema are more prominent on panel B (left) than panel A (left). C) Computed tomographic scan showing the cross section of the head of a TED patient at eye level. Displaying generalised enlargement of the extraocular muscles with distinct bilateral proptosis resembling the left panels. Excessive orbital tissues compressing the optic nerve can be seen (black arrows). D) Normal orbits are shown for comparison *(Bahn, 2010)*.

John Dalrymple identified the LPS as the source of the upper eyelid retraction and was first to differentiate it from exophalthmos. It is now known as Graves' upper eyelid retraction (GUER) and it can occur without the presence of exophthalmos (Eden, et al., 1942; Pochin, 1939).

GUER is the most common sign for Graves' ophthalmopathy and refers to a higher than normal upper eyelid margin at open state during rest (just below the superior corneal limbus). Nowadays the position of the upper eyelid is commonly measured from the center of the pupil; however, mid-pupil to upper eyelid margin distance was also used in some studies. GUER is a common symptom of TED due to an over-stimulated MM and the anatomical positions of the LPS between the enlarged extraocular tissues, causing LPS over-activation. LPS enlargement from inflammation or scar is also a factor in the upper eyelid retraction (Davies, et al., 2017). Lower lid retraction is primarily caused by overreaction of the inferior rectus muscle (Putterman, 1997). TED patients often have accompanied periorbital edema as a result of decreased venous drainage due to vascular compression within the orbital space after the inflammation and swelling of the extraocular muscles. In some patients, the proptosis and GUER is so prominent they were unable to close their eyes (even during sleep), leading to corneal dryness and other complications. GUER also brings about a decreased down phase blinking amplitude or incomplete blinking (Falcao, et al., 2008), increased tear evaporation and decreased in blink rate (Cruz, et al., 2013). The blink rate and amplitude in eyelid retractions are usually found to be abnormal and displaying Stellwag sign (frequent blinking) and Pochin sign (infrequent blinking), as displayed in figure 7. Such disturbance in blink rate can be detrimental for the maintenance of the corneal transparency and clarity of vision by reducing the spread of the tear film during spontaneous blink.

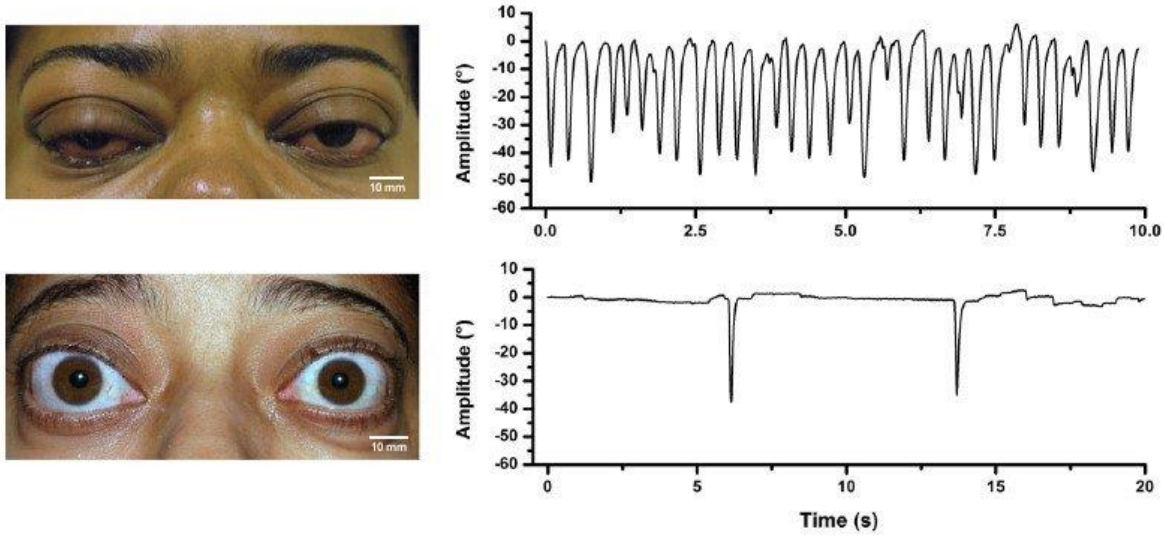

Figure 7.| Recorded blink rate and amplitude in GUER patients. Top panels shows Stellwag sign – frequent blinking of up to 155.2/min. Bottom panels shows Pochin sign – infrequent blinking of only 2.9/min. Scale bars are to 10 mm (Cruz, et al., 2013).

2.3.3a Current established treatments

There are many treatments for TED depending on the actual cause and current state of disease development. First would be to prevent the worsening of the condition by taking necessary steps such as to quit smoking, as treatments are less effective in smokers. In cases where TED or Graves' ophthalmopathy had developed from Graves' disease with hyperthyroidism, the common approach would be to control the thyroid level by administering anti-thyroid drugs/ systemic glucocorticoids, owing to its ability in anti-inflammatory and immunosuppressive effects. Orbital radiotherapy directed to the orbital tissues, surgical treatments such as orbital decompression and rehabilitative surgery could be considered.

The pathogenesis of TED is still incompletely understood, but physical changes in the orbit and the increased thyroid level have given indications to how best approach the disease. It was found that the majority of the physicians preferred to initiate treatments with glucocorticoid and some 23% select orbital radiotherapy. Orbital decompression and rehabilitative surgery wasn't widely considered as the first line of treatment (Weetman, et al., 1998). To address the proptosis in TED, it was understood that the reason is enlargement of the tissues behind the globe and as a result, the eyeball is being pushed out as a means for decompression. This leads to eyelid retraction, exposure keratitis, pain, photophobia and extraocular muscle dysfunction that causes restriction of eye movement with diplopia and blurred vision. In more severe cases, inflammation and the increased orbital content may apply pressure to the optic nerve thereby impairing vision. To resolve the root problem, upstream treatment should be aimed at reducing the volume of the orbital content or increasing the space available in the orbit. Medical decompression by utilising drugs and orbital radiotherapy reduce the inflammations and act on the etiology of the disease, but no immediate result or relieve to the patient. To maximise the effectiveness of these treatments, the degree of activity of the disease must be assessed. Glucocorticoids and radiotherapy respond best to active eye disease but unlikely to be of beneficial in patients with inactive TED (Bartalena, et al., 2000). These patients are the best candidates to be considered for orbital decompression or rehabilitative surgery.

Orbital decompression aims to increase space to accommodate the increased orbital content by removing one to even four walls of the orbit (Burch, et al., 1993). Although this method treats only the mechanical effects of the disorder, it has proven to be very effective, especially with patients who had little or no improvements with medical decompression alone, for immediate relieve of proptosis and other complications arise from venous congestions and

optic nerve compression. Further, side effects must be considered as this procedure has high incidence of post-operative diplopia (Garrity, et al., 1993; Nunery, et al., 1997). Orbital fat can also be removed as an alternative approach to decompress the orbital content, but this method seems to produce a limited decrease in proptosis (Trokel, et al., 1993), therefore the removal of bony components is carried out more frequently. Other rehabilitative surgery aims not only to improve the cosmetic appearance of the patient, but also the function of the eyes. Extraocular muscle surgeries may be carried out when the disease has not been active for 4-6 months (Burch, et al., 1993). The muscle recess is usually performed on the most affected, restricted muscle. The down side is that often more than one surgical procedure is needed. To have the best result for patients, both medical decompression and surgical interventions shall be utilised together if functional and or rehabilitative results are not satisfactory.

On a different note, eyelid surgeries including the correction for upper eyelid retraction may be done subsequently. Earliest attempts to control mild eyelid retraction with topical administration of adrenergic blocking agents (Gay, et al., 1966) has proven effective by reducing retraction, but side effects such as vasodilation, ocular irritation and discomfort have since render this type of drugs undesirable. Alternatively, botox injection to the upper eyelid retractor muscles was a quick and reliable method to lower the eyelid margin. It acts on the neuromuscular junction and prevent acetylcholine release, thereby reducing LPS contraction and relaxing the muscle. However, the effect is only temporary and lasts between 3-6 months and poses a risk of diplopia and ptosis. Still, this is the preferred method especially for patients who cannot undergo or do not wish for surgical treatment (Uddin, et al., 2002; Costa, et al., 2009; Shih, et al., 2004).

Other than pharmaceutical interventions, myotomy, blepharoplasty, LPS and LPS aponeurosis recession, and mullerectomy with anterior and posterior approach were also used to treat upper eyelid retraction. Residual lateral retraction is very common after the initial recession, therefore most surgeons increase the debilitation of the retractors laterally and this was accepted as a key step in surgical procedures (Hintschich, et al., 2005; Kazim, et al., 2011). Lid retraction may also be improved by orbital decompression surgery, however this treatment does not fully correct the condition as the causative mechanism is multifactorial (Cruz, et al., 2013).

Such wide divergence in the therapeutic approach to TED suggests a current lack of knowledge for the best practice.

2.3.4 Dermatochalasis

Human aging can have a variety of side effects on appearance, many of which are visually apparent such as thinning of the skin, caused by degeneration of type I collagen, the loss of connective tissues and reduced elasticity of the skin (Quan, et al., 2015), most notable around the area of the eyes such as sagging eyelids. Dermatochalasis is an ophthalmic condition caused by excess skin on the upper eyelid resting on the eyelashes, creating a 'hooding' effect which could affect peripheral vision as well as appearing tired with puffy and swollen eyes. Age is merely one of many risk factors for the development of dermatochalasis, but the sagging eyelids tend to gradually increase in heaviness as the person ages. Other intrinsic and extrinsic factors include ethnic background, sex, skin colour, body mass index,

and smoking, but the strongest influence is genetic predisposition and familial inheritance (Jacobs, et al., 2014).

Dermatochalasis may occur bilaterally and may affect the lower eyelid. It is typically a cosmetic concern, although in cases where it causes superior visual field loss, ocular or eyelid discomfort and ptosis due to increased mass of the upper eyelid, then treatments become medically necessary (figure 8). Usually, the body compensates such efforts by overworking or straining the frontalis muscle to force brow elevation to increase the visual field, which could potentially induce headaches. Moreover, a study using pre- and post-operative bilateral dermatochalasis (and or ptosis) facial photographs and questionnaires has revealed that the droopy eyelids of the condition were viewed negatively by members of society, therefore affecting the patients not only visually but also through psychosocial implications (Bullock, et al., 2001).

The aging process contributes to the formation of dermatochalasis the majority of the time, but ultraviolet-induced collagen degeneration and age-related degeneration are also attributable alongside worn elastic fibres subcutaneously. Together they are responsible for the thinning and overhang of the tissues beyond the eyelid margins. It was found that gravitational forces acting on the brow, superficial musculo-aponeurotic system and the submuscular fibroadipose tissue (SMFAT) causing descent and undergoes stretching and eventual attenuation contribute to the sagging of the eyelid skin above the eyelid margin (Gosain, et al., 1993; DeAngelis, et al., 2002).

Other factors that cause eyelid swelling may also lead to dermatochalasis. This condition is also seen in some rare skin conditions like cutis laxa. Caused by mutations in the elastin or fibulin genes, it is characterised by accelerated aging of the skin, loose and inelastic skin that

hangs in loose folds, causing the face and other parts of the body to become extremely wrinkled and display a droopy appearance (Mitra, et al., 2013). This condition can be congenital or acquired and affect all age groups. Another connective tissue disorder such as Ehlers-Danlos Syndrome can also give rise to dermatochalasis. Connective tissues are important as they form the basis of skin, tendons, ligaments, blood vessels, internal organs and bones. Therefore connective tissue disorders, even dermatochalasis, should not be taken lightly.

Dermatochalasis shares a similar phenotype with blepharoptosis, in which the appearance of their eyelids seems familiar. To avoid incorrect diagnosis, one has to pay close attention to the eyelid margin. In dermatochalasis, the eyelid margin might still be at a normal height despite the tired look, whereas ptosis patients have a lower than normal eyelid margin. These conditions can also occur simultaneously on the same patient, but more frequently in older people.

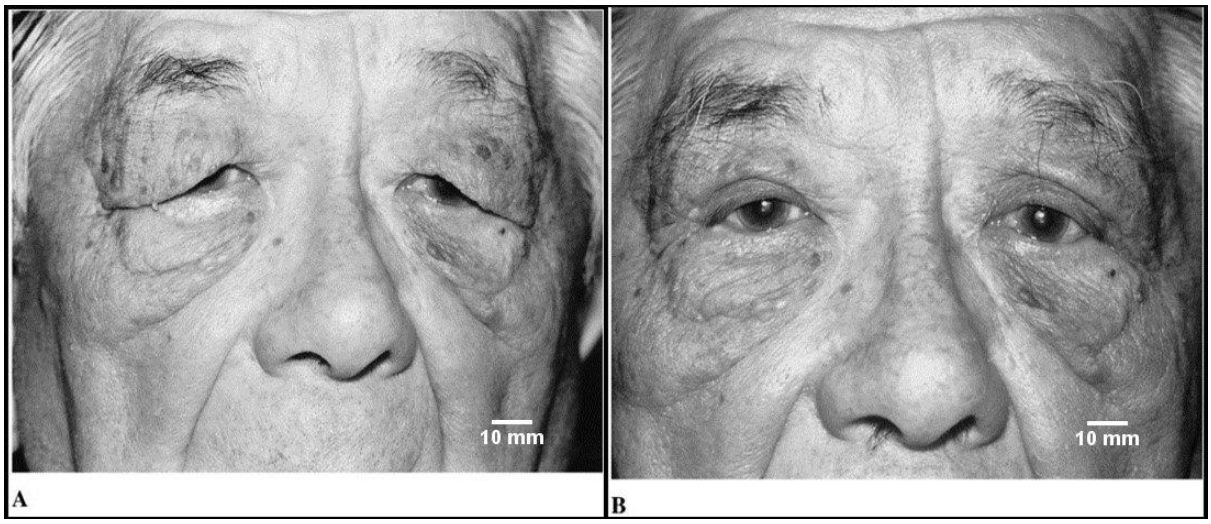

Figure 8.| Before and after blepharoplasty surgery in a dermatochalasis patient. (A) Patient with severe upper and lower eyelid dermatochalasis bilaterally. The excess upper eyelid tissues droops down, inducing lash ptosis, ocular discomfort and corneal irritation, and mechanically obstructs the central visual axis. (B) The same patient post-operative of dermatochalasis correction. Notice the upper eyelids have been significantly reduced and pupil is now visible. Dermatochalasis of the lower eyelids was not corrected (DeAngelis, et al., 2002).

2.3.4a Diagnosis and management of dermatochalasis

A thorough eye examination is beneficial to work-up a patient with dermatochalasis. To mention a few, visual acuity and visual field test with eyelids in their natural state and with the excess tissue elevated is necessary to determine the significant of the dermatochalasis. Measurement of the upper eyelid crease will also help to determine possible underlying levator dehiscence. As surgical intervention for dermatochalasis will not correct true ptosis, examination for ptosis is essential. Moreover, patients with brow ptosis are not suitable for this type of surgery as it may further descend the brows (DeAngelis, et al., 2002).

To address both functional and cosmetic problems of dermatochalasis, surgical procedure: upper (and or lower) blepharoplasty may be performed under local anaesthesia to remove excess skin, muscle and periorbital fat that can lead to bulges of the upper lid. This simple operation is a solution to the heavy and tired appearance of the upper eyelid, restoring youthful and appropriate periorbital contour of the eyelids. It is also life changing for the patient as it provides a dramatic but positive change to their appearance.

Blepharoplasty is considered the gold-standard to correct dermatochalasis, although other novel and modified techniques have been introduced (Perkins, et al., 1994; Carter, et al., 2001; Huang, 2000), the principle remains unchanged. Even though this procedure has been performed for centuries, there are still no defined amounts of skin, muscle or fat to be removed in relation to the post-surgical blink kinematics. The tissues are excised primarily based on experience and testing, thus the surgical outcome is unique to each patient. While the individuals may have improved quality of life, it is possible that they may still present diseased blink kinematics and not recover to 'normal' blink dynamics.

2.4 Blink dynamics and existing methods of measurement

Eyelid blinking system is a good experimental model to study spontaneous, reflex and voluntary blink dynamics, because the eyelid responses and blink stimuli can be quantitatively recorded and controlled, allowing them to be studied in more details. Eyelid motility can be used to assess ptosis and other diseases such as 3rd nerve palsy, blepharospasm and Graves' disease by neuro-ophthalmologists and eyelid surgeons. Static measurements of the PF and

the amplitude was the principal method to measure lid health. However, although more studies have trialled different ways to measure kinematics of eyelid movements very few studies have investigated the dynamics of normal and abnormal lid motion. In this section, various methods to measure blinking will be discussed.

High-speed cameras have been used for vision research since 1970s. 2 to 3 blinks were recorded with up to 500 frames per second (fps), however these studies were not specific on the type of blinks measured, i.e. voluntary, reflex, spontaneous or forced blink (Hayashi, 1977; Hung, et al., 1977). Doane recognises the significance of the differences between voluntary and spontaneous blinks, the study was designed in such a way to ensure that only truly spontaneous blinks were recorded (Doane, 1979). The test subjects were asked to read from a standard Snellen-type visual acuity chart by reflection through a mirror 10 feet away. A high-speed camera was focused on the subject's eyes, placed behind this one-way mirror, which allows the camera to record without the subject being aware of the filming and thereby affecting the blink mode (Figure 9). The subjects were only told after the filming that blinking was the topic of interest and that photography was being done.

Although spontaneous blinking was achieved, the authors failed to take into account that concentration reading or processing information also affect the blinking dynamics, such as the blink rate (Orchard, et al., 1991; Bentivoglio, et al., 1997). Another major problem in this study is that at 500 fps, the effective shutter speed was 1/1500s. This short exposure time combined with the 60% light loss through the one-way mirror means that a high intensity light is required to light up the subject. Even though lights were directed at an oblique angle to the eye being photographed, the brightly lit-up room will have substantial effect on the PA. Nevertheless, Doane reported that the upper eyelid accelerates rapidly downwards and

reaches its peak velocity at the point it crosses the visual axis and then decelerates and comes to rest before achieving full closure. During the opening phase, the eyelid again accelerates rapidly but at a lower velocity and gradually decelerates from approximate halfway point, then moves even slower for the final few millimetres of movement to return to its original PA (Doane, 1979).

Other methods of detecting blinking include placing electrodes immediately above the eyebrow and below the lower eyelid and amplifying these oculometric signals for offline analysis (Orchard, et al., 1991). However, this method raises the issue of subject comfort and the weight above the eyelid, affecting the data being collected.

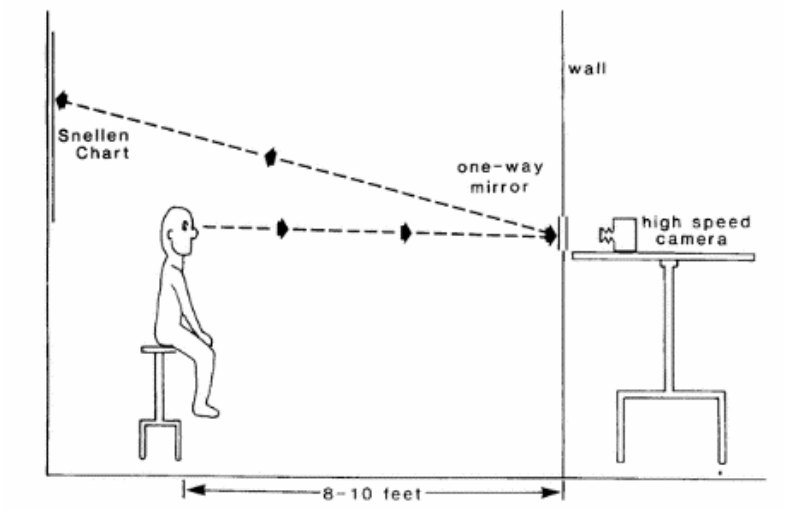

Figure 9.| High-speed camera set-up behind the one-way mirror in the adjacent room. The subject can see the Snellen visual acuity chart through the reflection, but unaware of the camera filming, until after the test *(Doane, 1979)*.

A method to record horizontal and vertical eye movements in monkeys using principles of electromagnetism was described in 1966 by Fruchs and Robinson. Essentially, a fine strand of

stainless steel conductor coated with Teflon (due to its biological inertability) was made into a coil and implanted into the eyes of the monkeys. This coil is then subject to horizontal and vertical alternating magnetic fields. During the eye movement, a voltage is generated in the coil. This DC voltage is proportional to the angle between eye position and the magnetic field and is detected against both horizontal and vertical reference voltages (Fuchs, et al., 1966). Other kinematics can then be obtained by calibrating and analysing the signals recorded. Such coil is embedded in a contact lens or annulus to be worn by human subjects under local anaesthetic (Robinson, 1963; Collewijn, et al., 1975; Kenyon, 1985). This method allows accurate and reproducible recordings for visual tracking in the test subjects disregarding the head position, and provides a high degree of temporal and spatial resolution. However, this is not used to study disjunctive eye movements as it induces slight diplopia and minor strabismus in the implanted subjects.

This is known as the scleral or magnetic search coil technique and has since evolved to measure eyelid movements as well, following the same principles, with the coil affixed to the upper eyelids (Gruart, et al., 1995) and using only vertically directed alternating magnetic field. It is a popular method to measure the kinematics of blinking.

Using a magnetic search coil, one study with 9 human subjects was able to measure maximum velocity versus amplitude and duration versus amplitude in the upper eyelid during voluntary blinks and lid saccades (Guitton, et al., 1991). The authors separated the down and up phases of the blink/ lid saccades and found that maximum velocity and duration increases linearly with the increment of amplitude during the down phase of a blink, whereas the maximum velocity is nonlinear against increasing amplitude in lid saccades. However, the duration increases linearly with increasing amplitude in eyelid movement of lid saccades. This study

also established that down phase maximum velocity is always greater than the up phase in the voluntary blinks, but were largely similar during the saccadic eyelid movements. With large inter-subject variations, the authors suggested that caution should be taken when using normative data to interpret abnormal lid motion for clinical purposes (Guitton, et al., 1991). A group tested 40 healthy human subjects to investigate age related changes in upper eyelid motions with spontaneous and voluntary blink amplitude, duration and maximum velocity using also magnetic search coil technique. Although they found no trends that the eyelid kinematics is consistent with eyelid movement disease as a direct result of aging, they have generated a reliable normative database of eyelid blinking metrics (Sun, et al., 1997).

Magnetic search coil technique was also used to investigate abnormal blinking activities, such as GUER (Garcia, et al., 2010), Graves' orbitopathy (Garcia, et al., 2011), ptosis (Cruz, et al., 2014), Bell's phenomenon (Takagi, et al., 1992; Iwasaki, et al., 2005), etc.

Garcia *et al.* recorded spontaneous blinks of 15 GUER patients and compared the results to a control group of 15 healthy subjects. It was found that blink rate per minute is significantly lower in patients compared to controls (P= 0.016) due to a longer inter-blink interval in patients (P=0.05), but the amplitudes were not significantly different from the controls (Garcia, et al., 2010). However, they noted that majority of the patients' upper eyelid did not even reach the centre of the pupil during the blink, which is over 3-folds more than the control group. Furthermore, the maximum velocity during the down phase is proportional to the amplitude and this was found to be the same for both groups. This is in agreement to the above study by Guitton (Guitton, et al., 1991). Although there is a trend of faster blinks in controls than GUER patients, the mean differences were not significant, so as for the duration of blinks between the two groups (Garcia, et al., 2010).

In all of the above studies, the coil was taped to the upper eyelid, above the eyelid margin, although it was suggested that it does not impair normal eyelid motions (Evinger, et al., 1984; Robinson, 1963; Sun, et al., 1997; Stava, et al., 1994; Garcia, et al., 2010), any foreign objects will add weight to the upper eyelid and therefore the force exerted on the LPS will increase and as a result could affect the blinking dynamic. It may also induce discomfort on the volunteer during the experiment. The slipping of the coil annulus resulting in a lower maximum velocity reading compared to infrared-oculuography method has also been reported (Traisk, et al., 2005). However, comparing the electronic circuitry of magnetic search coil technique to analogous eye movement measuring system, magnetic search coil technique is simpler to use because only a single channel magnetic field generator and demodulator is required.

An infrared-oculuography (IR-OG) has been developed to detect eye blinking (Castro, 2008). Based on certain ocular parameters such as the percentage of eye closure over time, eye closure duration over time and the average eye closure speed, the person's level of fatigue can be monitored. This method works in two parts: infrared light is directed to a particular point on the surface of the eye; a fixed infrared detector detecting the infrared reflected on the surface of the eye. Together, due to a different angle of reflection during eye movement, the position of the eye and the eyelid can be recorded. This device is portable, wearable (fixed onto the glasses) and cheap, but the disadvantage is its poor ability to detect vertical eye movements and it can only provide the measurement of the eyelid at a fixed point. It is impractical for continuous measurements such as acceleration at various point of the blink. Other studies have also investigated methods to monitor drowsiness or fatigue in drivers (Ma'touq, et al., 2014; Lenskiy, et al., 2012). These methods have emphasized safety and intrusiveness. Various techniques have been used, such as electrooculuography (EOG) and

electromyography (EMG) by recording activities in the muscles involved in blinking, namely LPS and OOM.

Other ways to measure eyelid movements include a lever attached to the lower margin of the upper eyelid: this was used to monitor the eyelid position during blinking in humans, guinea pigs and rabbits. This lever moves a small infrared light-emitting diode past a photosensitive position detector and the signal was amplified and recorded for offline analysis (Evinger, et al., 1984). This method produced results similar to those with high-speed photographic analysis but was not easy to attach the lever to the smallest animal used in the study with double-stick tape, it also produce a very noisy recording.

More and more new methods have been introduced in this field to measure eyelid movements during blinking. A novel analytical technique was proposed by Radlak and Smolka, involving static image analysis using a high-speed camera. It is based on the eye area approximation, grey scale, brightness and contrast detection algorithms of the face and eyelid edges to identify blinking dynamics. A single frame is analysed and algorithms are applied to subsequent images to track eyelid motion (Radlak, et al., 2012).

Some studies have used high precision optoelectronic systems that are able to capture rapid movements through digital video cameras and sensitive sensors to record eyelid movements. Bologna *et al*. have used the *SMART* analyser system (BTS, Milan, Italy), which comprises three infrared cameras that are capable of tracking the displacement of markers that were taped on the upper eyelids of the patients. In this study, they looked at the spontaneous, voluntary and reflexive blinking. Kinematic features like blink rate, duration, maximum velocity and the pause between closing and opening phases of patients with progressive supranuclear palsy (PSP) were compared with controls (Bologna, et al., 2009). A similar method was also used to

study blinking kinematics of Parkinson's disease (Agostino, et al., 2008). However this method relies heavily on technology and makes it much harder to troubleshoot when there is a problem in the analysis.

2.4.1 Velocity, duration and amplitude in blinking

Certain eye conditions often lead to a change in blink patterns, and this in turn affects the dynamics of blinking. Blepharospasm is a good example where the blink rate increases drastically. TED patients with eyelid retraction show larger than normal PA, whereas ptosis displays abnormally low upper eyelid margin, or a decrease in PA. These changes in upper eyelid metric could potentially provide valuable insights into the pathological mechanisms and facilitate developments of new diagnostic techniques.

Upper eyelid was also known to elevate or lower involuntarily with the change in vertical direction of the gaze. When a person looks up without changing the position of the head, the upper eyelid retracts. The eyelid drops down with the person looking downwards. This is known as the saccadic movement of the upper eyelid, and has been studied relatively extensively.

A study compared the lid saccade kinematics between various forms of ptosis and found that congenital ptosis, involutional and rigid-contact-lens-induced ptosis are significantly different (Wouters, et al., 2001). Average velocity (measured in degrees per second) is also significantly different between the groups. This study found that eyelid saccadic peak velocity decreases significantly with age. The authors concluded that there are distinctive differences in the

blinking dynamics amongst different forms of ptosis. In a separate study, blink velocities were also reported to be increased post ptosis operation (Watanabe, 2012).

Multiple system atrophy (MSA) is a progressive neurodegenerative disorder, its blinking was evaluated in patients with Parkinsonian (MSA-P) and cerebellar (MSA-C) phenotypes compared to controls. A longer interphase pause duration was reported in both types of patients compared to controls, and they also found that peak velocity and amplitude during voluntary opening and closing phases were lower in MSA-P and MSA-C compared to controls, but not during reflex blink. That led the authors to suggest that basal ganglia dysfunction may play a role in generating this abnormality (Bologna, et al., 2014).

Apart from discriminating clinical conditions, blink dynamics can also be used as an indicator of fatigue in professional drivers. The blink duration and frequency was studied and used as a measure of sleepiness. As a result, effective treatment was developed to prevent deteriorating driving performance during prolonged driving and to reduce the risk of traffic accidents (Hakkanen, et al., 1999). Another study used the data captured from gaze direction and blinking sequences with a camera to create a control system for electric wheelchair for people with physical disabilities (Purwanto, et al., 2009).

2.5 Force of blinking

Many studies have compared normative data of blink dynamics such as velocity, amplitude and duration to various disorders to be used as additional diagnostic tools. The force of eye blink, however, has received very little attention. As an example, BEB produces forceful exaggerated blinks and often leads to apraxia of eyelid closure (as mentioned in section 2.3.2). It is therefore safe to assume that force changes in certain diseases compared to controls, but there have been very few studies on this topic.

There has been an attempt at measuring the strength of the OOM in the 1950s. H.B. Jacobs suspected that some ophthalmic disorders may be correlated with variations in the strength of the OOM. However, there wasn't any equipment built for this specific purpose. Jacobs decided to develop a simple and portable instrument to measure such force generated by the OOM in a random sample of refractive patients and a group of normal subjects (his medical students). Essentially, he assembled a piston and cylinder connected to a pair of specula that is also connected to a pump, an air reservoir and a mercury manometer (Jacobs, 1954).

The instrument was introduced into the PF and by increasing the air pressure inside the piston (measured in mm Hg) it worked against the volunteer's forced eye closure (figure 10). Jacobs was able to take readings at the moment the eyelid parted and by assuming that the force generated in the cylinder is equal to that exerted by the muscle, he compared the individuals in attempt to gain an idea of variations to be found in the strength of the OOM. For one of his groups of subjects, he obtained an average measurement of 120-140 mm Hg, or 60-70 g in weight for the force of eyelid closure with a wide range on either side of the mean. This study

failed to establish a norm but instead an extremely wide range of variation in overall eyelid closure power (50-186 mm Hg). Amid much experimental errors, its primitive design and technology, and the intense invasiveness without the use of topical anaesthetic, the subjects are bound to produce unstable results and Jacobs was unable to obtain a consistent results. There is a need to properly define the mechanical characteristics and properties of the muscles involved in blinking in order to improve disease diagnosis. Jacobs's study has laid the first step towards the investigation of how force of blinking differs in various ophthalmic disorders.

Decades later, a study evaluated the force exerted by LPS during blinking as a diagnostic tool for the cause of ptosis (Frueh, et al., 1996). A clamp was placed on the margin of the upper eyelid on the eye lashes and connected to a force transducer. The authors evaluated 187 patients with different forms of ptosis and measured the LPS force generated on up gaze and found significant differences in levator force between aponeurotic, myogenic/neurogenic and the control group. Average force was measured to 67.50±24.20 g (± standard deviations), 26.90±19.80 g and 74.10±21.20 g (or 0.66±0.24 (N), 0.26±0.19 N, 0.73±0.21 N) respectively in the three groups. The study also demonstrated a 97.30% correct ptosis diagnosis by levator force measurement alone, up to an impressive 97.90% with clinical evaluation (183 out of 187 patients).

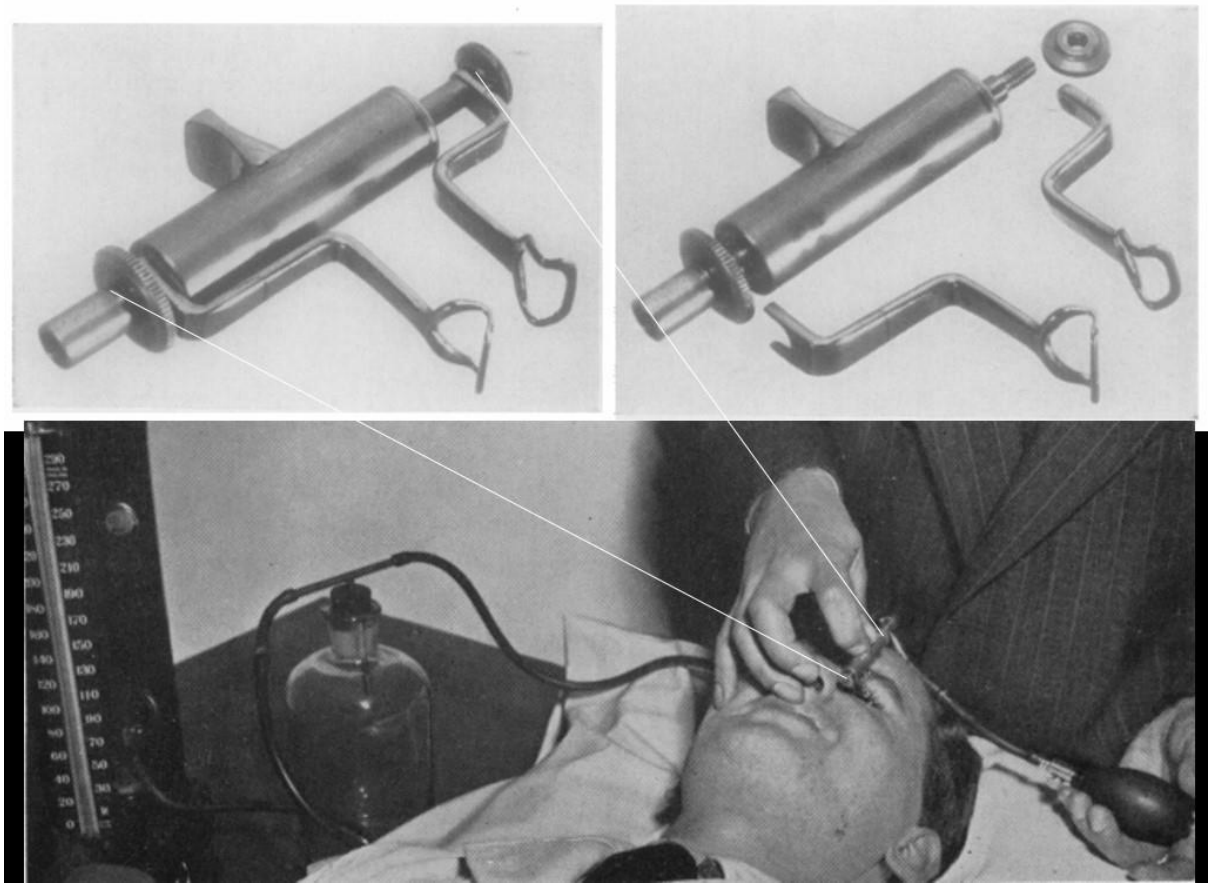

Figure 10.| Instrument assembly and experimental set-up in Jacobs's study. Top two panels display an instrument's assembly. The specula can be detached for sterilisation. The instrument is formed of a piston and a cylinder connected to a pair of specula. The lower panel shows the device connected to the pump, an air reservoir and the mercury manometer. The subject is at the supine position with the instrument inserted in the PF. The subject was encouraged in his efforts at all times. The white lines across the pictures depicts the size of the instrument in use *(Jacobs, 1954)*.

Not only the force of eyelid closure could provide useful information on ophthalmic conditions, the LPS function measured by the maximum lid excursion is also being evaluated clinically these days. The first attempt to measure force generation by LPS was in the 1980s. After an injection of local anaesthetic, the active contraction and passive stretching was recorded by a spring scale connected to the upper eyelid via a suture through the eyelid. The

subject was asked to look up and the scale read (Madroszkiewicz, 1980). This is not a preferable technique as this involves surgical interventions with the otherwise healthy subject. A decade later, B.R. Frueh improved upon this method by not requiring a local anaesthetic injection or any piecing of the skin. This also provides a more accurate assessment of the LPS force generation in conditions that are more acceptable for the subjects (Frueh, et al., 1990). The apparatus consists of a lash clamp (weighing 2 grams) that can be connected to a load cell force transducer. The procedure involves an application of a topical anaesthetic in the eye being tested and the lashes being clamped by the lash clamp at the down gaze position with the subject at a seated position (figure 11). This is then linked to the force transducer placed in tangent in front of the eyelid and the recorded signals are amplified. The subject was asked to stabilise his/her head with a bite bar and to look up as high as possible for 20 seconds and look back down as far as possible. The maximum force recorded was then considered as the maximum levator force. Both studies have acquired similar results of a mean force of 58 g (Frueh, et al., 1990; Madroszkiewicz, 1980). No age effects on LPS force generation were seen in Frueh's study but they have demonstrated a significantly greater force generation in men than women. Although only healthy controls were tested in this study, Frueh suggested that the method described will be helpful in detecting congenital myogenic ptosis and characterising LPS functions in patients with TED and diagnosing myopathies.

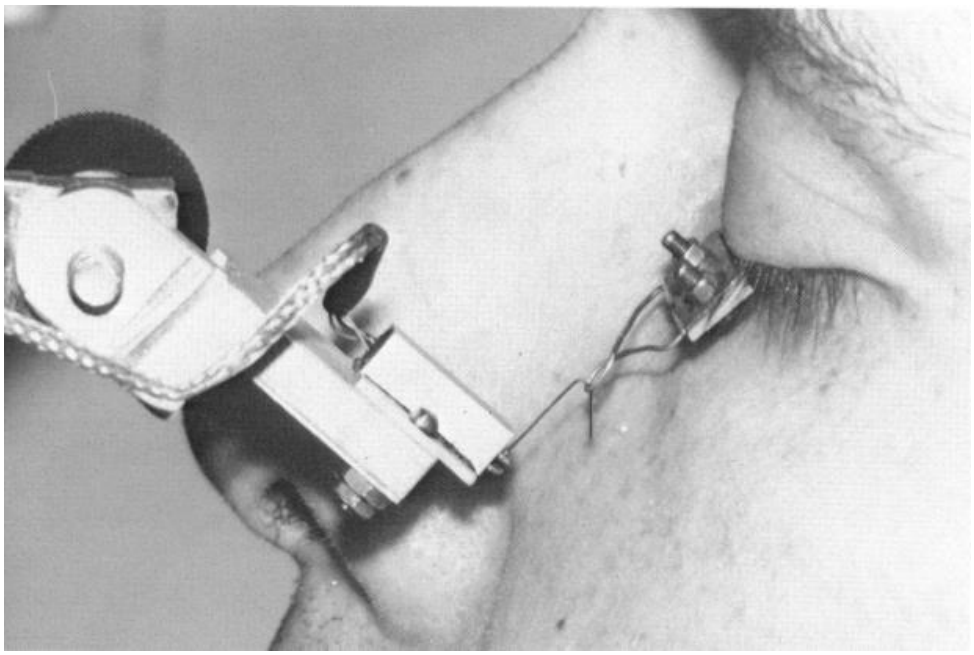

Figure 11.|A lateral view of the subject being tested. The subject was looking down and his upper eyelid lashes were clamped and linked to a small force transducer with a wire hook *(Frueh, et al., 1990)*.

The results from these studies indicate that the hidden patterns in the blinking kinematics could potentially help clinicians diagnose diseases earlier and more accurately, and also provide advanced treatment for the condition. This has also inspired us to investigate forces in blinking and to develop a modern device to measure forces during eyelid closure (chapter 7).

CHAPTER 3: EXPERIMENTAL DETAILS, SET-UP AND METHODOLOGY

This chapter on experimental details are dedicate to the analysis of blink dynamics in chapter 4, 5 and 6. Chapter 7 will have its own method section.

The magnetic search coil technique was a popular choice of method to measure eyelid blinking dynamics, it is also widely accepted for high accuracy. After reviewing a list of different methods in the previous chapter, a video imaging system was selected as the preferred measurement tool. Not only does it provide continuous recording in respect to time, it is also non-invasive, inexpensive, quick to set-up, and still able to provide accurate, reproducible results. A more recent study which compared a magnetic search coil technique to a portable video system in blinking dynamic analysis revealed that the blink traces registered by magnetic search coil were identical to the portable video recording system. The study concluded that blinking kinematics can be measured by both methods interchangeably (Wambier, et al., 2014). However, it should be pointed out that the video system they employed was coupled with a blue light emitting diode taped on the upper eyelid, near the margin. This could have impact on the natural blinking dynamics as the upper eyelid now bears the weight of the tape, the diode as well as a wire connecting to it. The tape also fixes the upper eyelid skins together, and could also contribute to a less than natural blinking dynamics.

With a slight modification to this video imaging system, we propose to measure the eyelid movements as naturally as possible, without any external apparatus that could possibly affect

the blink dynamics. Natural diffused light was also used to prevent glare, distraction or any reflexive action of the eyelids caused by high intensity light. In this chapter, we will discuss the experimental set-up and how the subjects were tested.

3.1 Experimental set-up

Patients of various conditions were recruited for each of the following studies (chapter 4, 5, and 6) but share the same set of controls. A total of 45 healthy subjects (14 males, 31 females) were used in this research, including twenty-five from our previous study (Kwon, et al., 2013). Only 45 healthy subjects was available on site, given the time frame we had at MEH. However, a power analysis could be done to measure whether this sample size is adequate to detect an effect in the full population when compared to the patient groups; to calculate the minimum sample size required to produce more significant results. Male and female patients were not considered separately and are tested one at a time because no statistically significant differences were found between the different genders (discussed in more detail in Chapter 4.2.1). After informing the patients how this test will be carried out, they were seated comfortably in a controlled environment inside the hospital at room temperature (22.6 ± 1.6°C) and standard humidity (28.3 ± 2.2%) with natural light. All patients are recruited from the oculoplastic service at Moorfields Eye Hospital (MEH) National Health Service (NHS) Foundation trust, and the healthy subjects were recruited from a combination of University College London and MEH. However, individuals of oriental Asian origin were not included in

this study due to their different eyelid anatomy compared to those of western origin, as explained in Chapter 2.2.

It was decided that high-speed camera capturing of voluntary blinks is the quickest, simplest and least invasive way to measure blinking dynamics for the subjects, also the easiest to set-up in a hospital environment where space is very limited. The idea here is to record voluntary blinking in diseased and control groups, both follow the same protocol. The resulting video will be analysed frame by frame with an external image analytical tool to extract the PA with respect to time. Afterwards, blinking dynamics will be analysed and a model will be generated in attempt to distinguish diseased individuals from the controls.

The following section of the thesis will cover the details of the method used to capture and analyse the data.

3.1.1 Protocols

All recordings were done in the Moorfields National Institute for Health Research (NIHR) clinical research facility. As we wanted to match this study with the previous data of healthy subjects, we kept all experimental details as similar as possible. However, two different high-speed camera models and settings were used.

In our previous study (Kwon, et al., 2013), a PHANTOM (v. 7.3, Vision Research Ltd, UK) high-speed camera was placed in front of the volunteers at their eye-level. The camera was mounted with a Nikon 24–85 mm f/2.8 macro zoom lens and had 800x600 pixel resolution. Blinks were induced by asking the volunteers to blink as normally as possible after a verbal

command. The motion of two voluntary blinks was recorded at a rate of 600 fps. The PA, which is the vertical distance between the central points of the upper and lower eyelid margins, was measured every 5 ms of the recorded videos, using the dedicated software PHANTOM CINE VIEWER v. 2.14 (Vision Research software). The measurements started from 30 ms prior to the start of a downward movement of the upper eyelid and continued until the initial PA value was reached. The second recorded blink was used for this analysis, considering the possibility that the volunteer was more comfortable and relaxed after the first blink. All participants were informed about the general purpose of the study.

In the present research, the protocol follows the above described principles with only minor differences in the equipment used and analytical techniques. Subjects were seated in front of the high-speed camera, which was set-up at eye level in front of each subject. 12.3 seconds of high-speed recording of voluntary blinking was taken for each patient with a monochrome Photron Ultima APX12K Camera (Photron – Europe Limited, Buckinghamshire, UK), operating at 500 fps with full 1024x1024 resolution; a total of 6144 frames per patient was recorded in 8 bit grey scale. The same lens, Nikon f/2.8 macro zoom lens with focal length of 24-85 mm was used. Subjects were asked to relax, look straight into the camera and blink as normally as possible; a brief pause prior to recording allowed the subjects to familiarise themselves and be as natural as possible. A verbal command was also given before each blink was captured. These control data were collected every 5 ms with two different cameras of different frame-rates (500 fps and 600 fps) settings, which produces an effective frame rate of 200 fps. Smooth curves were therefore fitted to the raw data to ensure that differences in collection protocol had a negligible effect on the results.

A desktop computer running Windows 7 operating system with the high-speed camera's default software (Photron FASTCAM Viewer – for High-speed Digital Imaging, version 3.5.1.0) was used to capture the data, in real-time, and record it directly to an external hard-drive. All images were captured in RAW format and converted to TIFF, using the same software.

In cases of patients with the ocular conditions we are interested in, they will have their ocular surface examined after filming and key oculoplastic measurements were taken manually – namely, vertical PA; Levator function (LF), the maximum excursion of the upper eyelid margin in mm; and MRD, the distance between the central corneal light reflex and upper eyelid margin in primary gaze. LF is the commonly employed standard for classifying LPS function, and the PA and MRD indicate the static severity of ptosis (Sudhakar, 2009; Fox, 1976; Nerad, 2010).

3.2 High-speed camera

The high-speed digital imaging system allows study of motion that happens faster than our eyes can perceive by offering extremely high frame rates, from 2,000 fps at full resolution and up to 120,000 fps at reduced resolutions in some models. The reason behind the switch in high-speed camera (from Phantom to Photron Ultima APX12K) in this study was not only due to the availability of the camera, but also the full mega pixel image resolution at the same/ higher frame rate. The Photron camera also provides a higher light sensitivity at the same or higher performance and reliability. This higher light sensitivity allows clearer images to be captured without external light sources indoors, and therefore improves the accuracy

of manual measurement done in the later process. It is favourable to avoid external lighting shining toward the eyes because it has an enormous impact on the PA and the blink rate.

3.3 Anonymity and confidentiality of patient data

All patient data collected are treated with the highest confidentiality in our study. Only researchers directly involved in the study had access to the data. All data were stored in accordance with the Data Protection Act 1998. The data were used only on informing the research question in these studies and in cases of publication in peer-reviewed scientific journals resulted from these information, the subjects cannot be identified.

Data collected were locked and stored securely at all times, and data that can allow identification of the specific patients were held only in the MEH Clinical Research Facility. Whilst working on the data analysis outside of the hospital, patient's name, date of birth and hospital numbers were deleted and a new patient number was assigned for ethics compliance.

3.4 Data analysis

All selected blinks in the captured videos were analysed frame by frame. The central PA are measured manually using the open source freeware ImageJ (W. Rasband, National Institute of Mental Health, USA). In this software, the isolation of a complete blink (100% PA recovery) from each subject was attempted, it being considered a blink if their upper eyelid

margin reached below 50% of the starting PA during the closure phase. Some subjects did not achieve 100% recovery, and were therefore analysed to the closest maximum percentage recovery. Only the affected eyes were considered in the diseased patients and both eyes were included for the healthy subjects but were not treated as pairs.

Each individual's PA will have a different scale on a 2-dimensional image for each subject due to the different distances they sat before the high-speed camera. The PA were determined by calibrating the horizontal corneal diameter to a standard of 11.70 mm (Salouti, et al., 2009). The measurement starts from the moment the upper eyelid begins to descend and continues until the initial PA value is recovered, or until the eye ceases to open further (figure 12). The resulting data were normalised to prevent data redundancy and improve integrity. Subsequent master curves were produced for each disease group.

Blink duration and peak blink speed were also analysed and compared to the control group. Blink frequency was not measured both because it is highly variable and also because this project focuses on voluntary blinking. Speeds were calculated as a magnitude from the upper lid excursion for each frame (by a one-sided finite difference approximation). Means and standard errors of the means were calculated for both groups.

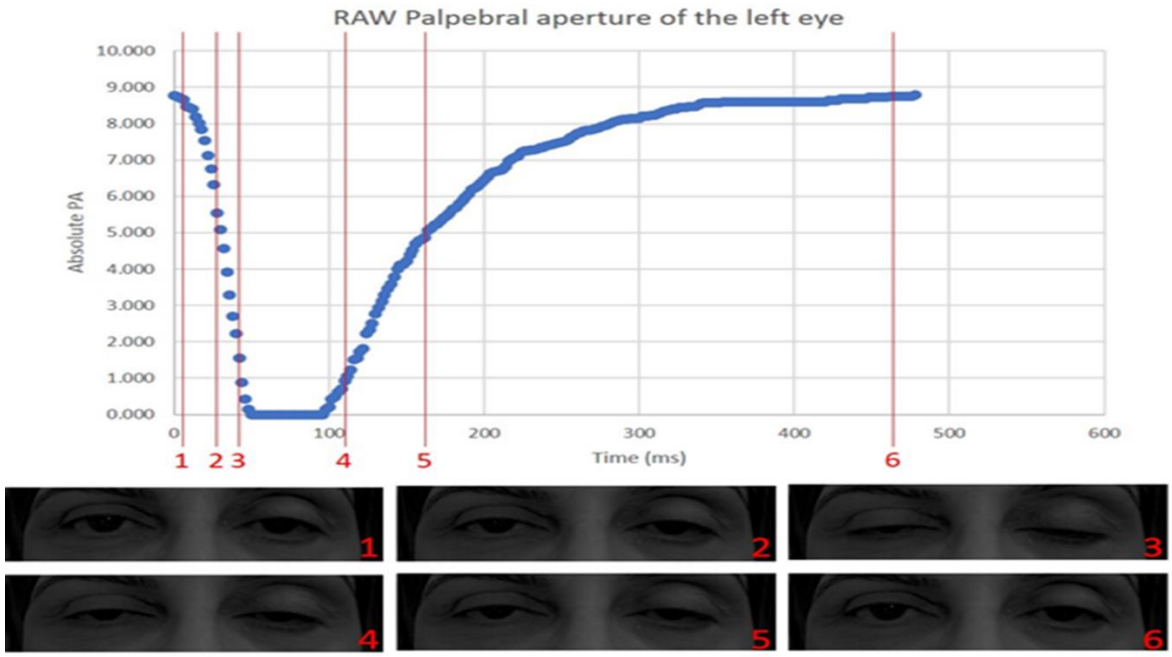

Figure 12.| Example plot of a randomly selected a patient's left eye PA for the complete duration of a single blink. These RAW data have not yet been normalised and therefore are labelled 'Absolute PA'. This demonstrates different phases of a blink labelled 1-6. 1 is at the beginning of the closing phase; 3 is just before complete closure; 5 is mid-recovery and 6 is returning to the initial aperture.

3.5 Statistical analysis and eyelid blink modelling

The measurements extracted from the RAW data were fed into a program written in Mathematica (Wolfram Research Champaign, Illinois, USA) and investigated using Fisher's linear discriminant analysis (LDA) and Gaussian classifiers.

To model the eyelid motion in order to differentiate diseases from controls, recreating the blinking profile was attempted. Key features of the PA *versus* time plot were broken down into different parameters to fit a function to best represent each feature (figure 13). These parameters include initial % opening; time offset for closing (t_1); minimum opening; rapidity of closure (v_1); time offset for opening (t_2); rapidity of opening (v_2); time offset for slow opening (t_3); rapidity of slow opening (α) and final % open. Analysing the data was performed in order to allow Mathematica to characterise the diseases blink dynamic and to determine if they are different from the control group. In this project, five parameters used to describe the shape of the blinking profile are detailed in the next section (section 3.5.1).

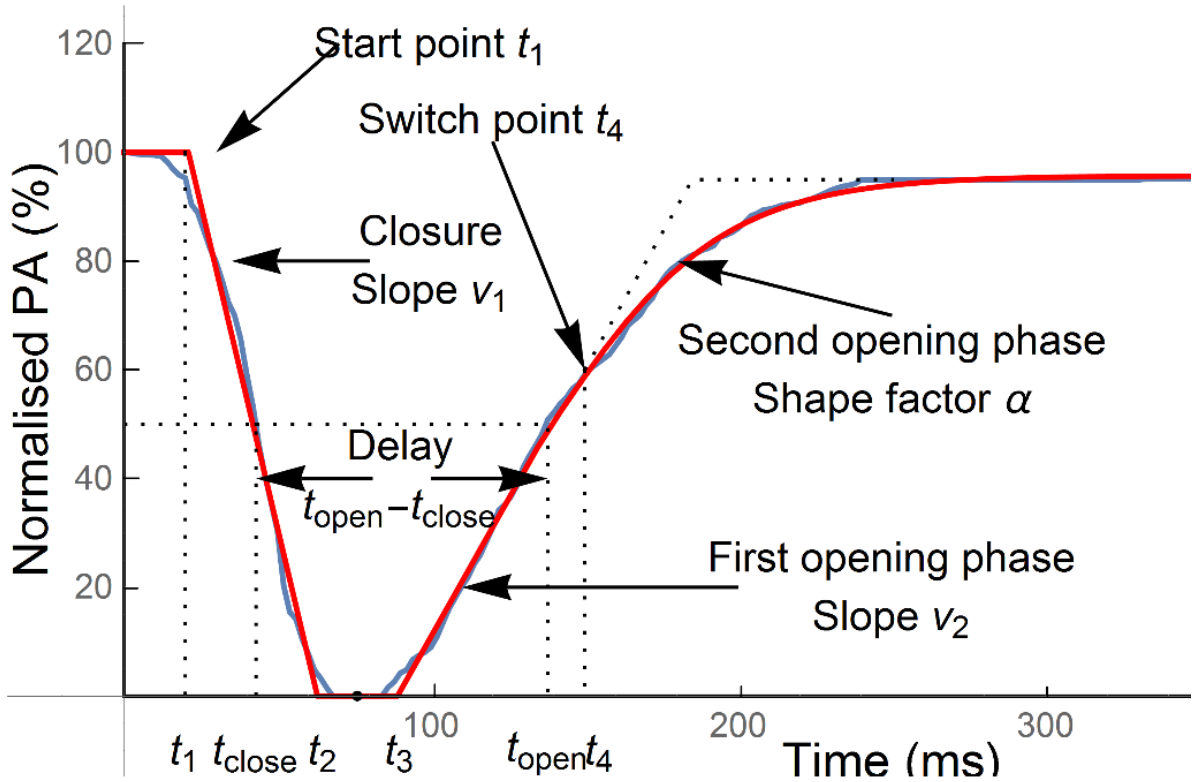

Figure 13.|Fitting the blinking profile. An example breaking down the blink PA vs time curve into possible key features – parameters that could be used in our analysis. The blue trace is the PA measurement against time, and the red trace is fitting of the functions designed to represent the key features of the blink profile.

3.5.1 Coding in Mathematica

There are two main aspects to the Mathematica coding: extracting parameters from the data and analysing them statistically. The time trace for each blink was first normalised, with the maximum PA set to 100%, and then divided into five segments, as follows (figure 13):

1. Constant at the initial PA, PA_{start}, from time 0 to t_1;
2. Constant-velocity closure at a rate v_1 to the minimum PA, PA_{min}, between t_1 and t_2;
3. Constant at PA_{min} from t_2 to t_3;

4. Constant-velocity opening at a rate v_2 from t_3 to the switching time (to the next parameter; change of rate of opening) t_4;
5. Smooth approach to full opening from t_4 to the end of the trace, PA(t)=A+B tan$h$(α(t-t_4)).

The values of A and B were determined by the value of PA at t_4 and by the requirement that the PA should asymptotically tend to its final value PA_{end} and the best fit of this piecewise smooth function was determined for each time trace by using Mathematica's *NonlinearModelFit* function, assuming the distribution of blink dynamics are normal across all subjects. The fitted parameters were PA_{start}, PA_{end}. v_1, v_2, α, t_{close}= (t_1+ t_2)/2, t_{open} which is defined similarly to t_{close} as the time at which the PA would reach (PA_{min}+PA_{end})/2 at a rate v_2, and t_4, the switching time. The value of PA_{min} was not used as a fitting parameter, but was set to the observed minimum percentage PA.

The fitted parameters characterise the time trace, but in order to remove any constant offsets from the time traces the five quantities which were used for further analysis were v_1, v_2, α, T_1= (t_{open}-t_{close}) and T_2= (t_4-t_{open}). The measured value of PA_{min} was also taken into consideration, as it was observed that whilst healthy eyes were all able to close fully, some diseased eyes tested could not: cases with full closure were analysed separately from those with partial closure.

The initial analysis was to assemble a linear combination of the five quantities described above which best distinguishes between the diseased and healthy eyelids, and this was done using the Fisher Linear Discriminant procedure (Bishop, 2006), which maximises the ratio of "between-class" and "within-class" variances; this finds the best plane in the five-dimensional space of the parameters for separating the classes. However, a planar separation may not

always yield the best results for all diseases. In cases when the covariance of the classes are not equal, one requires an elliptical (or ellipsoidal in higher dimensions) separation as the discriminant. This was achieved by using a Gaussian classifier that involves calculating the means (μ_c) and covariance matrices (σ_c) for each class (c) and then assigning an eye with parameters x to class c with a probability.

$$p(c|x) = \frac{|2\pi\sigma_c|^{-1/2}\exp[-\frac{1}{2}(x-\mu_c)^T\sigma_c^{-1}(x-\mu_c)]}{\sum_c |2\pi\sigma_c|^{-1/2}\exp[-\frac{1}{2}(x-\mu_c)^T\sigma_c^{-1}(x-\mu_c)]} \quad (1)$$

In expression (1), as is conventional, || denotes a determinant and a superscript T denotes a transposed vector. Note that this assumes equal prior probabilities for all classes – that is, before any measurements are taken any eye is assumed to be equally likely to be diseased or healthy.

CHAPTER 4: ANALYSIS OF BLINK DYNAMICS IN PATIENTS WITH BLEPHAROPTOSIS

4.1 Introduction

Ptosis is characterised by abnormal drooping of the upper eyelid and affected individuals have difficulty raising their lids to the normal vertical PA. It may cause obstruction to the visual axis causing functional blindness. The severity of ptosis can be usefully measured by the PA but different ethnicity (details covered in section 2.2), especially of oriental origin, has significant impact on the PA (Le, et al., 2002).

Possible pathogenesis of ptosis was covered in previous section 2.3.1, but the precise mechanism for development of an aponeurotic ptosis is poorly understood. It has been suggested to arise from a disinsertion of the levator muscle from the tarsal plate (Dortzbach, et al., 1980; Fujiwara, et al., 2001; Paris, et al., 1976) which would, in theory, affect the blinking dynamics. At present, manual measurement of the PA height and the eyelid excursion ("LPS muscle function") are the major determinants for diagnosing ptosis. This method also involves experienced judgements at early stages of the disease. Our limited knowledge of blinking dynamics in ptotic patients suggested that an accurate and detailed analysis of different aspects of the blink cycle could further our understanding of the mechanics and pathogenesis in ptosis. In addition, appropriate modelling of the blink cycle may enable clinicians to diagnose ptosis more accurately and at an earlier stage, where the condition is

less likely to be of concern to the patients. Subsequently, this can also provide avenues for monitoring and adequate treatment.

Characteristics of blink dynamics such as height of the PA, blink speed, duration and frequency vary significantly between healthy and affected groups, but no data has been published to compare the blink dynamics of patients with ptosis as compared with unaffected subjects. Various methods to study blink dynamics have been published and discussed in section 2.4. Static image analysis using a high-speed camera has also been used (Radlak, et al., 2012). Also, other techniques, such as infrared-oculuography (Castro, 2008) or a magnetic search-coil technique have been used to investigate the rapid blink movements (Evinger, et al., 1991; Korošec, et al., 2006; Sun, et al., 1997; VanderWerf, et al., 2003).

Due to the lack of invasiveness, high accuracy of measurements and being able to produce meaningful results, a high-speed camera ws used to record and characterise voluntary blinking. The blink dynamics of ptosis patients were compared to a control group. For each blink cycle in an individual patient, the images were analysed for central height of the PA as a function of time. A model was constructed to quantify the characteristics of ptotic blink dynamics, and the results compared with those for healthy subjects. LDA and Gaussian classifier were used to discriminate between diseased and healthy subjects and the results could potentially improve clinical evaluation and provide a reliable method for the diagnosis and quantification of ptosis.

4.2 Methods

4.2.1 Subject selection

There is ethnic variability in facial structure, especially between Western and Oriental Asian faces. These differences in facial structures might be reflected in varied muscle attachments and, combined with a narrower PA, could affect the blink mechanics and dynamics that were measured in this part of the study. Consequently, volunteers of Oriental origin (very few in number) were excluded from the study. The study received local ethical approval.

Twenty-six ptosis patients (11 males, 15 females) and 45 healthy volunteers (14 males, 31 females), including the 25 healthy subjects from our previous study (Kwon, et al., 2013) were included in the present work. A comparative histogram of the probability distribution of values of the discriminant function was plotted and confirmed that there is no statistically significant difference between the genders (figure 14).

All ptosis patients were awaiting surgical correction of their aponeurotic disinsertion ptosis and were recruited from the oculoplastic service at Moorfields Eye Hospital NHS Foundation Trust. Ptosis patients ranged from age 22 to 84 (mean of 52) years (for a detailed breakdown of causations, see Table 3), and the control range was 25 to 67 years (mean of 41). Seven additional subjects (1 male, 6 females) were not used for primary mathematical modelling, but were used retrospectively to assess for reliability of the derived model.

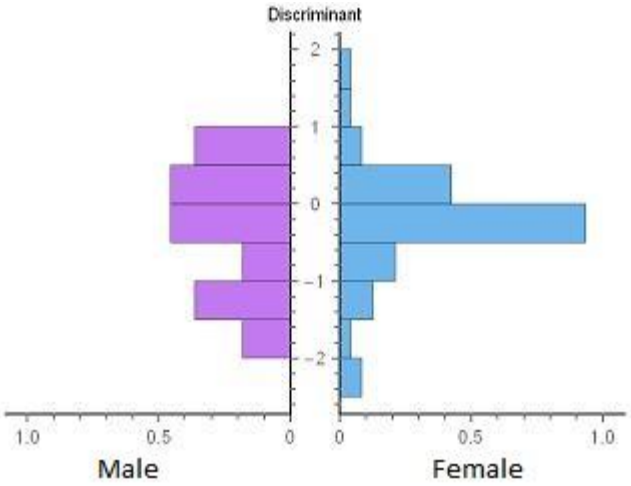

Figure 14.| Comparative histogram of the probability distribution of the discriminant function between genders of the subjects.

4.2.2 Protocols

The present protocol followed the principles described above (section 3.1.1) using high-speed camera imaging to analyse blink dynamics, and will therefore be covered briefly only.

Ptosis patients who agreed to participate in this study had their blinking recorded by a high-speed camera and all participants were briefed before filming, explaining what would be measured and how it would be accomplished. While seated comfortably, subjects were asked to relax, look straight into the high-speed camera and blink as normally as possible after a verbal command. No external devices or any attachments were affixed to the subject's upper eyelids, nor there were any intense light sources focusing on the subject's face.

- There were 18 aponeurotic ptosis:
    - 10 cases of primary surgery for aponeurotic ptosis correction (2 of then due to long standing use of contact lens and 8 was age related involutional ptosis);
    - 8 cases of redo aponeurotic ptosis correction (1 case ptosis induced by cataract surgery in childhood, 1 case of long standing contact lens, 6 cases age related involutional ptosis).
- 2 cases of TED ptosis induced by over correction of previous lowering upper lid surgery (both cases were a redo ptosis correction).
- 1 case of III nerve palsy with aberrant degeneration.
- 2 cases of ptosis in an ophthalmic socket.
- 1 case of VII nerve palsy ptosis
- 1 case related to parathyroidectomy surgery.
- 1 case of Horner syndrome surgically induced following a sympathectomy.

Table 3.|Breakdown of causations of the 26 ptosis patients included in this study.

4.2.3 Data analysis

Data analysis follows the same procedures as outlined in section 3.4. Only the affected eyes were considered in the ptosis patients and both eyes were included in the control group but were not treated as pairs because the diseases in question do not necessarily affect both eyes. The central PA in 71 subjects (26 ptosis patients and 45 controls) were measured in

every frame of the recorded videos manually after horizontal corneal diameter calibration. The measurement started from the moment the upper eyelid began to descend and continued until the initial PA value was recovered, or until the eye ceased to open further. The resulting data was normalised to generate a comparable master curve in order to include patients with a range of PA measurements. Blink duration and peak blink speed were also analysed and compared to the control group. These results are presented in section 4.3.

Ptosis has been indicated as age-dependent (will be discussed in section 4.3.3), therefore this analysis has been carried out in several ways: i) Ptosis group *versus* control group (irrespective of age), data not shown for reasons given in section 4.3.3. ii) Control subjects only – age 40 or over *versus* age below 40 (section 4.3.3). iii) Ptosis group *versus* control group – patients of age 40 or over only (section 4.3.4). The cut-off point for the control group at age 40 was chosen to select the best age-match for our two study groups whilst maximising the sample size: for age ≥40, the mean control age became 51 years (with sample size of 22), compared to a mean age of 52 years for all 26 ptosis patients.

As mentioned in section 3.5 under eye blink modelling, we have recreated the blinking profile using key features of the PA versus time plot. Mathematica was used to characterise the ptotic blink dynamics and to determine if they are different from the control using the Fisher's linear discriminant procedure. It has revealed a fair ability to separate the classes, and showed that ptotic eyelids have much larger variances in the parameters than healthy eyelids – this implying that better results could be expected with a curved (rather than planar) surface separating the classes (Gaussian classifier, section 3.5.1). Another group of subjects was gathered from Moorfields Eye Hospital to act as masked controls in a retrospective test of our model.

4.3 Results and discussion

4.3.1 Palpebral aperture, blink duration and peak blink velocity

The cinematographic PA in this study ranged from 1.15 to 10.45 mm with a mean of 6.90 ± 0.30 mm (standard error of the mean; hereafter abbreviated as SEM in text) in 26 ptosis patients; compared to the range of 6.29 to 12.78 mm with a mean of 9.08 ± 0.15 mm (SEM) of all 45 control subjects. Ptosis patients have a significantly smaller PA (P=0.003; table 1). These measurements were made during the high-speed camera image analysis rather than being real-time measurements on the volunteers. The PA master curve is shown in figure 15 and 16 for controls and ptosis patients.

Total blink durations were calculated from the start of upper eyelid descend until maximum recovery in each isolated blink in ptosis and the control subjects. Only 14/131 eyes did not achieve 100% recovery, of which 3 were from ptosis patients. The incompletely recovered blinks have a mean of 96.8% recovery, ranging from 79.0 to 99.7% across all subjects. Ptosis patients have average blink duration of 560 ± 50 ms (SEM), greater than that of the control group; 530 ± 22 ms (SEM) of the controls. However, while there was a trend for blinking duration in ptosis patients to be greater than controls, the data were not significantly different (p=0.28; t-test). A summary is presented in table 4, together with the peak speed achieved in ptosis and in control patients.

			Blinking dynamics (2 s.f.)		
References	Number of test subjects	Age	Maximum velocity (mm/s)	Palpebral aperture (mm)	Duration (ms)
(Kwon, et al., 2013) Controls	25	25-63	240±9	9.8±0.17	570±25
This study: Controls	20	29-67	290±16	8.2±0.18	490±40
Ptosis	26	22-84	260±14	6.9±0.30 *	560±50
Additional subjects	7	22-77	210±29	7.9±0.51	810±130

Table 4.|Results of upper eyelid blink dynamics from this study and *(Kwon, et al., 2013)*. * indicates significantly different from the control subjects.

Figures 15 and 16 showed how the normalised PA changed over time, with the average speed overlay. They share similar key features such as a rapid decrease in PA and then a slower and distinctively two-stage opening phase – after which they reach approximately 97% recovery, in agreement with (Kwon, et al., 2013). The speed master curve exhibits two parabolic curves; one for the closing phase and the other one for the opening phase. In comparison, ptosis patients have very similar upper eyelid closure acceleration to the control group, with peak speed at near-mid closing and then decelerating until reaching their full closure. However, the initial opening speed (second parabolic speed curve) seems to have diminished in the ptosis patients compared to the controls. Ptosis patients have a mean peak speed of 258.7±13.7 mm/s (SEM), (range 105.5 to 459.5 mm/s) and the control subjects have 260±8.5 mm/s (SEM) (range 128.5 to 482 mm/s), with a significance of 0.79; thus, the null hypothesis of there being no difference between the two peak speed means could not be rejected.

The speed of blink was then considered as two components in each subject: the closing phase and the opening phase (figure 17). During the closing phase, the peak speed in controls ranges from 130 to 480 mm/s (mean 260±9 mm/s; mean±SEM), as compared to the ptosis group, ranging from 110 to 460 mm/s (mean of 254±15 mm/s; mean±SEM). Considering the opening phase as a single entity, the peak speed in the control group ranged from 90 to 260 mm/s (mean of 156±4 mm/s), compared to the ptosis group ranging from 50 to 375 (mean of 160±14 mm/s; mean±SEM); figures were rounded to the nearest integer. These findings might suggest that altered intrinsic LPS muscle function has a role in the development of acquired ptosis, rather than dehiscence of the LPS from the tarsal plate, and might explain the long-observed feature of reduced eyelid excursion in acquired ptosis. However, the above SEM values of the ptosis group were insignificant compared to controls.

Whilst it was expected that the closing phase would always achieve higher speed than the opening phase, a small number of ptosis patients (4/26) achieved a faster upper eyelid opening speed than closing. The reasons for this are unclear, but these data might suggest a more widespread motor dysfunction, extending to orbicularis function, presenting in patients with ptosis.

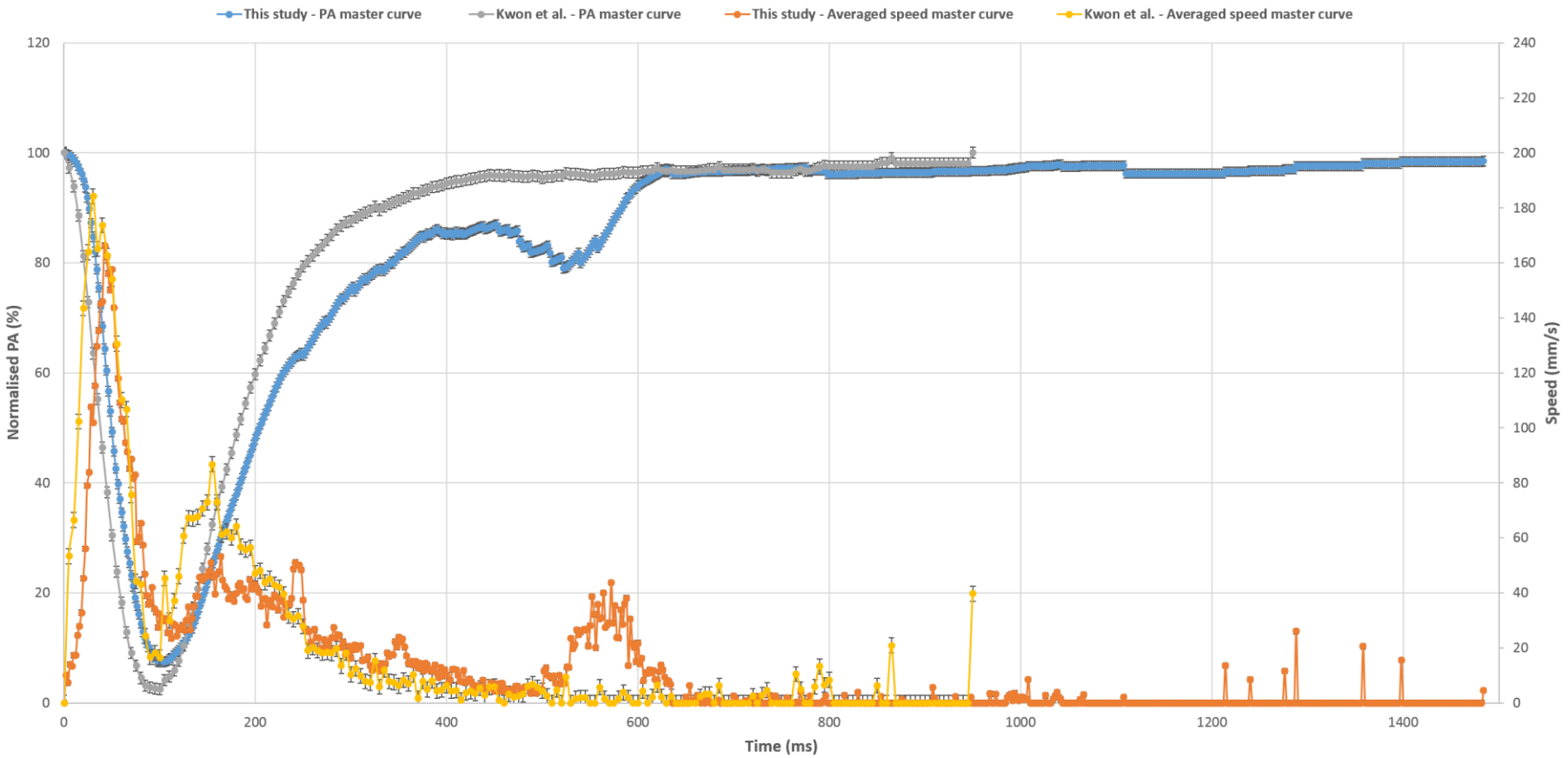

Figure 15.|PA and speed master curves for all controls. Two sets of normal subject's blinking: (Kwon, et al., 2013) PA master curve is shown in grey and its respective speed is shown in yellow. The PA master curve is shown in blue and its respective speed is shown in orange. Secondary axis for the speed master curve is on the right hand side, measured in mm/s. The chart is plotted with mean±SEM.

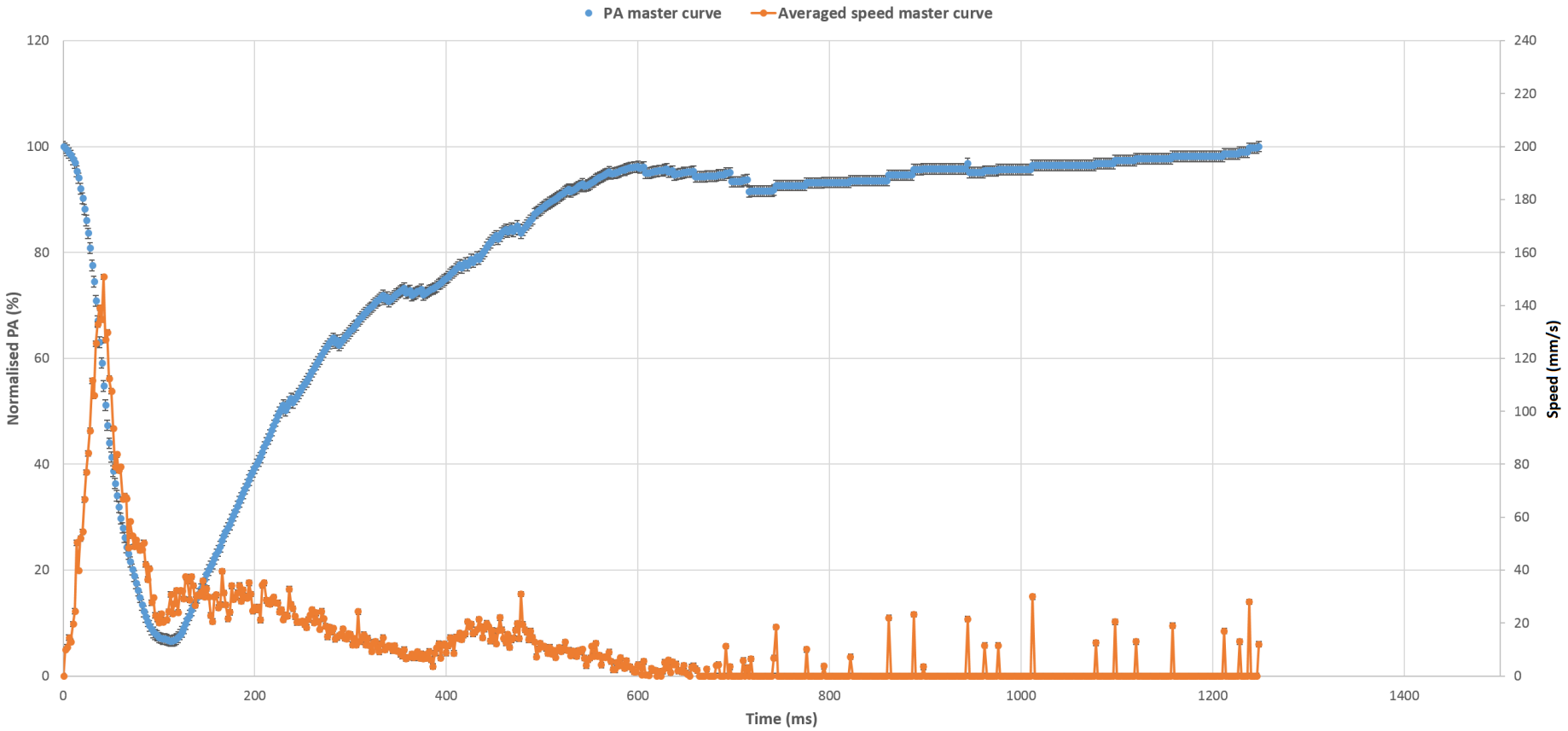

Figure 16.|PA and speed master curves for ptosis patients. PA vs speed master curve for both left and right eyes in ptosis patients. The PA master curve is shown in blue and its respective speed is shown in orange. Secondary axis for the speed master curve is on the right hand side, measured in mm/s. The chart is plotted with mean±SEM.

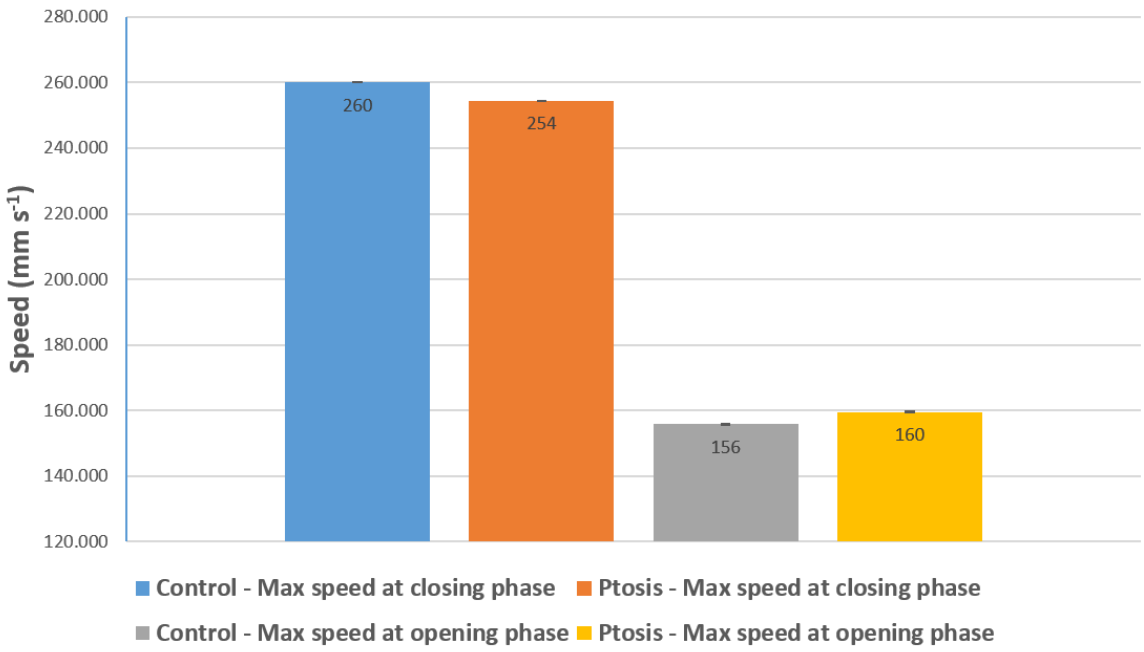

Figure 17. | Maximum speed during opening and closing phases: control vs ptosis (to the nearest integer). The bars represents the averaged maximum speed during different phases of blinking: Blue is control closing compared to orange for ptosis closing; and grey is control opening comparing to yellow for ptosis opening. Error bars are shown as SEM.

4.3.2 Distinctive two-stage recovery

A characteristic two-staged PA recovery was observed in each individual PA *versus* time graph, indicated as 'switch point' in figure 13. The outcome of the Mathematica model was greatly improved after this parameter was introduced, compared to the beta tests without this 'switch point'. One possible explanation for this phenomenon may be the extensive internal connective tissues and the activation of different muscle fibres in the extraocular muscles. The LPS muscle consists of a mixture of muscle fibres with fast-twitch fibres similar to those seen in the global layer of the extraocular muscles and also unique

slow-twitch fibre types. The singly innervated global/slow type accounts for about a third of this layer and has a high mitochondrial content and has a high fatigue resistance. The global/fast type, on the other hand, has a low mitochondrial content with low fatigue-resistance (Porter, et al., 1989). These muscle fibre subtypes work in parallel with different functional properties, and this might explain the distinctive two-staged recovery during the opening phase of a blink. The faster initial opening rate may be caused by a combined effort of MM working together with LPS, whereas the shorter, smaller MM has completed its contraction and cease to help in the later phase. The much slower recovery may be contributed by the LPS muscle alone.

The curved traces of the PA *versus* time graph during the initial closing and the latter opening phase is likely to be due to the muscle architecture. Most muscle fibres are short and do not extend to the tendons (Harrison, et al., 2007). The myofibres in each muscle are concentrated in the mid-section and decrease in density as they approach their insertions, contributing to the nonlinear contraction properties in the PA *versus* time graphs.

4.3.3 The effect of age

It was necessary to explore the possibility that the results of the present study are merely age-related effects rather than a true difference between the controls and the affected eyelids.

All normalised PA *versus* time graphs for the control subjects were plotted with their respective speed plot over-laid. All parameters were calculated and full details are provided

in appendix 1. When the functions were applied to the individual eyelids, in order to have the best fit, some did not start at 100% due to the stepwise fitting of an initial constant PA followed by closing at a speed v_1, the rate at which the upper eyelid descends; an example of the fitting can be seen in figure 13. For example in appendix 1, subject ID 2C4 [left eyelid, LE], 2C33 [LE and right eyelid, RE] did not start at 100%, and it was noted that 63% of these subjects also have incomplete closure.

These data were analysed using LDA and before being separated into their respective age groups (≥40 and <40), there were some major overlaps. However, there was an obvious separation of the two means when divided into two groups (figure 18). Mahalanobis distance (2) was used as the discriminant to measure how many standard deviations a data point is away from the mean of the distribution in a multidimensional space; the closer the distance to the centre of distribution, the more likely it is to belong to that class. The function used to describe this distance is defined as:

$$\sqrt{(x-\mu_c)^T \sigma_c^{-1} (x-\mu_c)} \tag{2}$$

Symbols were defined before in equation (1).

A significantly large separation between the means of the two groups (figure 18) shows that age is a factor in blinking dynamics and that it would be appropriate to conduct further analysis with a group of controls selected to age-match the patients suffering from ptosis.

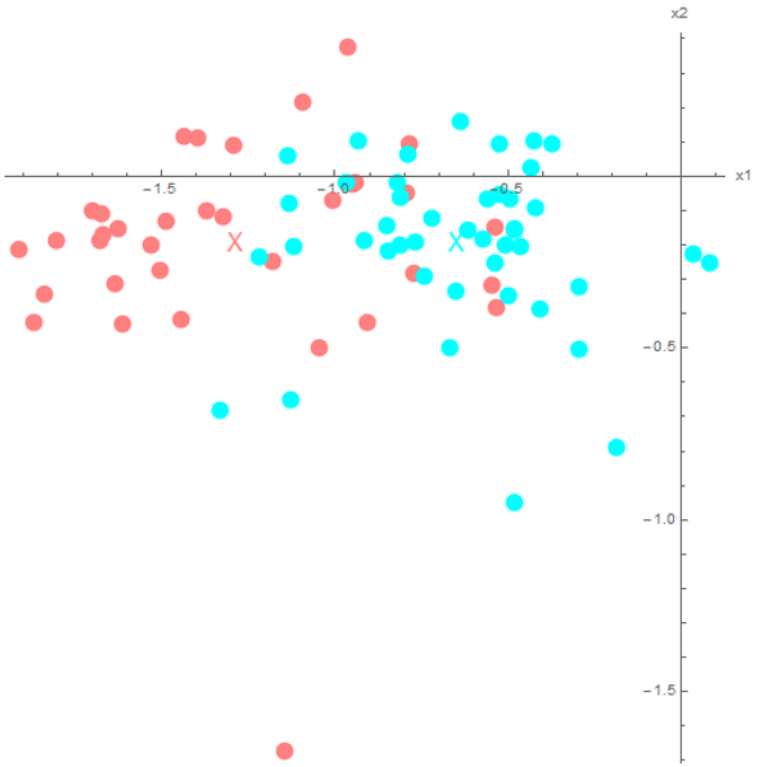

Figure 18. | Blinking discriminant between control subjects of age ≥40 (pink) vs <40 (cyan). This analysis used the 5 parameters mentioned in the text: rate of closure, delay between opening and closing, initial rate of opening, switch point and rate of slow opening. The coloured X is the mean of the respective group. Values on x1 and x2 axes are merely numbers representing the reduced dimension in LDA.

4.3.4 Ptosis versus control

It has been shown that age is a factor in blink dynamics in the previous section (4.3.3) and, to remove this effect in further analysis, we have compared the ptosis group with the control subjects aged ≥40. Using the same parameters as described above, all the PA *versus* time curves were reconstructed for all ptosis patients and the selected control subjects and the key features extracted (figure 19). The value of the minimum is only included if the eye

closure was not complete (because otherwise would be zero). The start and end percentages were not included because they are not really shape parameters (full details are presented in appendix 2).

The three-dimensional display (figure 19) was reduced to generate figure 20. There is a clear difference between the class means, but there are still overlaps in the middle portion. A probability-based discriminant was used to differentiate between the two classes because the data are differently spread in the classes. Therefore a dividing curve that curls around the class that is less widely spread out is better to separate the two of them: a linear discriminant function leading to a planar separation was inadequate in this case.

A slower rate of eye opening in ptosis patients compared to controls, characterised by v_2 was observed and therefore a more quantitative measurement was sought. A histogram was generated for comparison of the v_2 parameter between the ptosis patients (mean of 0.87 with the variance of 0.108), and controls (mean of 1.01 with the variance of 0.057). Figure 21 demonstrates a heavy overlap between the two sets of data but Mann-Whitney tests have revealed a significant difference in the mean at the p=0.005 level. Although this might serve as an indicator for distinguishing ptosis from controls, one must note that this is just one of the features used in the discriminant process and would not be sufficient for diagnostic purposes.

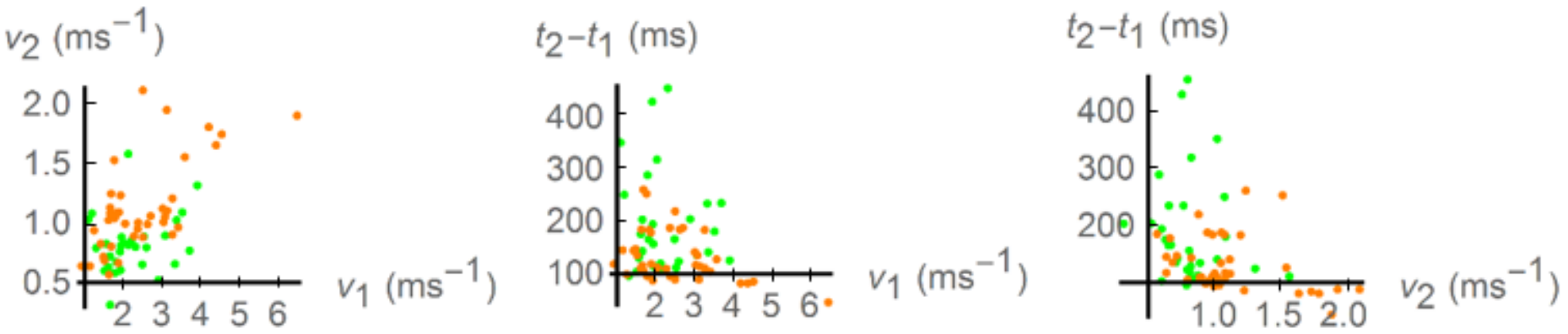

Figure 19. | Three-dimensional discriminant display of the parameter used for ptosis (all ages; green) and controls (≥40year-old; orange). v_1, v_2 t_{open} and t_{close} are defined in text (section 2.5). The value of minimum is neglected as it does not have much significance, as the real value of the minimum is often at a cusp. Also the start and end % were not considered because they are not really shape parameters.

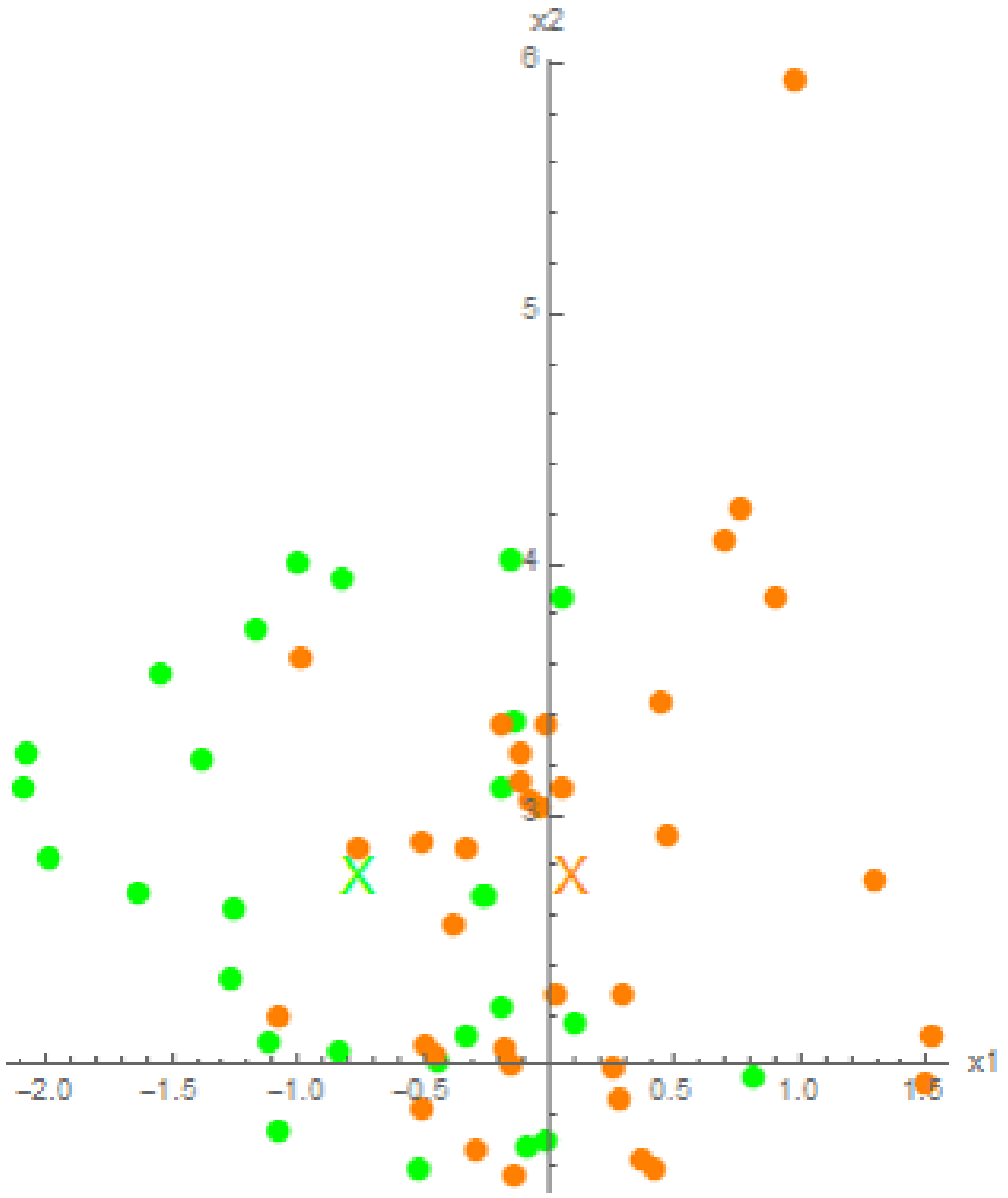

Figure 20. | Ptosis patients (green) vs ≥ age 40 controls (orange) in the reduced dimension of the linear discriminant. Axes x1 and x2 are the first two principal directions in the space of the linear discriminant. The class means are shown as the X marker in its respective colour.

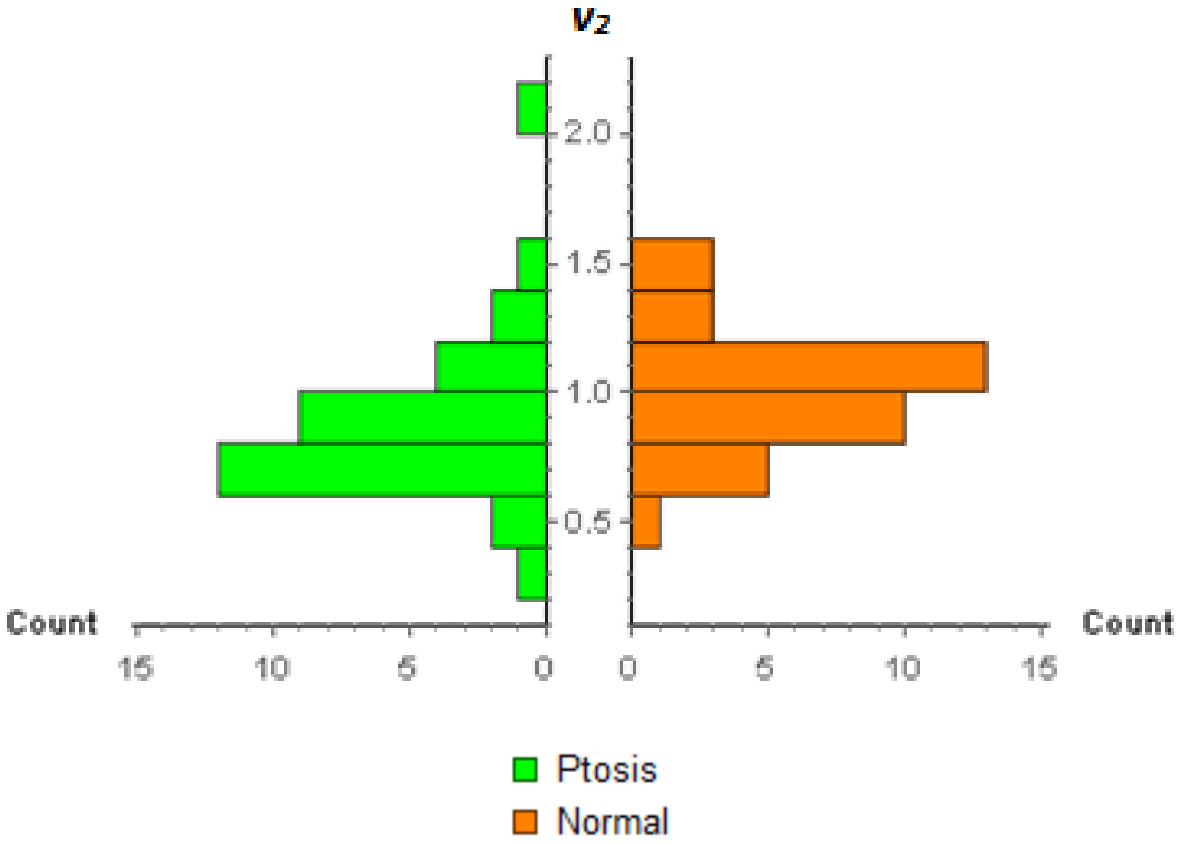

Figure 21.|Comparison of v_2 parameter between ptosis and control patients are displayed on this histogram. It demonstrates a slower rate of opening in the ptosis patients than the controls by a small, but significant amount.

This analysis gives us a model to discriminate ptosis from normal cases and this data-set constituted the 'learning' set of data. The discriminant can be applied to a new set of untested subjects, and hence a further test-set of seven additional subjects was acquired to investigate the robustness of the procedure (table 5).

ID	Probability for normal	Probability for ptosis	Model prediction		Clinical diagnosis
1-19 [LE]	0.10	0.90	Ptosis	√	Ptosis
1-19 [RE]	0.00	1.00	Ptosis	√	Ptosis
1-23 [LE]	1.00	0.00	Normal	X	Ptosis
1-23 [RE]	1.00	0.00	Normal	√	Normal
1-24 [LE]	1.00	0.00	Normal	√	Ophthalmoplegia
1-24 [RE]	0.65	0.35	Normal	√	Ophthalmoplegia, myopathy (worst side)
1-25 [LE]	0.22	0.78	Ptosis	√	Ptosis
1-25 [RE]	0.01	0.99	Ptosis	√	Ptosis
1-37 [LE]	1.00	0.00	Normal	X	Ptosis
1-37 [RE]	1.00	0.00	Normal	√	Normal
1-6 [LE]	1.00	0.00	Normal	√	Normal
1-6 [RE]	1.00	0.00	Normal	X	Traumatic Ptosis
1-7 [LE]	1.00	0.00	Normal	√	Tarsorrhaphy
1-7 [RE]	1.00	0.00	Normal	√	Normal

Table 5.|Probability test for the 7 additional test subjects (in 2 decimal places). This group of subjects has all been assumed to have ptosis for the purpose of this exercise and after applying our model on Mathematica, 4 out of 6 eyes were correctly considered ptotic; 10 cases were considered normal of which, 3 cases were misclassified. Correct prediction from the model was represented by tick marks on the right and misclassification by cross marks.

ID 1-24 [LE] & [RE] and 1-7[RE] in table 5 have been classified as normal and the clinical diagnosis is of ophthalmoplegia and tarsorrhaphy, respectively. The present model was programmed to detect ptosis, and therefore other diseases are likely to be classed as 'normal': this does not mean they are completely healthy. Note ID 1-24 [RE] in table 5 achieved 65%/35% as normal/ptosis, suggesting some abnormality or borderline ptosis. This was understandable as the patient has been diagnosed with myopathy, ocular muscle paralysis,

and this right eye is the worse of the two eyes. Other normal cases (table 5) have been correctly classified as normal, such as ID 1-23 [RE], 1-37[RE], 1-6 [LE] and 1-7 [RE].

4.4 Summary

Resting maximum PAs in ptosis patients were significantly lower than those of controls and ptosis patients also had a greater range of PA (1.15-10.45 mm, compared with 6.29-12.78 mm in controls). The average duration of a single blink in ptosis patients was 560±24 ms (SEM), a small but statistically insignificant increase from the 530±22 ms (SEM) of the controls.

The speed master curve in control subjects exhibits two parabolic curves; one for the closing phase and the other for the opening phase, with the peak speed of 260.0±8.5 mm s^{-1} (SEM). However in ptosis patients, this curvature during the initial opening phase was reduced, demonstrating a much lower rate of recovery during opening phase. The speed curve in the PA versus time plot could also be the combined effect of LPS, MM, frontalis muscle and other accessory muscles. Therefore a reduced rate of opening/ acceleration at the initial opening phase was observed. Peak speeds were found to be 258.7±13.7 mm s^{-1} (SEM), both peak speed and range were very similar between the two groups. Not all subjects achieved higher closing speeds as compared to opening: 4 subjects, all with ptosis, had faster opening of the upper eyelid – all within the first 50 ms after opening phase was initiated.

The analysis in this study showed a significant separation in PA between the control subjects of age ≥40 and those <40. Recognising that age is a factor statistically, the ptosis group was compared with the control with subjects aged ≥40. Using some of the key features of the

blinking profile, PA versus time curves were reconstructed for each subject. A model was generated using these data and was able to discriminate ptosis from a set of data with good accuracy.

An additional seven subjects (14 eyes) were used to test the model's robustness and achieved 11/14 (80%) successful predictions, discriminating ptosis from controls. In one instance, the model failed to diagnose the one case of ptosis caused by trauma, having predicted 0% probability for ptosis for case 1-6 [RE] (table 5). It might also be insensitive to weakness and atrophy of ocular muscles from myopathies or paralysis. With more sophistication this model has the potential to predict specific causations of ptosis with relatively good accuracy. On the other hand the type of blinking captured in the high-speed recordings may be a factor. It is possible that even clinically-diagnosed ptosis patients may have some aspect of blinking dynamics that are comparable to controls. This is an aspect that could be investigated further.

On fitting models, not all PA versus time curves have been matched as tightly as they could be. For example in figure 22, the starting point has been replaced by a kink in a piece-wise linear function, but the original trace has a smoother shape. Similarly some curvature was seen in a small section just before full closure and at the beginning of the opening phase. For future improvements, a function could be designed with extra parameters that could also capture these minute, but possibly significant features. Furthermore, it would be beneficial to add more ptosis and control cases into the learning data set and also introduce the severity of the ptosis as an extra parameter to improve the 'learning' in the present model.

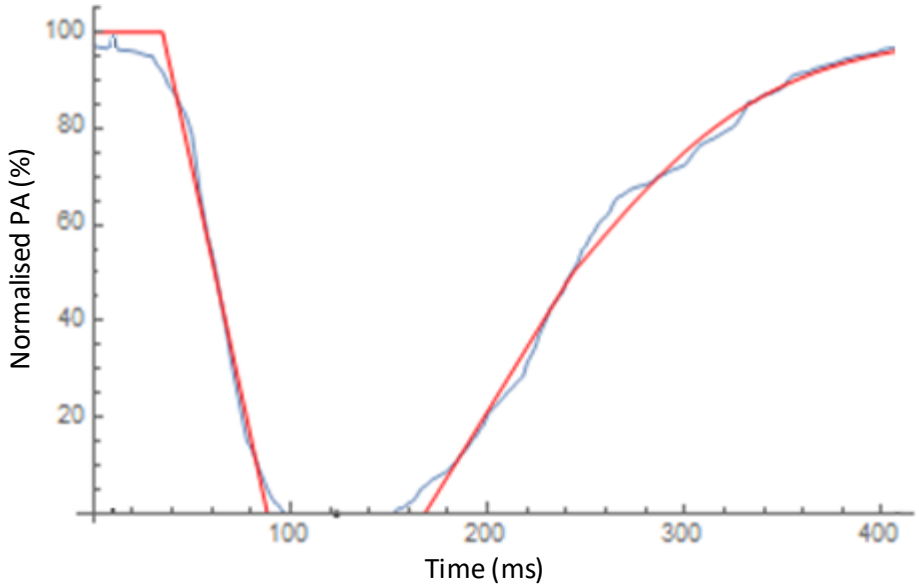

Figure 22.|Fitting of the blinking profile on the PA vs time curve for a control patient. It is clear that the blinking profile is not fitting every detail if we only have linear functions for closure and initial opening. Some of the information is lost after conversion into the fitting function.

CHAPTER 5: CHARACTERISING UPPER EYELID MOVEMENT DISORDERS USING BLINK DYNAMIC ANALYSIS

5.1 Introduction

BEB, TED and aponeurotic blepharoptosis (hereafter abbreviated as ptosis) are all conditions which affect the dynamics of eyelid opening and closure. BEB is characterised by involuntary spasm of the OOM and corresponding inhibition of the LPS muscle. The combined effect increases the blink rate considerably with forceful, exaggerated blinks and often associated with ALO. TED is a manifestation of Graves' disease, it has long been observed to be associated with upper lid retraction, variability of upper lid position, exophthalmos and lagophthalmos, and also abnormalities of LPS function. Aponeurotic ptosis describes a low upper eyelid position, typically associated with a high skin crease and reduced levator function. It is thought that aponeurotic ptosis results from some form of dissociation between the LPS and the lower part of the eyelid with an impaired transmission of mechanical force. Much of these ophthalmic conditions have been covered in depth in chapter 2.

Various diseases can affect the blink rate, speed and duration of closure. It is therefore intriguing to speculate what role altered blink states have in patients suffering from various ocular conditions. This study explores the potential of high-speed camera analysis of blinking dynamics in BEB, TED and ptosis patients compared to healthy volunteers. Generating a predictive model based on statistical methods to separate these diseases from controls may

lead to earlier and more accurate diagnosis for physicians and provide avenues for monitoring and adequate treatment for the patients. We hypothesised that analysis of LPS dynamics in these diseases may identify characteristic patterns of abnormalities which may support diagnosis. This may have clinical relevance in some contexts where diagnosis is unclear, especially in the early stages of the disease: this applies particularly to BEB and TED, where diagnosis is often delayed (Estcourt, et al., 2009; Perros, et al., 2006).

5.2 Methods

The experimental details, protocols and the method of analysis have been described in chapter 3. Informed consents were obtained from all participants. The study adhered to the tenets of the Declaration of Helsinki and received local and regional ethics committee approval (REC: 15/ES/171).

5.2.1 Subject selection

Individuals of oriental Asian origin were not included in this study due to their different eyelid anatomy compared to those of western origin.

Thirteen consecutive BEB (3 males, 10 females), nine consecutive TED (3 males, 6 females) and fifteen consecutive aponeurotic ptosis (6 male, 9 females) patients were recruited. It is noted that the sample size might be small, but as these conditions are not very common in

the general population, as well as hospital visits/ data collection days were limited and can not always accommodate the patient's visits. Therefore these are the number of cases we can work on. Power analysis could be used here to reveal potential sample size significance as dicussed in section 3.1. These patient's blinks were recorded, analysed and compared to 45 healthy volunteers (14 males, 31 females), including the 25 healthy subjects from our previous study (Kwon, et al., 2013).

All patients were recruited from the oculoplastic service at Moorfields Eye Hospital NHS Foundation Trust. BEB patients ranged from age 54 to 83 (median of 69) years; TED patients ranged from age 38 to 66 (median of 55) years; ptosis patients ranged from 21 to 78 (median of 49) years and controls ranged from 25 to 67 (median of 39) years. Demographic data from the control cohort have been mentioned above in chapter 4 and are summarised in table 6 under the Results and Discussion section (5.3.1).

5.2.2 Video capture

Volunteers were seated comfortably in a controlled hospital environment, one at a time, at room temperature (22.6 ± 1.6°C) and standard humidity (28.3 ± 2.2%), with natural light (not directly shining on their faces). A monochrome high-speed camera was set-up in front of the volunteer at eye level. The vertical distance of PA was recorded at 500 fps with full 1024x1024 resolution in 8 bit grey scale. All patients were asked to blink as normally as possible and a verbal command was given before each (voluntary) blink was captured.

5.2.3 Method of analysis

A single (complete) blink was isolated from each patient and the PA was measured manually in each frame: frames were 2 ms apart. Blinks were only analysed if the eyelid margin excursion reached below 50% of the PA during closing phase, and a blink was determined as being complete when the eyelid margin returns to the original PA after closure, as previously described. For the subjects who failed to achieve 100% PA recovery were therefore measured until the maximum percentage recovered. Diseased eyes were considered individually, whereas in control subjects, both eyes were included and analysed but were not treated as pairs.

ImageJ was used to measure the central PA for every frame of the isolated blink. The horizontal corneal diameter was calibrated to a standard of 11.7 mm (Salouti, et al., 2009) for all subjects to standardise the measurements as corneal diameter is the same across all ages and genders beyond full growth at around 1yr after birth (Augusteyn, et al., 2012). The recorded data were normalised to include a range of PA measurements when generating master curves as previously described (chapter 3).

5.2.4 Statistical analysis

Similar to chapter 4, the statistical analysis was carried out using Mathematica to investigate the raw data using Fisher's LDA and Gaussian classifiers, as detailed in section 3.5. Curves describing eyelid excursion as a function of time were generated with key component

features described (see figure 13). Analysis of those key parameters for each patient allowed Mathematica to distinguish and separate each disease's blink dynamics from the dynamics of controls.

Key definitive features of the PA versus time curves have been selected and plotted in three-dimensional space (figure 23). V_1, V_2 and delay between closing and opening phase (t_{open}-t_{close}) have been calculated for each of the disease groups and for the healthy volunteers. Figure 23 showed heavy overlapping and it is therefore difficult to discern to which group a particular set of values belongs. For this reason, in order to best separate and classify them into groups, Fisher's linear discriminant procedure was used to derive the three linear combinations of the original parameters which gave the best separations between the groups. A cross-section of this three-dimensional plot is shown in figure 24. Mahalanobis distance described by function (2) was used to measure the distance of a point from the mean of each class. Using this distance measure, multivariate Gaussian probability distributions centred on the class means were used to determine the most probable classification for each sample.

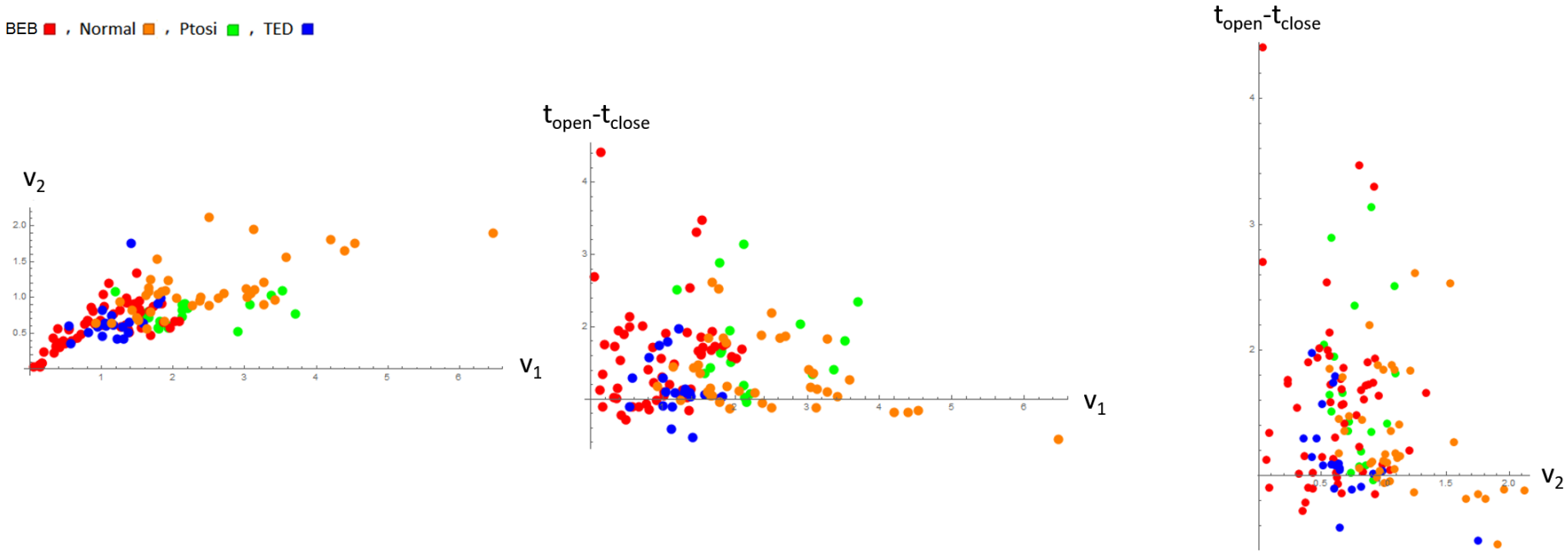

Figure 23.|Two-dimension projections of points representing ptosis (green), BEB (red), TED (blue) and normal (orange) in the 3D space of V_1, V_2, and delay (t_{open}-t_{close}).

The starting percentage, minimum PA and the end PA were ignored because they do not define the shape of the curves.

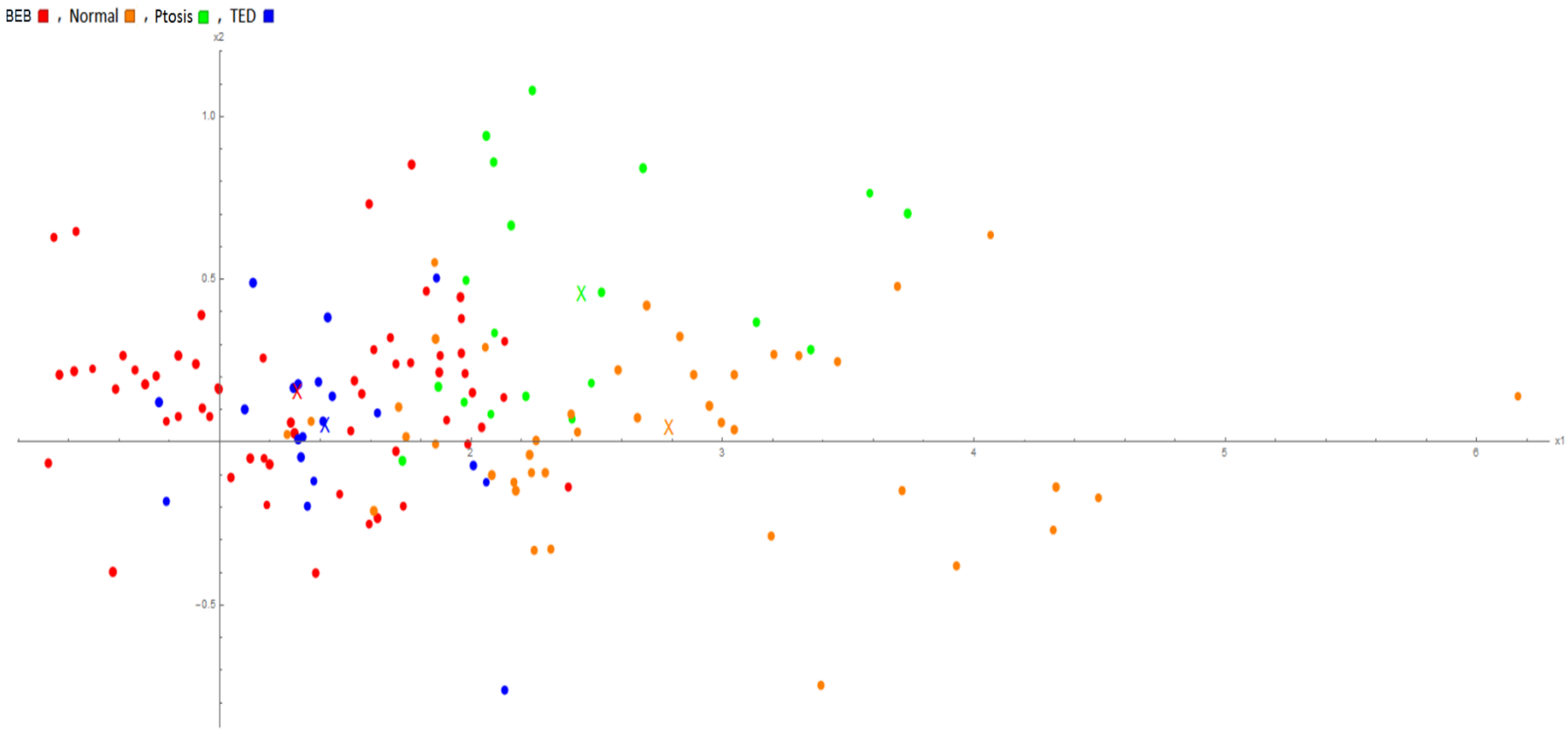

Figure 24.|Linear discriminant analysis: reduced dimensional plot of ptosis, BEB, TED patients and normal volunteers. This analysis used v_1, v_2 and t_{open}-t_{closoe} as the parameters. 'X' represents the mean of the category in its respective colour group. Values on x1 and x2 axes are merely numbers representing the reduced dimension in LDA.

5.3 Results and discussion

5.3.1 Palpebral aperture, blink duration and maximum blink speed

Fifteen patients with aponeurotic ptosis, thirteen BEB and nine TED patients were recruited; their demographics and basic lid parameters summarised in table 6. The PA measurements, defined as the vertical distance between the upper and lower eyelid at the initial open phase, for the different conditions are shown figure 25a. The PA of BEB and TED patients ranged from 4.9 to 11 mm, with a mean of 8.50 ± 0.28 mm (SEM) and 7.2 to 14 mm with a mean of 10 ± 0.43 mm (SEM) respectively. Ptosis patients had a PA of 5.0 to 10.5 mm with a mean of 7.04 ± 0.38 mm (SEM) and controls ranged from 6.3 to 13 mm with a mean of 9.10 ± 0.15 mm (SEM) of all 45 subjects. TED patients have significantly higher PA, whereas ptosis patients have a significantly lower PA than controls (figure 25a).

					Blink dynamics (2s.f.)		
Reference	**No. test subjects**	**Sample size (eyes)**	**Age**	**Age median**	**Max speed (mm/s)**	**Palpebral aperture (mm)**	**Duration (ms)**
Kwon et al., 2013	25	50	25-63	33	240±9	9.8±0.17	570±25
Controls	20	40	29-67	50	290±16	8.2±0.18	490±40
Ptosis	15	19	21-78	49	250±22	7.0±0.38	520±36
BEB	13	26	54-83	69	210±12	8.5±0.28	1008±150
TED	9	18	38-66	55	230±17	10±0.43	670±74

Table 6.|Average measurements for BEB, TED, ptosis and controls in 2s.f.

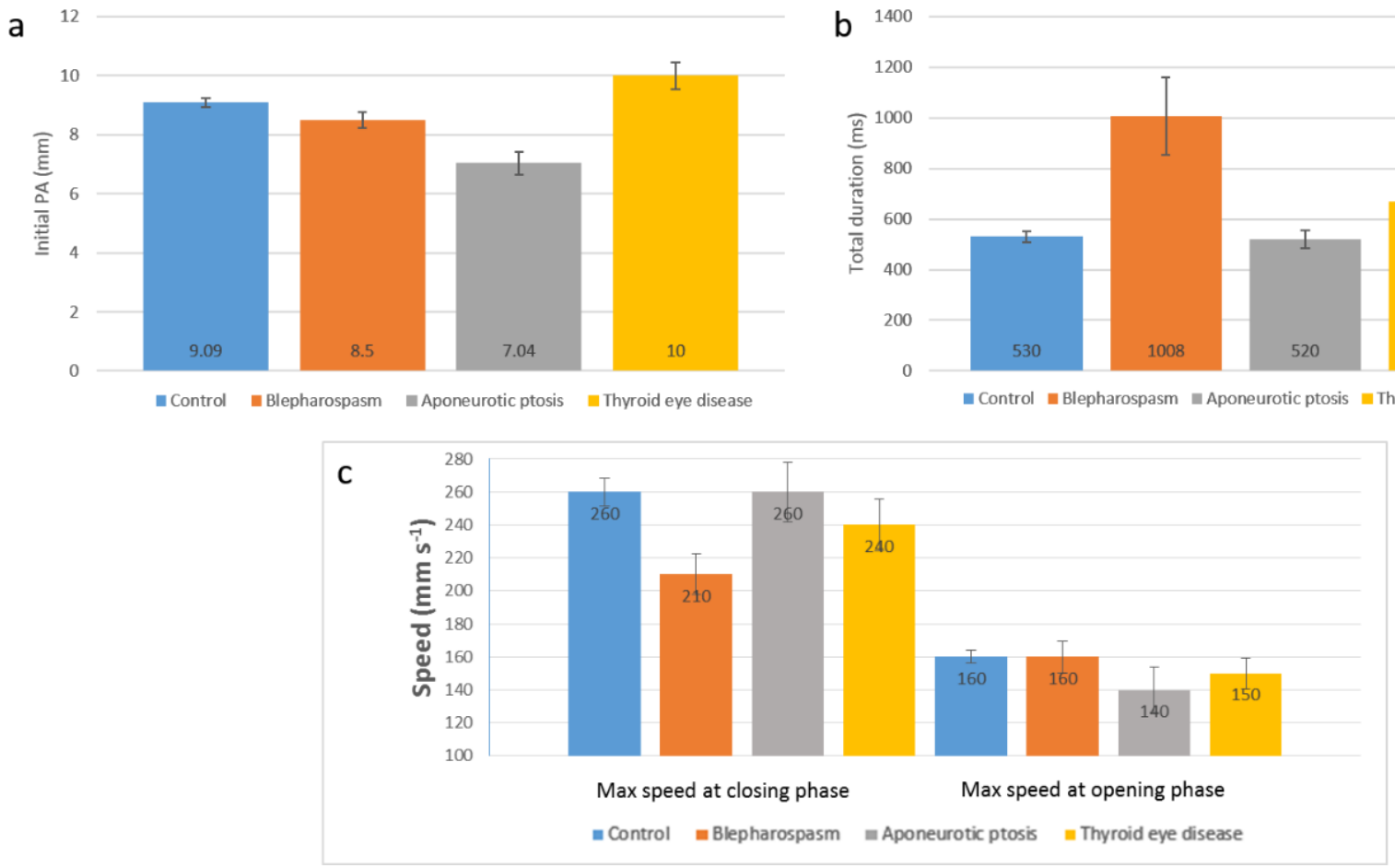

Figure 25.|a. Initial PA of all patients compared to control. b. Total blink duration in BEB, TED and ptosis compared to control. c. Averaged maximum speed of blink for each of the disease category for closing and opening phase. All chats are presented in 2 significant figures and error bars are shown as ± standard error of the mean (SEM).

Blink duration is measured from the start of descent of the upper eyelid to the maximum recovery. There were a total of 16% of eyes which did not achieve 100% recovery, of which there are 4/19 in ptosis, 6/26 in BEB, 3/18 in TED and 11/90 in control. The average incomplete maximum recovery is 98.3%, ranging from 90.1% to 99.9%. The mean blink duration for control, ptosis, BEB and TED are 530±22 ms, 520±36 ms, 1008±150 ms and 670±74 ms respectively (figure 25b).

The speed of blink was analysed in two parts: the closing and the opening phase (figure 25c). During the closing phase, the maximum speed ranged from 130 to 480 mm s^{-1} (mean of 260±8.5 mm s^{-1}) for control; 100 to 380 mm s^{-1} (mean of 210±12 mm s^{-1}) for BEB; 190 to 460 mm s^{-1} (mean of 260±18 mm s^{-1}) for ptosis and 110 to 360 mm s^{-1} (mean of 240±16 mm s^{-1}) for TED patients. Mean maximum opening phase speeds are significantly slower than their mean maximum closing phase counterparts across all subjects (figure 25c). During the opening phase, speeds ranged from 88 to 260 mm s^{-1} (mean of 160±4 mm s^{-1}) for control subjects; 89 to 280 mm s^{-1} (mean of 160±9.6 mm s^{-1}) for BEB; 80 to 340 mm s^{-1} (mean of 140±15 mm s^{-1}) for ptosis and; 87 to 250 mm s^{-1} (mean of 150±9.3 mm s^{-1}) for TED patients (table 7). However, not all individuals have lower speed in opening than closing. 23%, 5.3% and 4.5% of the BEB, ptosis and TED eyes were found to have a higher maximum opening speed than their corresponding maximum closing speed. This phenomenon was not observed in the control group.

	Average maximum speed (2s.f.)	
	Closing phase (mean±SEM)mm s^{-1}	Opening phase (mean±SEM)mm s^{-1}
Control	260 ± 8.5	160 ± 4
Blepharospasm	210 ± 12	160 ± 9.6
Ptosis	260 ± 18	140 ± 14
Thyroid eye disease	240 ± 16	150 ± 9.3

Table 7.| Average maximum speed for all subjects during closing and opening phases.

5.3.2 Comparisons between controls and disease groups

Figure 23 shows projected plots for three variables describing the blink dynamics: rate of closure (v_1), rate of initial opening (v_2) and the delay between closure and opening at 50% (t_{open}-t_{close}) for XYZ axes. These plots demonstrate heavy overlapping of all patient groups in all directions and it is difficult to discern disease states from normal. However, there is a trend of controls achieving higher rate of closure and rate of initial opening compared to the diseased groups. BEB patients demonstrated the lowest rate of closure (v_1), then TED patients and finally the controls and ptosis patients (overlapping considerably); all conditions, including controls, have approximately the same 'delay' duration. These data were analysed using LDA and generated figure 24 after dimensional reduction.

Figure 24 showed great separation in mean between normal versus all the diseases, ptosis versus all other categories, BEB versus ptosis and normal, TED versus ptosis and normal. However, BEB and TED are shown to be close together in the parameter space. Figure 24 also

shows a small variation in the parameters for BEB and an even smaller region for TED compared to ptosis and healthy eyelids.

A probability-based discriminant was used to differentiate between the 4 classes. A predictive model was generated based on the likelihood of any of the collected data being classified as BEB, TED, ptosis or normal (table 8).

By feeding all the BEB patients' data into the model, BEB patients achieved the lowest accuracy of all categories: 54.8%. 29.0% of the incorrect predictions were misclassified into the TED group, and 16.1% of the eyes have been narrowly classified as BEB within the 0.5±0.1 region. Amongst those TED misclassifications, 19.4% of the cases were predicted with 0.8-0.9 confidence to belong to the TED group.

Looking at the normal cases, the same problems as above were encountered, namely that several eyes have been narrowly misclassified, around the 0.5 region as ptosis (i.e. 2C17 [LE] and 2C45 [L/RE]), and in some cases as high as 0.84 ptotic. Furthermore, it is worth noting that there was only one misclassification as BEB within this control group (2C21 [LE], at 0.402). 66.7% of the normal patients have been correctly classified.

Patient type	Patient number[eye]	p(BEB)	p(Normal)	p(Ptosis)	p(TED)	Model prediction	
Bleph	#01[LE]	0.046	0.046	0.012	0.896	Thyroid	
Bleph	#01[RE]	0.502	0.347	0.147	0.004	Bleph	✓
Bleph	#02[LE]	0.192	0.391	0.381	0.036	Normal	
Bleph	#02[RE]	0.254	0.438	0.248	0.059	Normal	
Bleph	#04[LE]	0.930	0.062	0.008	0.000	Bleph	✓
Bleph	#04[RE]	0.209	0.230	0.189	0.372	Thyroid	
Bleph	#12[LE]	0.060	0.328	0.608	0.004	Ptosis	
Bleph	#12[RE]	0.149	0.034	0.014	0.804	Thyroid	
Bleph	#13[LE]	0.953	0.043	0.002	0.002	Bleph	✓
Bleph	#13[RE]	0.931	0.068	0.000	0.000	Bleph	✓
Bleph	#14[LE]	0.119	0.022	0.009	0.850	Thyroid	
Bleph	#14[RE]	0.067	0.006	0.030	0.897	Thyroid	
Bleph	#15[LE]	0.108	0.020	0.006	0.866	Thyroid	
Bleph	#15[RE]	0.053	0.046	0.008	0.893	Thyroid	
Bleph	#26[LE]	0.423	0.061	0.402	0.114	Bleph	✓
Bleph	#26[RE]	0.928	0.038	0.000	0.033	Bleph	✓
Bleph	#27[LE]	0.121	0.877	0.002	0.000	Normal	
Bleph	#27[RE]	0.481	0.447	0.072	0.000	Bleph	✓
Bleph	#28[LE]	0.729	0.193	0.027	0.050	Bleph	✓
Bleph	#28[RE]	0.802	0.146	0.034	0.019	Bleph	✓
Bleph	#30[LE]	0.265	0.307	0.016	0.412	Thyroid	
Bleph	#30[RE]	0.276	0.274	0.037	0.414	Thyroid	
Bleph	#31[LE]	0.720	0.082	0.198	0.000	Bleph	✓
Bleph	#31[RE]	0.725	0.015	0.260	0.000	Bleph	✓
Bleph	#32[LE]	0.313	0.331	0.084	0.271	Normal	
Bleph	#32[RE]	0.476	0.309	0.008	0.207	Bleph	✓
Bleph	#35[LE]	0.935	0.064	0.001	0.000	Bleph	✓
Bleph	#35[RE]	0.945	0.048	0.003	0.004	Bleph	✓
Bleph	#36[LE]	0.554	0.065	0.010	0.371	Bleph	✓
Bleph	#36[RE]	0.616	0.117	0.020	0.247	Bleph	✓
Bleph	#38[LE]	0.949	0.050	0.000	0.001	Bleph	✓
Normal	1C11[LE]	0.001	0.998	0.001	0.000	Normal	✓
Normal	1C11[RE]	0.000	1.000	0.000	0.000	Normal	✓
Normal	1C17[LE]	0.000	1.000	0.000	0.000	Normal	✓
Normal	1C17[RE]	0.000	1.000	0.000	0.000	Normal	✓
Normal	1C3[LE]	0.000	1.000	0.000	0.000	Normal	✓
Normal	1C4[LE]	0.000	1.000	0.000	0.000	Normal	✓
Normal	1C4[RE]	0.000	1.000	0.000	0.000	Normal	✓
Normal	2C11[LE]	0.068	0.440	0.004	0.488	Thyroid	
Normal	2C11[RE]	0.011	0.707	0.281	0.000	Normal	✓
Normal	2C14[LE]	0.000	1.000	0.000	0.000	Normal	✓
Normal	2C14[RE]	0.028	0.969	0.003	0.000	Normal	✓
Normal	2C17[LE]	0.031	0.469	0.470	0.031	Ptosis	
Normal	2C17[RE]	0.064	0.078	0.066	0.792	Thyroid	
Normal	2C19[LE]	0.238	0.607	0.148	0.007	Normal	✓
Normal	2C19[RE]	0.010	0.186	0.804	0.000	Ptosis	
Normal	2C1[LE]	0.000	0.984	0.016	0.000	Normal	✓
Normal	2C1[RE]	0.001	0.904	0.095	0.000	Normal	✓
Normal	2C21[LE]	0.402	0.168	0.269	0.160	Bleph	
Normal	2C21[RE]	0.135	0.217	0.569	0.079	Ptosis	
Normal	2C23[LE]	0.000	1.000	0.000	0.000	Normal	✓
Normal	2C23[RE]	0.001	0.980	0.018	0.000	Normal	✓
Normal	2C25[LE]	0.000	0.824	0.176	0.000	Normal	✓
Normal	2C25[RE]	0.000	0.656	0.344	0.000	Normal	✓
Normal	2C27[LE]	0.183	0.725	0.089	0.003	Normal	✓
Normal	2C27[RE]	0.126	0.619	0.117	0.138	Normal	✓
Normal	2C29[LE]	0.182	0.725	0.066	0.026	Normal	✓
Normal	2C29[RE]	0.233	0.585	0.149	0.033	Normal	✓
Normal	2C31[LE]	0.000	0.672	0.328	0.000	Normal	✓
Normal	2C33[LE]	0.142	0.725	0.132	0.001	Normal	✓
Normal	2C33[RE]	0.058	0.687	0.254	0.001	Normal	✓
Normal	2C39[LE]	0.334	0.655	0.010	0.000	Normal	✓
Normal	2C39[RE]	0.020	0.980	0.000	0.000	Normal	✓
Normal	2C43[LE]	0.125	0.087	0.071	0.717	Thyroid	
Normal	2C43[RE]	0.087	0.000	0.842	0.071	Ptosis	
Normal	2C45[LE]	0.009	0.420	0.571	0.000	Ptosis	
Normal	2C45[RE]	0.031	0.374	0.594	0.000	Ptosis	
Normal	2C4[LE]	0.034	0.025	0.008	0.933	Thyroid	
Normal	2C4[RE]	0.398	0.087	0.036	0.480	Thyroid	
Normal	2C6[LE]	0.109	0.037	0.017	0.837	Thyroid	
Normal	2C6[RE]	0.118	0.077	0.077	0.729	Thyroid	
Normal	2C7[LE]	0.000	0.902	0.098	0.000	Normal	✓
Normal	2C7[RE]	0.011	0.645	0.344	0.000	Normal	✓

Ptosis	#19[LE]	0.101	0.025	0.864	0.010	Ptosis	✓
Ptosis	#19[RE]	0.002	0.000	0.998	0.000	Ptosis	✓
Ptosis	2-13[RE]	0.000	0.028	0.972	0.000	Ptosis	✓
Ptosis	2-14[LE]	0.000	0.000	1.000	0.000	Ptosis	✓
Ptosis	2-24[LE]	0.000	0.028	0.972	0.000	Ptosis	✓
Ptosis	#23[LE]	0.241	0.275	0.365	0.119	Ptosis	✓
Ptosis	2-3[LE]	0.066	0.393	0.487	0.054	Ptosis	✓
Ptosis	2-40[LE]	0.244	0.265	0.259	0.232	Normal	
Ptosis	2-40[RE]	0.003	0.000	0.997	0.000	Ptosis	✓
Ptosis	2-47[LE]	0.401	0.562	0.037	0.000	Normal	
Ptosis	2-49[RE]	0.000	0.638	0.362	0.000	Normal	
Ptosis	2-55[RE]	0.017	0.596	0.387	0.000	Normal	
Ptosis	2-5[LE]	0.154	0.023	0.824	0.000	Ptosis	✓
Ptosis	2-5[RE]	0.310	0.091	0.599	0.000	Ptosis	✓
Ptosis	2-65[RE]	0.132	0.370	0.470	0.028	Ptosis	✓
Ptosis	2-6[LE]	0.000	0.043	0.957	0.000	Ptosis	✓
Ptosis	2-6[RE]	0.000	0.371	0.629	0.000	Ptosis	✓
Ptosis	#37[LE]	0.039	0.511	0.433	0.017	Normal	
Ptosis	3P2v[LE]	0.067	0.614	0.314	0.004	Normal	
Thyroid	#08[LE]	0.043	0.013	0.005	0.938	Thyroid	✓
Thyroid	#08[RE]	0.128	0.035	0.003	0.834	Thyroid	✓
Thyroid	#09[LE]	0.048	0.017	0.008	0.926	Thyroid	✓
Thyroid	#09[RE]	0.071	0.020	0.009	0.900	Thyroid	✓
Thyroid	#10[LE]	0.337	0.066	0.019	0.577	Thyroid	✓
Thyroid	#10[RE]	0.528	0.000	0.317	0.154	Bleph	
Thyroid	#16[LE]	0.078	0.040	0.005	0.878	Thyroid	✓
Thyroid	#16[RE]	0.041	0.019	0.007	0.933	Thyroid	✓
Thyroid	#17[LE]	0.074	0.141	0.076	0.709	Thyroid	✓
Thyroid	#17[RE]	0.094	0.226	0.063	0.616	Thyroid	✓
Thyroid	#20[LE]	0.096	0.000	0.827	0.077	Ptosis	
Thyroid	#20[RE]	0.204	0.105	0.075	0.617	Thyroid	✓
Thyroid	#34[LE]	0.000	0.001	0.000	0.998	Thyroid	✓
Thyroid	#34[RE]	0.224	0.025	0.027	0.724	Thyroid	✓
Thyroid	New #18[LE]	0.150	0.019	0.000	0.831	Thyroid	✓
Thyroid	New #18[RE]	0.125	0.030	0.004	0.841	Thyroid	✓
Thyroid	New #21[LE]	0.411	0.084	0.037	0.468	Thyroid	✓
Thyroid	New #21[RE]	0.355	0.081	0.049	0.515	Thyroid	✓

Table 8.| Mathematica generated predictive model based on probability of BEB, normal, ptosis and TED. The 'Patient type' column displays official clinical diagnosis of the volunteer and the tick marks under the 'model prediction' column represent a correct prediction of this model according to the probability found in the middle section (BEB/ Normal/ Ptosis/ TED columns). The values are the probability of such patient belonging to that class and the value 1 means 100% probability and 0 means 0% probability belonging to that class. The values of each row under BEB, Normal, Ptosis and TED add up to 1.

Moving on to TED patients, this was found to be the most consistently identified group with 11 out of 18 patients at greater than 0.7 accuracy. 88.9% of the predictions were correct and there were only two misclassifications. The confidence levels of those predictions were relatively high (i.e. #10 [RE] was predicted 0.53 BEB and #20 [LE] was predicted 0.83 ptosis).

Last but not least the analysis achieved 68.4% success rate in correctly categorising ptosis into its respective group. All of the misclassifications were misclassified as controls at around the 0.5 region apart from case #2-40 [LE], for which the model was unsure amongst BEB, control or ptosis (0.24, 0.27 and 0.26 respectively, and 2-47 [LE] with 0.40 BEB & 0.56 normal). Again there were zero BEB misclassifications (as well as TED), suggesting that BEB is a very niche condition. It could well mean that the BEB malfunction is completely unrelated to ptosis. It is also clearly separated from the controls.

5.3.2a Three-dimension representation for all classes

Five variables were considered in this exercise, which are v_1, v_2, t_{open}-t_{close} (delay), t_4-t_{open}, and α. There are a total of ten different combinations of three variables (5!/(3! 2!)) and they are all shown in figure 26 for each of the classes. The regions of the parameter space containing each class are represented by the space occupied by the mesh network within the cubic space. BEB appears to be occupying a small but distinct region in all the ten combinations.

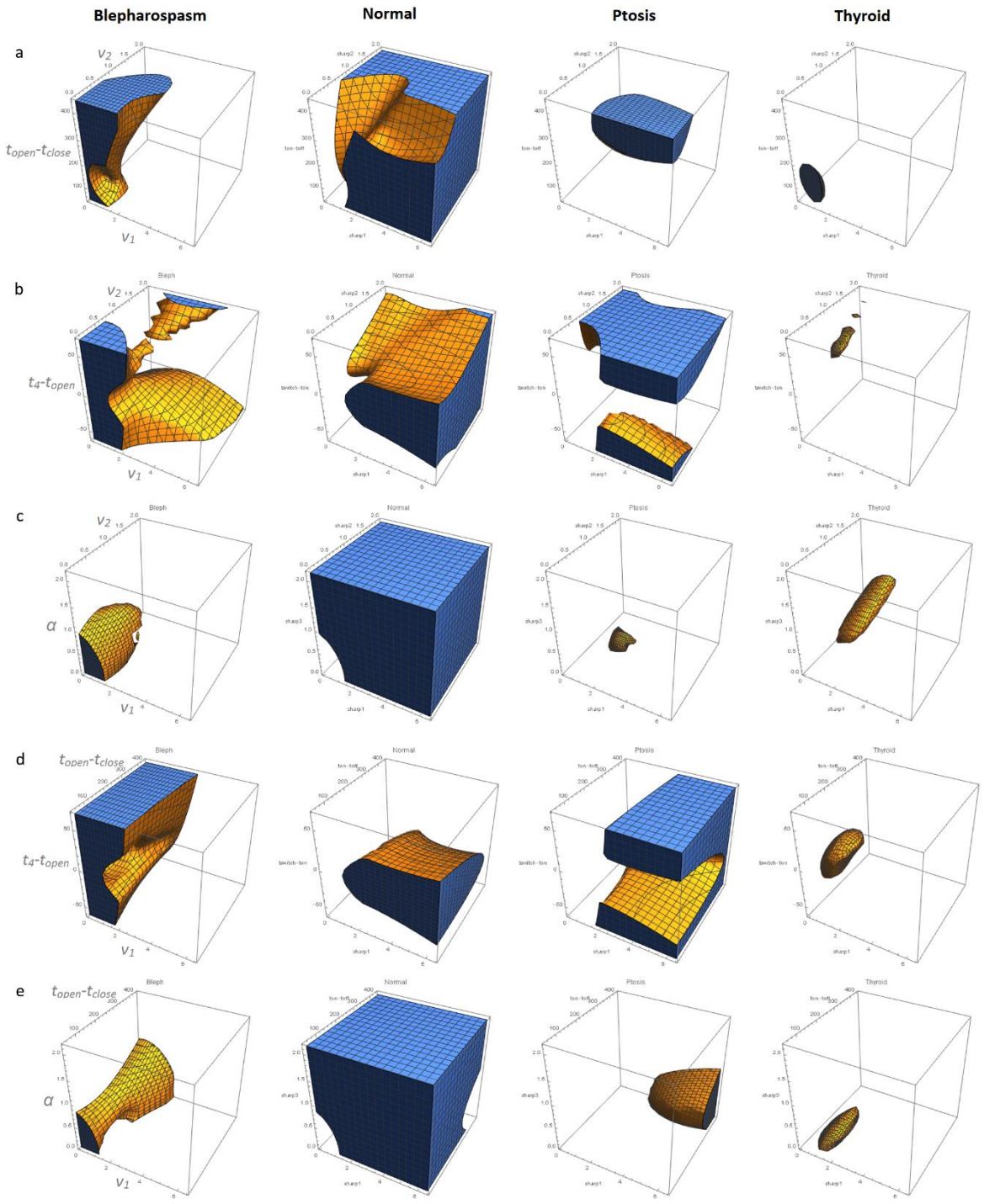
Blepharospasm
Normal
Ptosis
Thyroid
a
b
c
d
e
v_2
v_1
t_{open}-t_{close}
t_4-t_{open}
α
Bleph
Normal
Ptosis
Thyroid

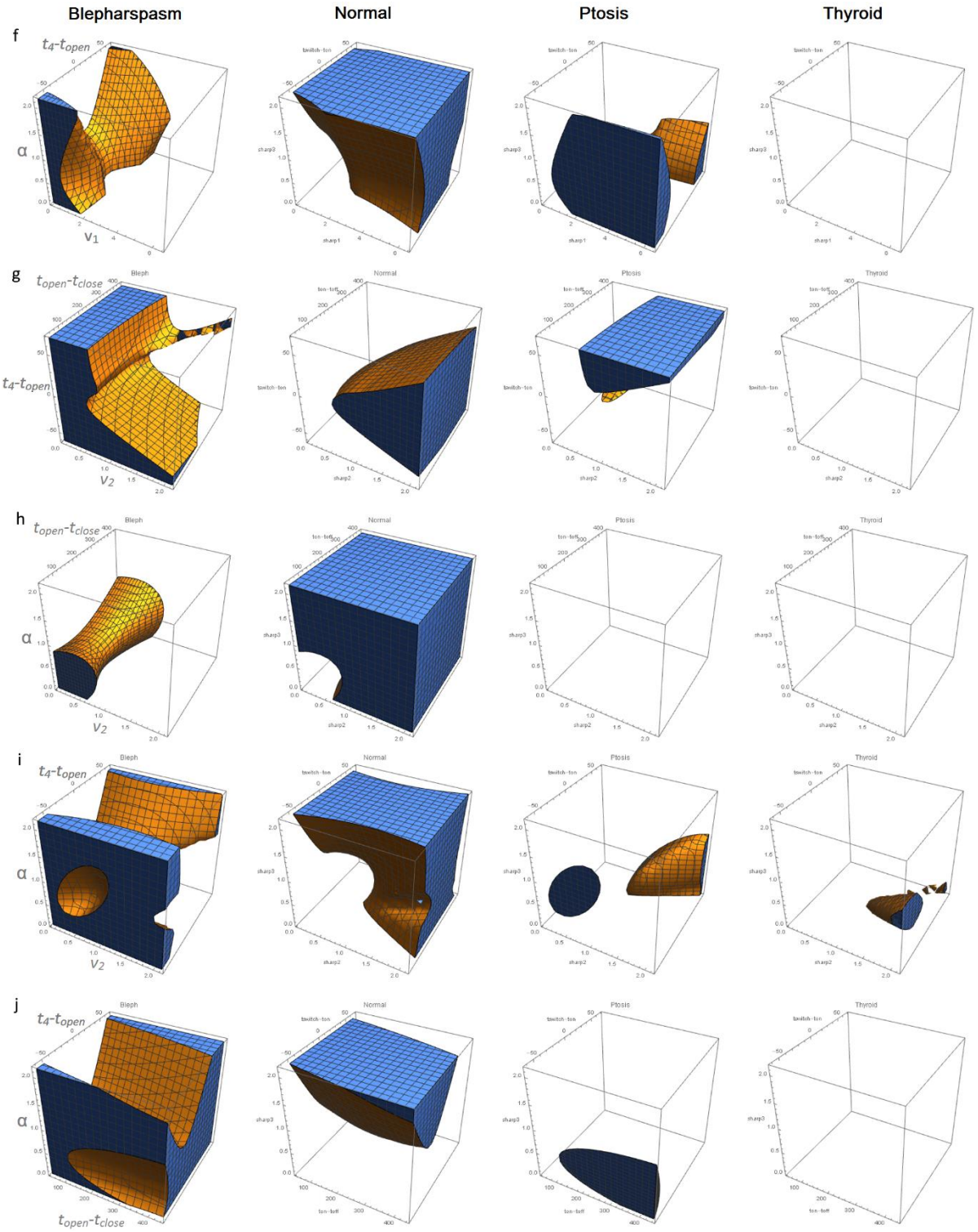

Figure 26.| a-j 3-dimensional representation of the model fitting parameters. The 3-dimensional mesh structures within the cubic space represents the probability of each class: BEB (blepharspasm), normal, ptosis and TED (thyroid). The columns show the space allocated for each class, and the rows a-j represent a different 3-dimensional projection from the 5-dimensional space. There are 10 rows because (5!/(3! 2!))=10. X, Y and Z axis labels remain the same for each row (graphics generated by Prof. Anthony Harker, whose permission has been obtained).

5.4 Future development

During the image analysis, it was noted that some patients exhibited multiple incomplete closures before reaching the closed state. Since the initial PA was not recovered after these incomplete closures, it was accounted as a single blink only when full initial PA recovery was achieved after a full closure. Due to this phenomenon, extra care was taken when constructing the predictive model; two methods of analysis were trialled and tested.

Method one was to focus the analysis at the initiation and the dynamics of the final closure, following the key feature (V_1) we extracted to form a model blink. Method two was to account every single peak and trough, thus including any partial closure and recovery phases within that single blink, therefore in the final summary the probabilities have been averaged for each eye. Both methods were tested and the accuracy for each is summarised in table 9.

	BEB (%)	Normal (%)	TED (%)	Ptosis (%)
Method 1 (initial & final)	45.2	69.1	66.7	68.4
Method 2 (peaks & troughs)	54.8	66.7	88.9	68.4

Table 9.|Model accuracy for each of the conditions by the different approaches to analyse the data. Results were displayed with 1 decimal place.

By accounting for all closures and opening phases, method two demonstrates an improved success rate compared to only considering the initial closure and final recovery (62.33% overall accuracy, a 7.37% drop from 69.7% of method two).

When looking at table 8, it is evident that diseased patients can sometimes exhibit normal blinking dynamics (e.g. one normal blink in five blinks), with the exception of TED group (majority were predicted as TED with one misclassification of ptosis #20[LE] and BEB #10[RE]). It is possible that the higher accuracy achieved in method two is due to not skipping the analysis of any defective blink dynamics. It therefore suggests that the more rules are applied in selecting a blink from the patient initially during the high-speed camera recording, the more accurate the result could be. It is possible that multiple blinks and single blinks of the same category will provide a more specific diagnosis, and focusing on one type at a time may allow substantial improvement on the predictive model.

On another note, the three-dimensional plot (figure 26) revealed a very small region for TED patients: this might due to an inadequate number of patients. Increasing the number of patients in all diseased categories in the learning-set data will clarify whether those small regions of parameter space are truly representative, and will improve the results and accuracy.

5.4 Summary

The resting maximum PA in TED patients was found to be significantly larger than that of controls (10 ± 0.43 mm compared with 9.09 ± 0.15 mm of controls), and ptosis patients have significantly lower resting maximum PA (7.04 ± 0.39 mm). Single blink durations were calculated for BEB, TED, ptosis and control patients and revealed an increase for BEB and TED but not ptosis patients compared to the controls. 16% of subjects did not achieve full recovery

(including controls), but the average incomplete maximum recovery was found to be 98.3%, ranging from 90.1- 99.9%.

The maximum speed of blink was analysed in two phases. During the closing phase, all conditions were comparable to controls, however the BEB patients were significantly slower (with the mean of 210 ± 12 mms^{-1} against the control 260 ± 8.5 mms^{-1}; p=0.002). This indicates that OOM function across TED and ptosis are comparable to normal. However, the reasons for slower OOM function in blepharospasm are unclear, but this suggests that although BEB causes excessive blinking, the physiology of the closure process is likely to be different from the normal blink circuitry, in terms of LPS-OOM coordination. During the opening phase, BEB, TED and control patients were very similar. However, although not significant, ptosis appears to be slightly slower compared to controls (140 ± 15 mm s^{-1} and 160 ± 4 mm s^{-1}, respectively; p=0.288). This suggestion of impaired velocity-related function of LPS in aponeurotic ptosis cases may offer new insights into the pathophysiology of this common form of ptosis. It is commonly observed that aponeurotic ptosis is associated with impaired levator function (excursion). However, these novel findings of attenuated LPS maximum velocity may suggest that this form of ptosis may be due to an inherent levator myopathy rather than a simple muscular dehiscence, although further studies with larger numbers of patients would be required to determine if this effect is significant.

By analysing all the closure and opening phases of the blinks from the learning-set of data, a more accurate model was generated. BEB has achieved 54.8% predictive accuracy in this model, whereas TED, ptosis and normal have achieved 88.9%, 68.4% and 66.7% respectively. BEB group has the lowest of all accuracy of 54.8%, and 29% of those misclassifications were identified as TED, with majority of the predictions as high as 0.8-0.9. Such high confidence combined with a high rate of misclassification suggests that BEB shares some similarities in

blinking dynamics with TED patients, particularly during the opening phase, which is primarily levator function.

Having established that the TED class has the highest accuracy in the model, it was also the most consistent class with the majority at over 0.7 for each learning-set patients. Furthermore, it has only two misclassifications: #10 [RE] at 0.53 for BEB and #20 [LE] at 0.83 ptosis. These results could suggest that these patients are also displaying the predicted condition's blink dynamics.

Normal and ptosis class success rates are very similar at 66.7% and 68.4% respectively. When assessing the normal class, some misclassifications were in the 0.8 regions. Although this is likely to represent limitations in the model, it is also possible that these misclassified patients may have a subclinical ptosis or dermatochalasis (both age-related) which could become apparent in the future and further assessments of these patients would be of interest. It was also noted that only one BEB misclassification was found at a low percentage prediction. Surprisingly, all ptosis misclassifications were controls and share similar predictions with ptosis, thus suggesting that the blink dynamics of ptosis and controls are largely similar. It is likely that a good separation for BEB from ptosis and TED has been established due to the low number of misclassifications found in the learning-data (ptosis and TED, table 8). The next step will be to increase the patient pool substantially for the learning-set of the model to be more accurate.

In conclusion, these data have demonstrated that a detailed analysis of blink dynamics has identified novel characteristics of LPS and OOM function in a variety of disorders affecting the movement of the upper eyelid, as well as describing the clinical phenotype of these conditions. These observations may also yield further understanding of the underlying pathogenesis of

these conditions. In addition, the modelling which has been demonstrated to discriminate between different conditions may have the potential of use as an additional diagnostic tool, or to monitor clinical progress and outcomes for treatment.

CHAPTER 6: EFFECTS OF BLEPHAROPLASTY SURGERY ON DERMATOCHALASIS PATIENTS – BLINK DYNAMIC COMPARISONS BETWEEN PRE-, POST-OPERATION AND AGE MATCHED CONTROLS USING HIGH-SPEED CAMERA

6.1 Introduction

In chapter 5, it was suspected that some of the misclassified normal class subjects may have subclinical ptosis, displaying probability as high as 0.8 in some cases (table 8). Having a similar phenotype to ptosis, dermatochalasis is also thought to be related to the human aging process (Jacobs, et al., 2014; Guinot, et al., 2002; Tenzel, et al., 1978). It is characterised by the loss of connective tissues and reduced elasticity of the upper eyelid skin, creating a 'hooding' effect in which the excess skin rests on the eyelashes. However the upper eyelid margin in ptosis is reduced, whereas in dermatochalasis the eyelid margin might still be at a normal height. More details of the condition, treatment and its management were covered in chapter 2.3.4. Although not sight-threatening, dermatochalasis is also a cosmetic concern for many. Along with weakened LPS, MM, decreased elasticity in the superior transverse ligament, palpebral ligament and dehiscence of the LA found in aging (Evinger, et al., 1991), skin redundancy and excess periorbital tissues could also induce additional burden to the upper eyelid and therefore affect the blink dynamics (Sun, et al., 1997).

This chapter investigates the blinking dynamics of patients suffering from dermatochalasis before and after blepharoplasty corrective surgery compared to a control group. A predictive model based on Fisher's LDA and multivariate Gaussian probability distributions was developed to separate pre-operation, post-operation and controls. This technique could give us more insight into how successful blepharoplasty surgery is in restoring dermatochalasis patients to normal eye performance by assessing it numerically; a novel approach which could complement visual assessment.

6.2 Methods

Informed consent was obtained from all participants. The study adhered to the tenets of the Declaration of Helsinki and received local and regional ethics committee approval.

6.2.1 Subject Selection

Seven dermatochalasis patients with age ranges from 52-78 (median age, 69, 1 male) and seven healthy controls with age ranges from 50-62 (median age, 53, 2 male) were included in the present work.

Control subjects were selected based on a two-stage process. First, they should not have been clinically diagnosed for dermatochalasis; second, all videos were reviewed to exclude any dermatochalasis-like and ptosis-like volunteers; this included abnormal lowering of the upper

eyelid margin and excessive loose upper eyelid skin resting on lashes with saggy appearances. This selection process is essential because dermatochalasis is not uncommon in the self-reported general public and many may live with it without knowledge until an advanced stage where the sagging upper eyelid becomes a problem in daily life. It is widely known that aging is one of the major risk factors in dermatochalasis, so the age range of the control group was narrowed to 50-80 years, compared to the dermatochalasis age of 52-78 years.

A cadaver dissection, histopathological and magnetic resonance imaging study has revealed that oriental Asians have lower or even absent upper eyelid creases and more subcutaneous and suborbicularis fat, with a pretarsal fat component than Caucasians (Jeong, et al., 1999). This is partly caused by the protrusion of the pre-aponeurotic fat pad and a thick subcutaneous fat layer that prevent the LPS muscle fibres from extending towards the superior tarsal border near the skin, and the LPS aponeurosis inserts lower down into the OOM and into the upper eyelid skin nearer to the eyelid margin in Asians (Jeong, et al., 1999; Le, et al., 2002). We have therefore decided to not include subjects of oriental Asian ethnicity in this study.

All dermatochalasis patients in this study have been screened before and after surgery, and were recruited from the oculoplastic service at MEH NHS Foundation trust.

6.2.2 Instrumentation

The present protocol followed the previously described principles introduced for analysis of blink dynamics using high-speed camera images (Kwon, et al., 2013; Mak, et al., 2016). A brief description will be provided here, but please see chapter 3 for more details.

A monochrome Photron Ultima APX12K high-speed camera was set up in front of the seated subject and their voluntary blinking (under verbal command) was captured at 500 fps. All subjects were recorded one at a time in a controlled hospital environment, with stable room temperature and humidity, with natural light from a tangent.

6.2.3 Method of analysis

ImageJ software was used to measure the recorded voluntary blinks. One complete blink was selected from each video clip and analysed frame by frame (frames being 2 ms apart) for the full duration of the blink cycle. A complete blink is defined here with the following specifications:

- Begins at the commencement of downward motion of the upper eyelid margin from the normal resting PA (initial closure);
- Reaches zero (full closure) or nearest zero PA (at least reaches below 50% of initial PA);
- Complete or nearest complete recovery from the initial PA (full recovery);
- Minimum number of downward motions by the upper eyelid.

The central PA was manually measured from each frame with horizontal corneal diameter calibrated to 11.7 mm for all subjects (Salouti, et al., 2009). This enables each image to be measured in the same scale, and nullifies the varied distances of subjects from the camera.

All patients had bilateral blepharoplasty and therefore all eyes were analysed as well as the controls. Moreover, blink duration and maximum blink speed were analysed and compared before and after the blepharoplasty procedure, and with controls.

6.2.4 Statistical tests

Raw data from ImageJ were normalised to generate the master curves for PA. The mean blink duration for each class was computed and the speed was calculated by one-sided finite difference approximation (the magnitude from the upper lid excursion between each frame of 2 ms).

The raw data were also imported into Mathematica for further mathematical computation, data analysis and modelling. The blinking PA profile was recreated using key features seen on the PA *versus* time plot and broken down into different parameters to fit a function that best represents these features (figure 13). These parameters include:

1. Initial percentage opening
2. Time offset for closing
3. Minimum opening
4. Rapidity of closing
5. Time offset for opening

6. Rapidity of opening
7. Time offset for slow opening
8. Rapidity of slow opening
9. Final percentage open
10. Root mean square deviation (RMSD) of measured from fit from half-open to first occurrence of maximum opening.

RMSD was included in the list of parameters because many of the pre-dermatochalasis operation blink profiles are rather spasmodic and almost step-by-step in the later opening phase. The equation (3) below provided a representation of the difference between such a spasmodic behaviour and a smooth opening profile.

$$RMSD = \sqrt{\frac{1}{N}\sum(\hat{y}_i - y)^2}$$

(3) Root mean square deviation. Where $\hat{y}_i$ is the observed value, y is the predicted value and *N* is the number of samples.

A three-class discriminant analysis based on Fisher's LDA and probability-based Gaussian classifiers was carried out for pre-operation, post-operation and controls to derive the best separations between these classes. Code and functions used in this modelling were described in chapter 3.5.1.

6.3 Results and discussion

6.3.1 Palpebral aperture, blink duration and maximum blink speed

A PA master curve for each class of subjects was generated. Figure 27 shows the normalised, mean PA plotted against time over a voluntary blink. The orange trace is the control group, green is the pre-operation and the red is the post-operation group. It is worth noting that only 3 recorded blinks in the control group have failed to achieve full closure, all eyes from pre- and post-operation group achieved full closure.

The initial PA for controls ranged from 6.6-9.6 mm, with a mean of 7.8±0.23 mm (SEM). The PA for patients with dermatochalasis (before blepharoplasty surgery) ranged from 6.3-9.4 mm, with a mean of 7.8±0.32 (SEM). For patients post-surgery the PA range was 6.2-11 mm, with a mean of 8.7±0.37 (SEM). All data are presented to 2 significant figures and the results are displayed on figure 28a.

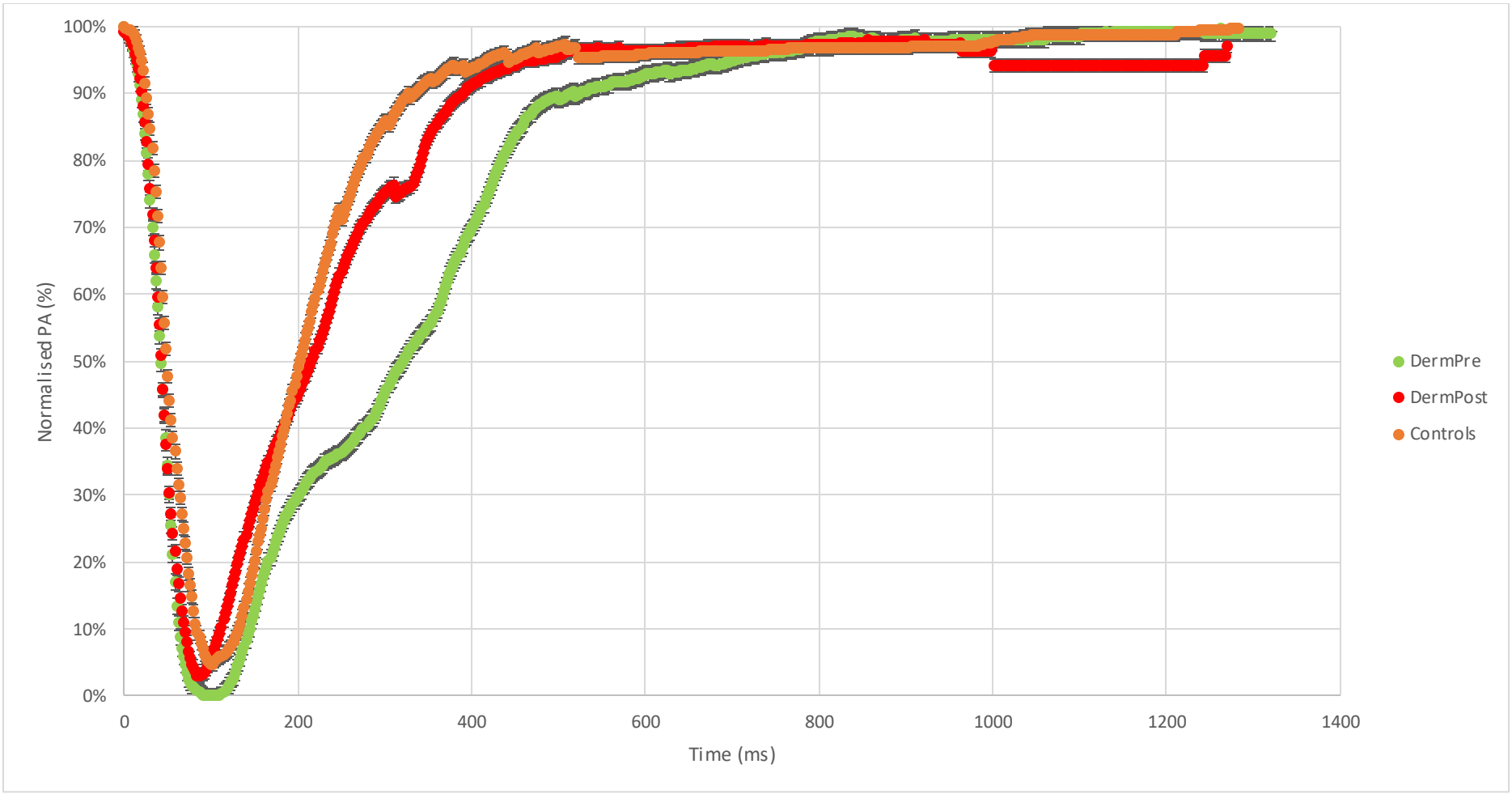

Figure 27.|Normalised PA master curve for control, pre-operation (DermPre) and post-operation (DermPost) patients. Values have been averaged across each group. Vertical error bars are SEM.

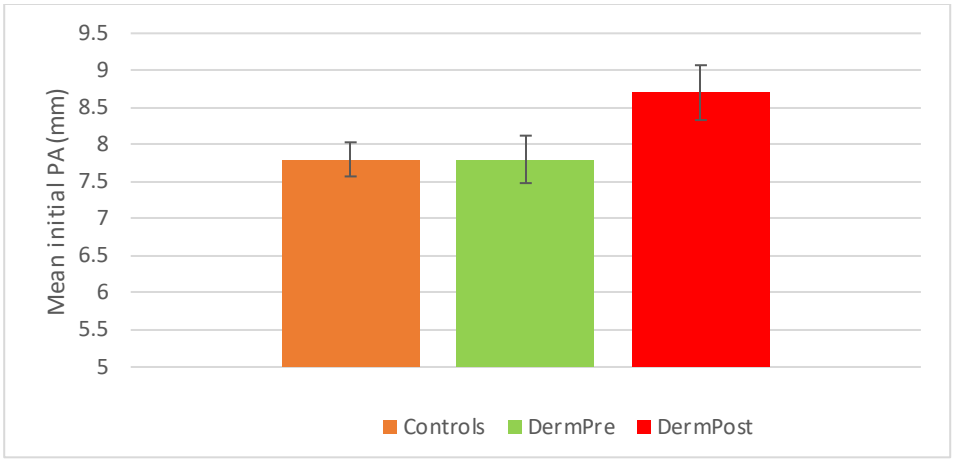

a.

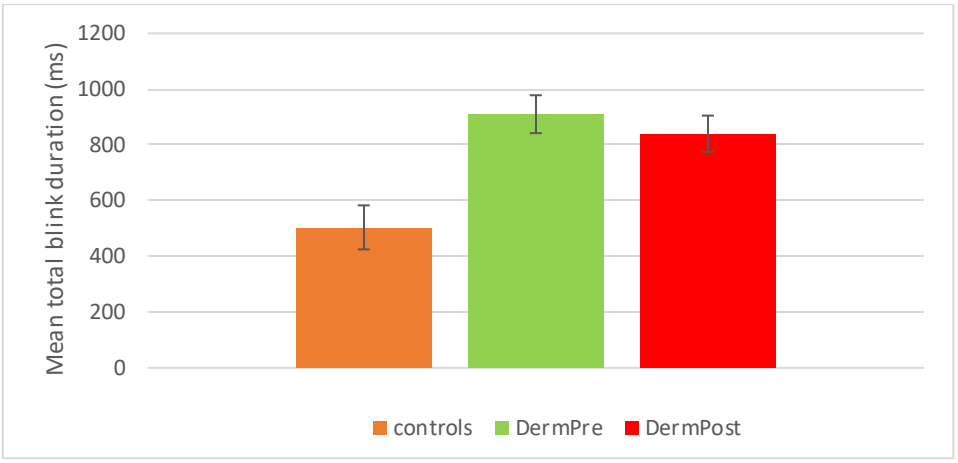

b.

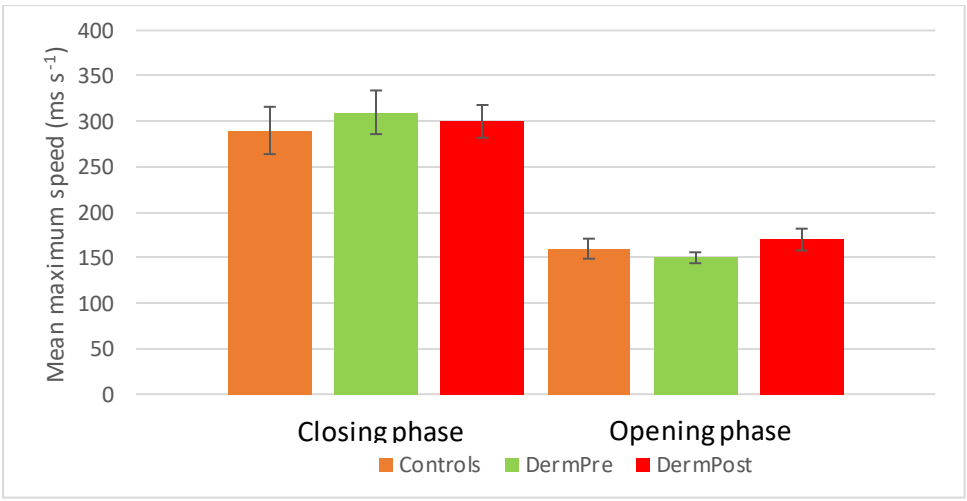

c.

Figure 28a-c.| **(a.)** Mean initial PA, **(b.)** mean total blink duration and mean maximum blink speed are displayed in colour coded bars with SEM error bars. Orange is control, green is dermatochalasis pre-operation and red is dermatochalasis post-operation. **(c.)** The Maximum speed of blink is measured in two phases, closing and opening phases that are separated by the zero or nearest to zero PA.

Total duration of a voluntary blink ranged from 250-1300 ms for the controls with a mean of 504±79 ms (SEM). Compared to 500-1300 ms, mean 910±68 ms for the pre-operation and 350-1300 ms, mean 840±65 ms (SEM) for the post-operation group (figure 28b). The maximum speed was also calculated for each group and shown in figure 28c. This was measured in two parts; the closing and the opening phases. For closing phase, the control group has maximum speed ranging of 140-480 mm s^{-1} with mean of 290±26 mm s^{-1} (SEM). For pre- and post-operation patients the range is 170-490 mm s^{-1} with a mean of 310±24 mm s^{-1} (SEM) and 190-440 mm s^{-1} with a mean of 300±18 mm s^{-1} (SEM) respectively. For the opening phase, the control group achieved 94-220 mm s^{-1} with a mean of 160±11 mm s^{-1}, the pre-operation 110-180 mm s^{-1} with a mean of 150±6 mm s^{-1} (SEM) and the post-operation 100-260 mm s^{-1}, with a mean of 170±12 mm s^{-1} (SEM).

The maximum speed during the closing phase is expected to be significantly faster due to OOM being a larger and stronger muscle than LPS, which is responsible for opening and maintaining the open state for long period of time. This closure force is also aided by gravity as well as the elasticity of the tendons surrounding the orbit. However, one eye in the control group exhibited higher maximum blink speed during the opening phase than the closing phase. This was unexpected and might be rectified by selecting an alternative blink from the recording because the speeds were very similar (closing speed of 182 mm s^{-1} compared to opening speed of 188 ms s^{-1}). The results are summarised in table 10.

		All values are to 2 s.f.		*Maximum speed (mm s^{-1})*	
		Initial PA (mm)	**Total duration (ms)**	**Closing phase**	**Opening phase**
Controls	**Minimum**	6.6	250	140	94
	Maximum	9.6	1300	480	220
	Mean	7.8	504	290	160
	SEM	0.23	79	26	11
DermPre	**Minimum**	6.3	500	170	110
	Maximum	9.4	1300	490	180
	Mean	7.8	910	310	150
	SEM	0.32	68	24	6
DermPost	**Minimum**	6.2	350	190	100
	Maximum	11	1300	440	260
	Mean	8.7	840	300	170
	SEM	0.37	65	18	12

Table 10.|Summary table for all three classes. All values are to 2 significant figures and SEM is standard error of the mean.

6.3.2 Multiple discriminant analysis: controls vs pre-operation vs post-operation

Four shape-defining parameters: the rate of closure (v_1), rate of initial opening (v_2), the delay between closure and opening at 50% (t_{open}-t_{close}) and the RMSD of the late opening phase after the switch point were analysed for each group using LDA and generated figure 29a after dimensional reduction. Dermatochalasis post-operation and pre-operation classes appear to be well separated; pre-operation and post-operation classes reasonably separated from the normal, although there is considerable overlap between post-operation and the normal class. However, in figure 29b, where the discriminant plot included v_1, v_2 and RMSD

but not the blink duration t_{open}-t_{closee}, all classes overlap significantly. This shows the importance of blink duration when determining the class memberships.

With the discriminant analysis achieving good separation between all three classes, a predictive model was generated based on the probability of any of the collected data being classified as pre-operation, post-operation or normal. This model achieved prediction accuracy as high as 81%. However, it was noted that without blink duration as a parameter, the probability for many individual cases became increasingly uncertain, i.e. 0.3-0.4 for each of the classes; a rise of nearly 3 folds from the model with blink duration as a parameter. This resulted in a 17% drop in accuracy.

In addition, a statistical analysis was carried out for each of the possible class combinations for each of the parameters. The most significant differences seem to be in t_{open}-t_{close}, or the blink duration, where pre-operation has a significantly longer duration than post-operation (p=0.0047) and controls (p=0.012). Interestingly, the post-operation class is not much different from the controls in almost every parameter (v_1, t_{open}-t_{close}, t_4-t_{open}, α and RMSD) except v_2. v_2 appeared to be moderately significant in differentiating post-operations from controls (p=0.0038) and those of the pre-operations class (p=0.044). The deviation parameter is moderately significant in differentiating controls from pre-operation as well (p=0.019).

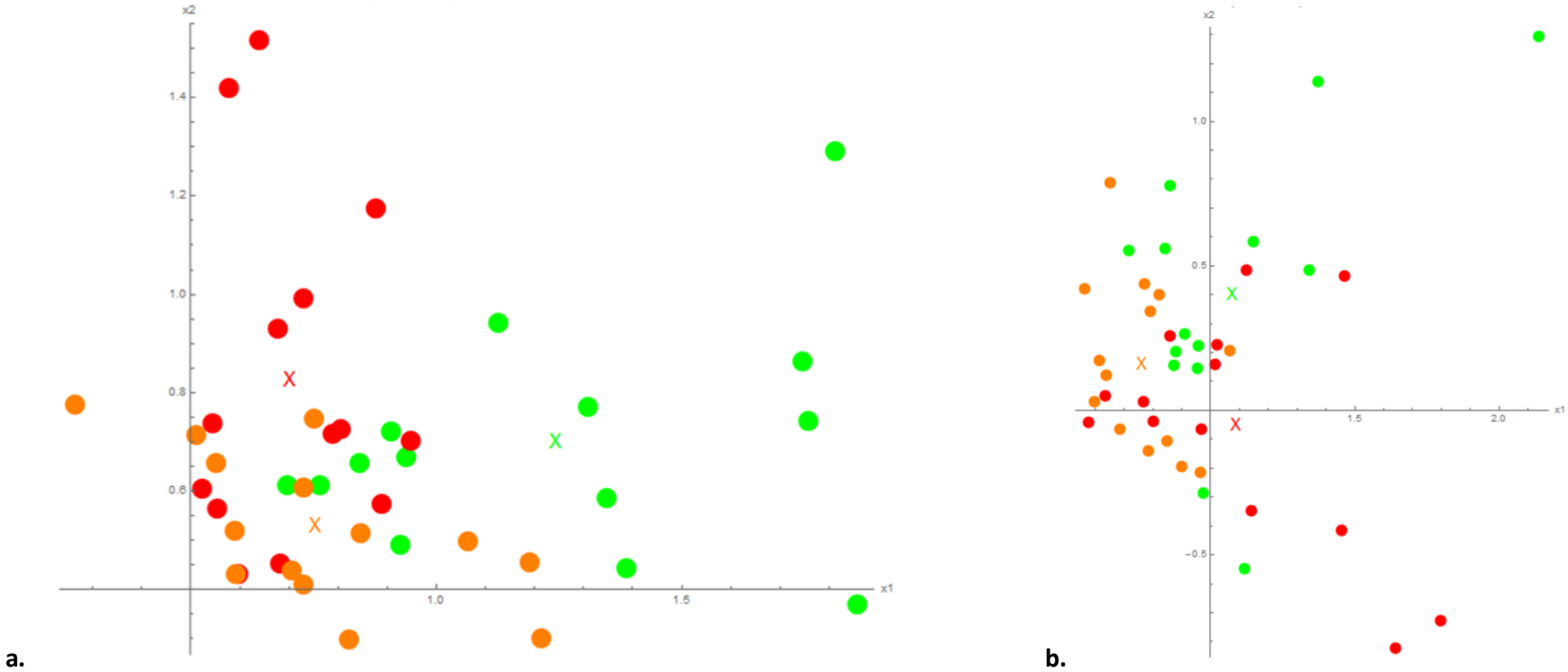

Figure 29. | Reduced dimensional plots were generated for control (orange), dermatochalasis pre-operation (green) and post-operation (red) to best separate these classes. **(a.)** This analysis used v_1, v_2, t_{open}-t_{close} and RMSD as the parameters and **(b.)** only used v1, v2 and RMSD. These two plots showed that the blink duration (t_{open}-t_{close}) is essential to differentiate all three classes by the more apparent separations between each classes when including blink duration. 'X' represent the mean of each of the colour coded individual classes. Values on x1 and x2 axis are merely numbers representing the reduced dimensions in LDA. †Mahalanobis distance was used here to measure the distance of a point from the mean of each class.

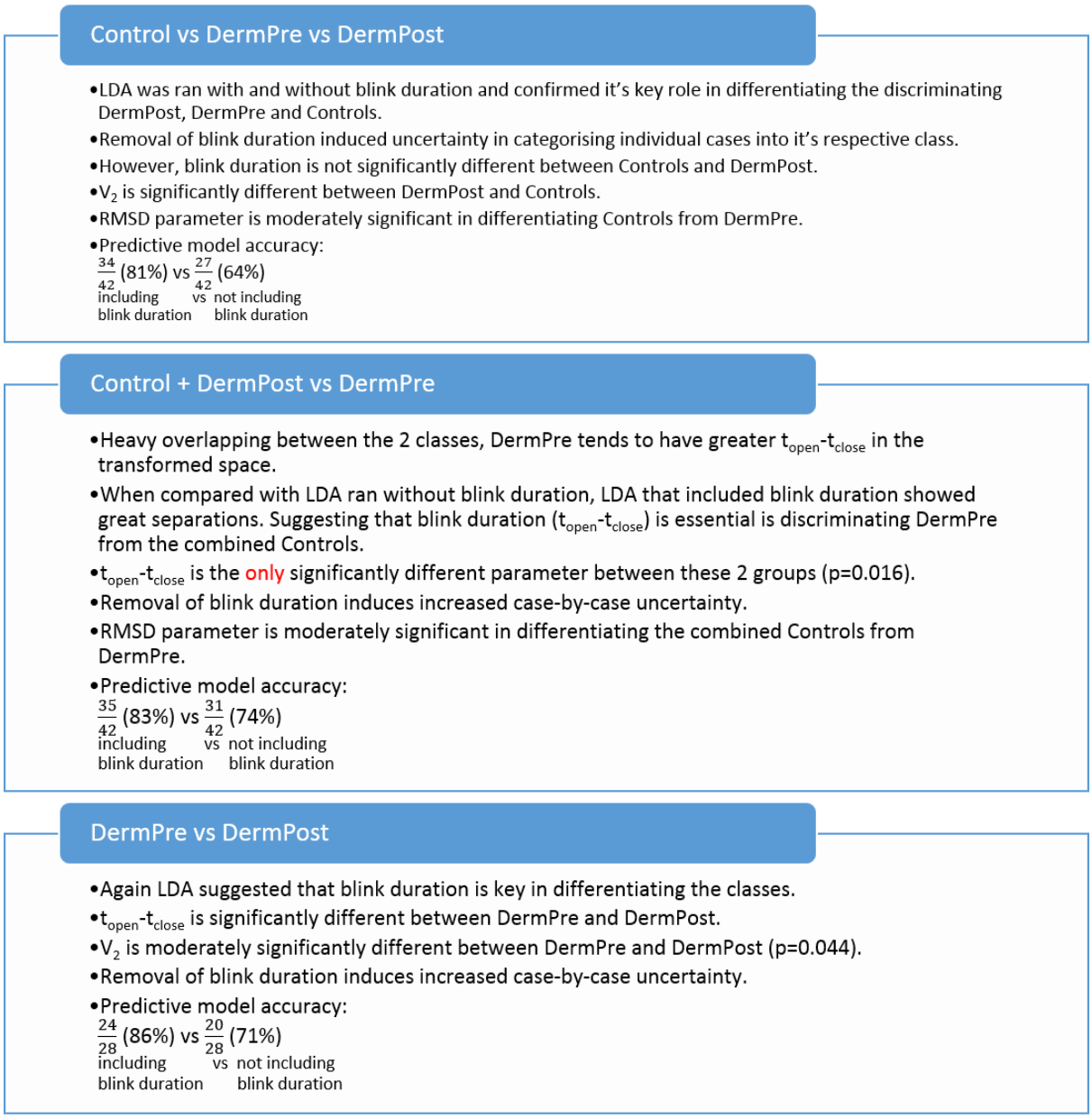

Figure 30.|Summary of different methods used to analyse the data. **Top**. Main method used in this investigation which established a predictive model with the accuracy of up to 81% in differentiating the three classes. **Middle**. Secondary method used to analyse the data – stemmed from the previous finding that suggest controls are similar to post-operated dermatochalasis patients. This method combined the original control group with post-operation class to form the new Control class. **Bottom**. Alternative method of analysis that only considered comparing pre-operation to post-operation. †DermPre is pre-operation and DermPost is post-operation.

6.3.3 Multiple discriminant analysis: combined controls vs Pre-operation and pre- vs post-operation

The high similarity between the control and the post-operation classes led to the investigation of combining those to form a new control class and comparing them to the pre-operation class. This analysis showed heavy overlapping of the two classes in v_1 and v_2, but the pre-operation class demonstrated a good separation from the combined controls. Parameter t_{open}-t_{close} appeared to be the only parameter that is significant in separating these classes ($p=0.016$). This agrees with the results of the 3-way discriminant analysis that blink duration is essential in discriminating the three classes.

Further, pre-operation was analysed against post-operation, ignoring the control groups. This again suggested blink duration is significant to differentiating the two classes. V_2 was found to be moderately significant ($p=0.044$). All three methods used to analyse the data are summarised in figure 30.

6.4 Summary

This part of the study explored the blinking dynamics of patients with dermatochalasis before and after blepharoplasty surgery, and compared them with a group of healthy volunteers using high-speed camera imaging analysis. Furthermore, by constructing the PA versus time curve and extracting key features from a standard blinking profile, we were able

to separate the condition from the control class as well as pre- and post-operation classes using LDA and multivariate Gaussian probability distribution. A predictive model was generated which achieved up to 81% accuracy in categorising a blinking profile into these three classes.

It was found that PA has significantly improved post-operation. Blink dynamics of the post-operation class were similar to that of controls as expected, due to the removal of excess skins during blepharoplasty procedures. Blink duration was longer than controls in both pre- and post-operation patients, most significant in the pre-operation class. The maximum speed of blink was analysed in two phases, closing and opening phase, and appear similar across all conditions. However, an observed rise in opening speed post-operation may be the result of a reduction in muscle mass of the upper eyelid.

Normal and post-operation blink dynamics are somewhat similar: not only do they strongly overlap in the discriminant analysis, but also five of six key features analysed in the blinking curves are not significantly different. Although similar in blinking profile, the parameter v_2 was demonstrated to be significant in separating between the two classes, as it is evident in figure 27. The steep nature of v_2 of the control group compared to post-operation suggests that, even though blink dynamics have improved from pre-operation to near control state after blepharoplasty surgery, the muscle dynamics responsible for initiating the opening phase (LPS) is largely different from the normal group. Most importantly, blink duration was flagged as the essential determinant for discriminating pre-operation to controls and post-operation. The blink duration was reduced significantly in both cases when comparing pre-operation to post-operation and controls, which suggest blepharoplasty alone was effective to address the defective blink dynamics in dermatochalasis.

CHAPTER 7: BLINK FORCE MEASUREMENTS

7.1 Introduction

OOM is the sole muscle responsible for eyelid closure. More specifically, the upper preseptal muscle serves as the main depressor of the upper eyelids, whereas the lower preseptal muscle is responsible for elevating the lower eyelid. Loss of function may result in an inability to close the eye, causing exposure that can lead to severe pain and sight threatening complications, or even removal of the eye in extreme cases. Upper and lower preseptal muscles of the OOM assist in the lubrication of the ocular surface during a blink (described in section 2.1). In cases where the OOM became malfunction, it may reduce the tear flow over the surface of the cornea and could lead to dry eye syndrome. Further, in excessive eyelid closure conditions such as ALO, patients are unable to open their eyelids due to involuntary levator palpebrae inhibition and a constant contraction of pretarsal potion of the OOM, causing functional blindness. Similarly in blepharospasm, forceful eyelid closure is caused by transient involuntary contraction of OOM (Marsden, 1976). In Bell's palsy, the cranial nerve VII that innervates OOM is trapped and compressed causing weakness to paralysis; the nerve is unable to relay signals sent from the brain to the OOM (Schwaber, et al., 1990). Patients found it difficult to impossible to blink or close the ipsilateral eyelid (Anwar, 2005; Hazin, et al., 2009). Subsequent lack of irrigation increases the risk of corneal inflammation and ulcers. These are just a few examples in which the OOM is affected by innervated problems. For myopathic conditions such as myotonic dystrophy and ocular

muscular dystrophy in the OOM, patients show weakness of eyelid closure (Ketelsen, et al., 1978). And patients suffering from facioscapulohumeral dystrophy cannot close their eyes completely during sleep, due to orbicularis oculi atrophy (Pandya, et al., 2008). Weakness of the OOM can cause incomplete eyelid closure, or lagophthalmos, which can lead to serious exposure keratitis and corneal scarring, a major ocular health concern. The above mentioned studies demonstrate that force of blinking is an important aspect in clinical diagnosis, and OOM function measured by the forces it produce may shed light on the pathological development of various eye conditions.

Muscular weaknesses in the OOM have not been measured numerically in the diagnosis of these diseases. By measuring the strengths of OOM in normal and abnormal patients, a comparison may allow categorisation or create a new grading system for OOM weakness to possible diseases. This may help in the diagnosis and promote early detection and, therefore, prevention in the field of diagnostic ophthalmology. As covered in section 2.5, Jacobs introduced an instrument that allows a measurement of forceful eyelid movements (Jacobs, 1954), measured by a mercury manometer (in mm Hg). Although he was unable to determine the norm, we suspect that the lack of accuracy in his results may be caused by experimental errors and the primitive measuring instrument, with the overly invasive procedures.

In this part of the project, a new apparatus was designed and constructed to measure the force in the eyelid closure, particularly maximum force of contraction and natural force of closure. This device has been used to test a very small sample of healthy volunteers and a patent is currently being filed. This chapter will go through the designs, its prototypes, measuring protocols and some preliminary results measured by the device.

7.2 Initial design considerations

There are several limitations to Jacobs's design which should be avoided, such as the instability of the hand-held instrument, discomfort of the volunteers relative to the positioning of the device, complication of mm Hg to force conversion and inconsistency of results.

In contrast to Jacobs' pressurised system (measuring in mm Hg), where he pumped air into the cylinder to generate opposing force, this design combined and integrated a Newton force meter within the speculum for direct force measurement (figure 31). To improve the overall precision of the experiment, the measuring device should be mounted on a stable position and be able to provide a high sensitivity and reproducible reading. The eyelid attachment should be adjustable (vertically and horizontally) to accommodate a variety of medial-medial canthal distance and PA; a three dimensional translational system is required to suit individual's facial contour.

To maximise volunteers' safety, comfort and enhance their experience, they were seated and allowed to rest their head firmly and comfortably on a chin-rest. This allows volunteers to remain still, thereby minimising errors caused by movement during the measurements. The structure of the device should be stable to ensure accurate measurement by a very sensitive device; operation should also be user-friendly as well as subject-friendly; and also the materials used for construction should be rigid, firm, easy to clean/ sterilise, if required, and commonly accepted in clinical settings.

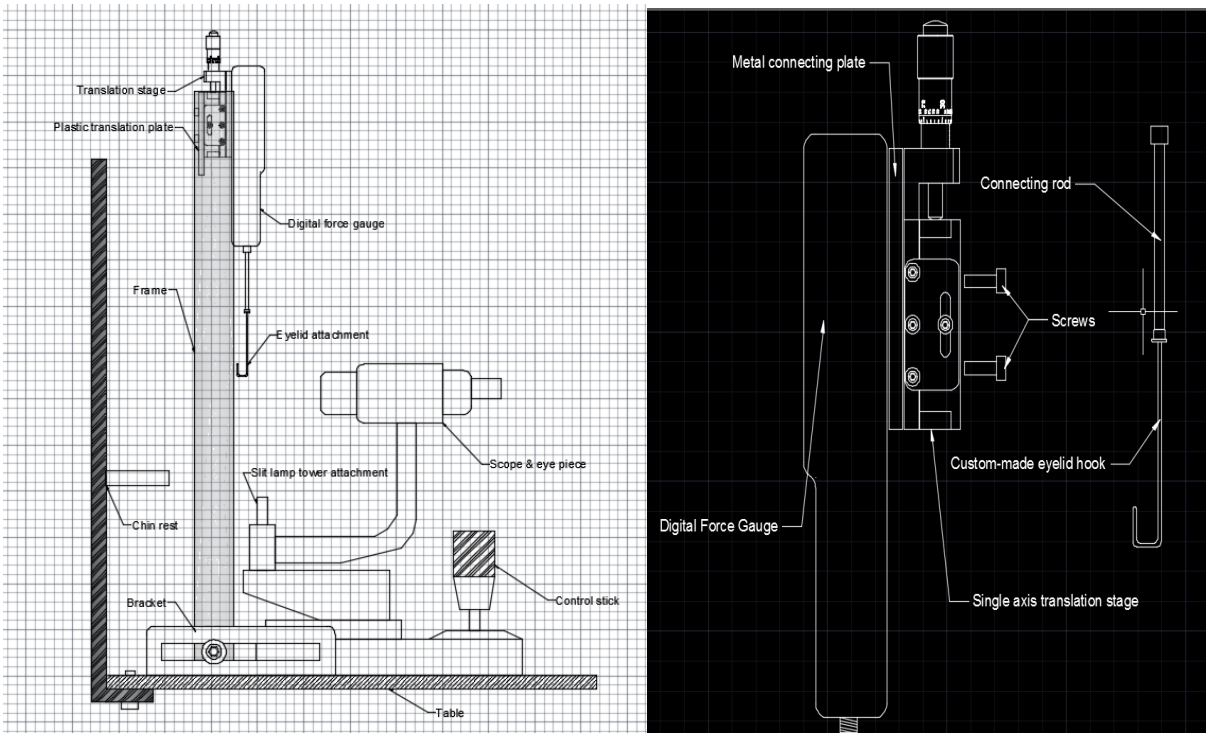

Figure 31.|Initial prototype design of the two dimensional Computer-Aided-Design (CAD) drawing of the eye blinking force measuring device. The device is based on a standard slit lamp table with a chin rest. The measuring unit is held up by a frame, which can provide X, Y, and Z direction movements. Right. Showing the attachment between the digital force gauge (DFG) and the single axis translation stage; allowing accurate up and down movements of the measuring device. Also showing a custom designed eyelid attachment.

7.2.1 Instrument prototype set-up

A prototype was designed (figure 31) on the software AutoCAD 2015 (Autodesk) and is illustrated in Figure 32a. The instrument consists of a frame on a standard slit-lamp and a DFG fixed with a single-axis micro translation stage. This frame permits the DFG to move in all X, Y and Z directions, it also provides a stable fixture for the functional parts. It is made up of two aluminium bars (each 610 mm high) and a light weight plastic plate (height adjustable)

with wide slots in the middle to allow the DFG to glide along the horizontal axis. The two aluminium bars that form the frame are wide apart at table width, allowing the full swinging motion of the rotational arm of the slit-lamp. The light tower is removed for convenience. The main measuring unit (figure 32b) consists of a combination of single-axis micro-translation stage (MT1/M Thorlabs Ltd., Ely, U.K.) and a DFG (FK10 Sauter, Lancashire, U.K.).

The translation stage has a steel linear bearing for precise motion and it was configured with the micro-meter drive, which has a 13 mm travelling range and 10 µm per division. To justify this selection, previous data showed that the PF was found to be between 7.4-12.8 mm with the mean of 9.8±0.2 mm (Kwon, et al., 2013) and with 61.7% lies between 9-10 mm aperture value (Fox, 1966). These figures suggest that the single-axis micro-translation stage with a vertical translation of 13 mm is adequate for our experiment.

This DFG is a uni-axial push/ pull force gauge. It contains a load cell, a transducer which is used to generate an electrical signal that is directly proportional to the force being measured. It senses the force through a mechanical strain gauge by converting the difference in voltage during its deformation (strain) into force values. This specific gauge has a data sampling rate of 1000 Hz and the accuracy of 0.5% of capacity. The real time/ peak hold mode allows observing transients or capturing peaks. Using Jacobs's values as a reference (Jacobs, 1954), I have decided to select FK10 model of the DFG. The FK10 provides resolution of 0.005 N (0.5 g) and the maximum reading of 10 N with 200% overload protection. This is sufficient to measure natural and forced eyelid closure with satisfactory accuracy. To ensure optimal functionality, the DFG was calibrated by Laboratory KERN (KERN & SOHN GmbH, Balingen, Germany; ISO Calibration Certificate CF-500).

At the measuring end of the DFG, a custom-made eyelid attachment was created (figure 32c), using a modified Pierce adjustable speculum (MMSU1270S, Malosa Medical, West Yorkshire, U.K.) which can be screwed on to the DFG to allow measurement. The complete unit is mounted on the plastic plate (removable) with a screw-in mechanism to allow stabilised horizontal movement. The Pierce adjustable speculum was selected because it is commonly used with patients during ophthalmic practices, and it is made of materials that are medically certified for use in a clinical environment.

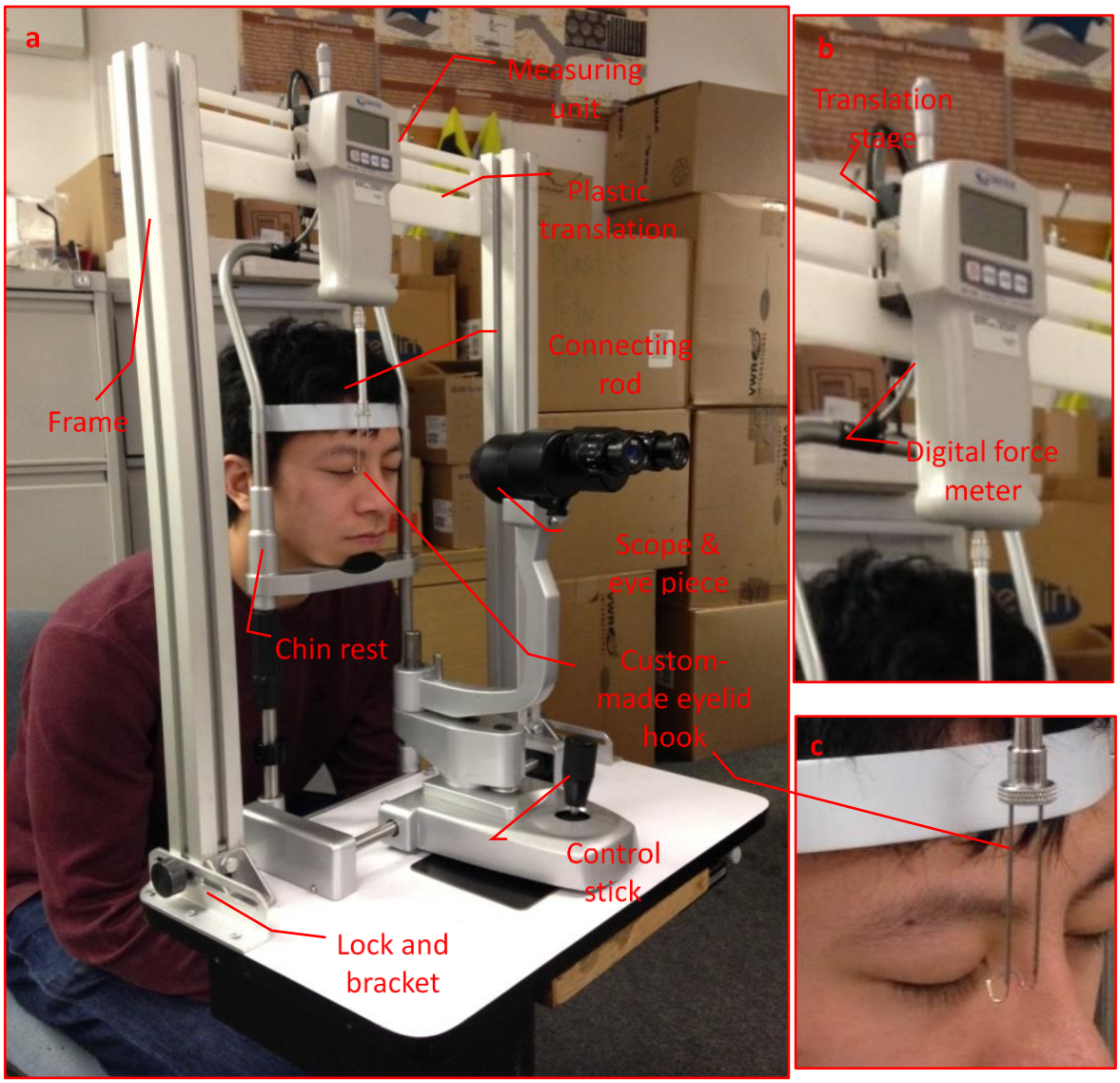

Figure 32.|Instrument in use. a. Adjustable frame made from 2 aluminium bars stood on either side of the slit-lamp table. They attach the main measuring unit across the top and allow height adjustment of the plastic plate. The frame is set wide enough to allow full swinging motion of the slit-lamp rotational arms (slit-lamp light and the binocular microscope). The slit-lamp light tower is removed for the purpose of this experiment. b. The main measuring unit. This consists of a single-axis micro-translation stage, and a DFG. The translation stage has a travelling range of 13 mm, controlled by the micro-meter drive for precise vertical motion. The DFG is attached to the translation stage via an aluminium plate. It has a maximum capacity of 10 Newton and a high data sampling frequency and high accuracy. It also has real time/ peak hold mode to capture transient peaks. This unit is mounted on a plastic plate. Horizontal translation is possible. c. Custom-made eyelid attachment. Made from modifying a Pierce adjustable speculum and screwed onto the base of the DFG. The speculum is inserted into the PF to begin measurement. Permissions have been obtained from the subject.

7.2.3 Method of measurement

It would be interesting to see how the blinking force in diseased patients compared to healthy individuals. However, before conducting widespread testing in patients and volunteers, it is crucial to test the safety of the device to operate in clinical environment and to confirm that this device can in fact produce robust and reproducible results.

The instrument was used to measure the:

1. weight of the eyelid,
2. natural blinking force and
3. the maximum eyelid closure force.

The volunteers were seated with chin on chin-rest and forehead resting firmly against the forehead-strip as they would be for a standard slit-lamp eye examination. Before the experiment, the subjects were briefed on the test and how it will be carried out using the instrument. Normal resting PA were measured and recorded for each subject.

There were 3 parts to this experiment. First, the speculum was introduced into the PF with the eyelids at the closed position. The DFG will be zeroed at this stage for the measurement of the natural force of closure/ weight of eyelid. Engagement value will be noted. The volunteers were asked to relax and allow the experimenter to elevate their eyelid to their normal PA value and the force was recorded. This value also provide an indication of the weight of the eyelid (perhaps combined with other neighbouring muscles and tendons). Second stage of the experiment continues after the result is recorded. With the DFG set to peak mode, the volunteers were asked to blink both eyes a few times, which will provide the

initial peak force for their blinks. This value was recorded. Lastly, with the eyelid prised open at the normal AP, the volunteer was asked to squeeze both eyes shut as tightly as possible. The peak value recorded indicates the maximum forced closure.

The volunteers were reminded to keep their head very still and were encouraged in their efforts at all time. Anaesthetic eye drop (tetracaine hydrochloride 1%) was used in this experiment as a precaution. A total of three measurements has been obtained from each eye and repeated again on the contralateral eye for each volunteer. These data were recorded and average value calculated. Variations between individuals are expected and two independent samples T-test were used to calculate the significance of these samples between the normal group and the diseased group of results.

This procedure allows a direct force measurement in Newtons and eliminates the complicated method of converting mm Hg. into force employed in Jacobs' experiment. The measuring gauge was mounted securely over-head for stability during measurements and underwent a rigorous calibration course to ensure accuracy and minimised the error margin.

7.2.4 Preliminary testing of the prototype

The device was custom built in the UCL Mechanical Engineering Workshop. Provisional testing with this device shows that the new method and apparatus is able to record different types of blinking forces and results are consistent, comparable with a similar but a very primitive one-off set of measurement done in 1954 (Jacobs, 1954). Table 11 below matched both studies and demonstrated comparable data of forced closure in healthy volunteers. We

have tested merely three volunteers, each with multiple measurements taken. The results were only used as a reference to improve the prototype, therefore we have not attempted to calculate the statistics in details. Averages have been used in table 11 below.

	Jacobs hand-held device (g)	Initial prototype (g)
Weight of eyelids	Not measured	10.0
Blink force	Not measured	11.5
Forced closure	60-70 with wide ± of mean	72.5
L/R eye variation	No	No

Table 11.|Comparison of previous study on forced closure in healthy subjects to initial prototype.

7.3 Evolution from initial design

During the tests, we felt that there were a number of problems which should be improved upon, including adjustment and major stability issues, both affect the accuracy of the measurement. The connecting rod is pushing against the volunteer's forehead and the custom-made eyelid hook is too far forward. It did not manage to accommodate all facial contours in every volunteer; the eyelid was not reaching the hook in its natural position. Furthermore, it required 2 people to carry out the test: one cannot easily adjust the frame proximal movement and plastic plate horizontal translation of the DFG measuring unit in parallel while keeping an eye for the safety of the volunteer. These sliding motions were quite jagged and the procedure was rather invasive. To rectify these problems, a new design was drawn and developed, with focus on the ease to use, smooth one-man operation, 'one-size-

fit-all' eyelid attachment with reduced invasiveness and most importantly, improvement on stability.

The previous structure of the table was rested on a single cylindrical supporting frame with 4 legs extended at the base to provide balance (not shown). With the table measured at 50cm in height, the volunteers have to sit on a small chair and hunch their back in order to rest the chin on the head-rest. With the volunteer's head in place, the shift in weight on the table created a tilt, affecting the DFG to eyelid engagement and therefore the accuracy of the measurement. Due to the height of the aluminium frame on the table top, the weight causes the DFG to rock back and forth, also affecting the measurement accuracy. The current design of the supporting table structure features a mobile, 4-legged base with a screw cap that can be tightened to lift and lock up the table into a fixed position, preventing movement. The height is raised significantly to 73cm, as a standard desk height (figure 33a). The aluminium frame that holds the measuring unit will be made redundant and replaced with a 4-legged structure that can provide parallel X, Y, Z direction movements with low friction sliding and lockable motions (figure 33b). However after evaluating the practicalities of the frame in figure 33b, such as space taken, stabilities, potential integration with conventional ophthalmic equipment, cost and materials required, a more suitable frame was designed figure 34.

This latest prototype was designed using SketchUp (Trimble Inc., U.S.). In figure 34a-d, different views of the model are displayed to allow the full understanding of this apparatus (figure 34e). It comprises an insertion part; a tri-axis (X, Y, and Z) positioning system for producing controlled motion of the insertion part to locate the insertion part on the surface of the eye of the subject in a neutral engagement with the eyelid; and an DFG for measuring

force produced by an eyelid of a human subject. For each of the X, Y, and Z-axis positioning rail, a threaded rod connects with a rotational handle allows the respective translation. The Y-axis positioning rail is fixed onto the table, whereas the moveable horizontal strut (X-axis positioning rails), which supports the vertical strut (Z-axis positioning rails) are supported by a base with roller-balls on the underside (figure 34d). The DFG is secured with a metal plate attached to the Z-axis positioning rail (figure 34a). The insertion part has also been improved in order the fit a variety of facial contours (figure 35). This eyelid attachment approximates a cantilever; when a patient applies a force to the engagement surface of the insertion part, this force is transferred to and detected by the DFG.

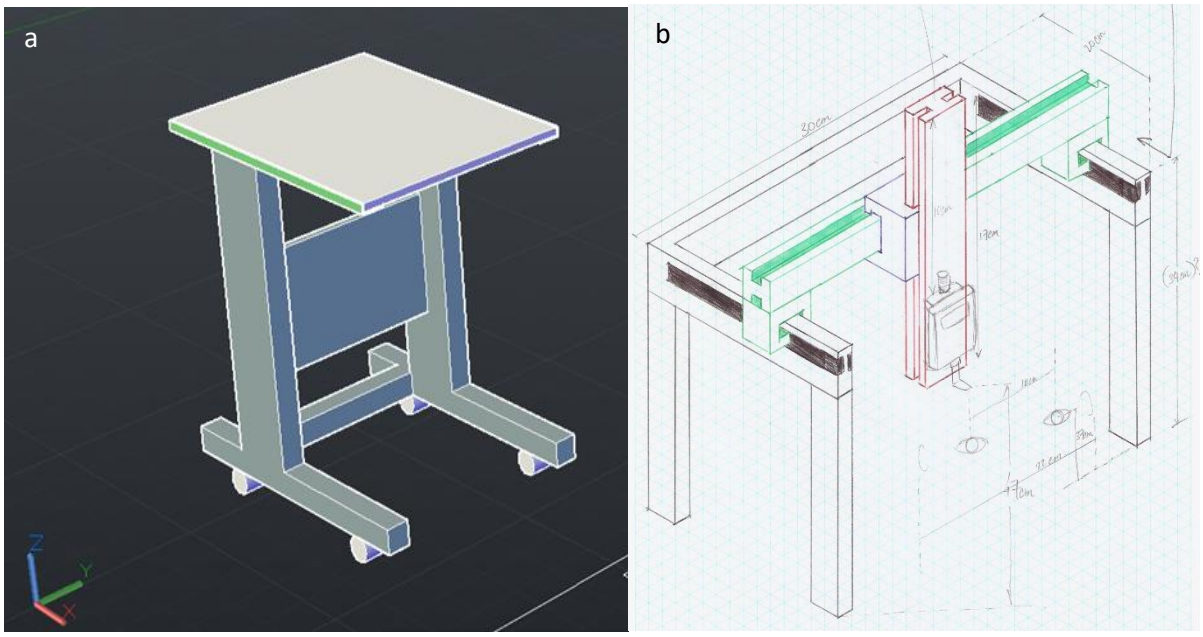

Figure 33.|Design of the eye blinking force measuring device. **a.** AutoCAD 3D drawing of a new table. **b.** Scanned drawing of a different frame to house the measuring unit.

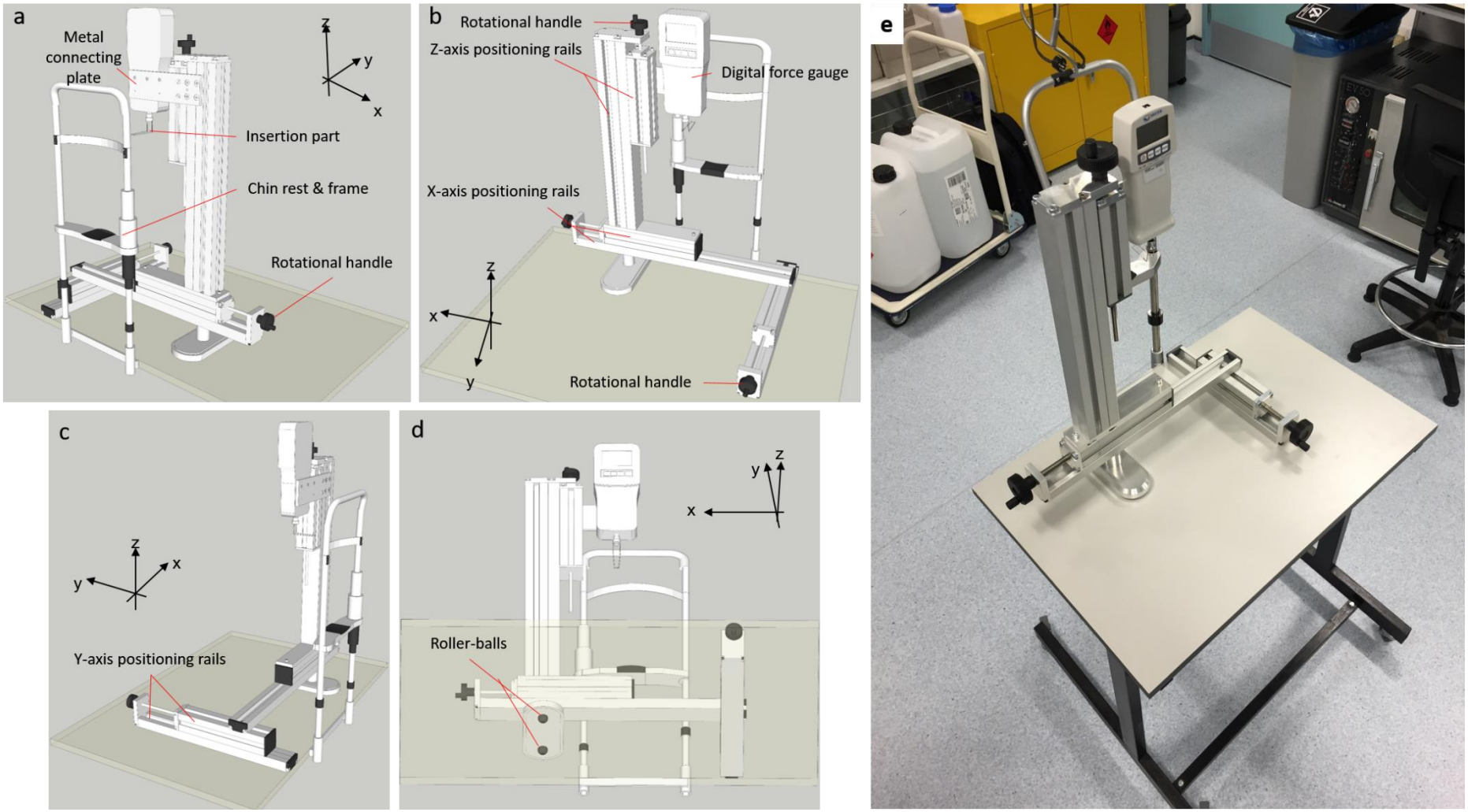

Figure 34.| Final design and the actual prototype build. **a-d.** Represent various viewing angles (in respect from the view of the subject being tested); front, back, left and under, respectively. X, Y, Z directional axis were labelled in each panel. **e.** A photograph of the final product.

Figure 35.| Eyelid attachment that connects to the DFG and produces direct force measurement in Newtons.

7.4 Protocol

This investigation involves recruiting two groups of volunteers to participate in an OOM strength testing study. We began with recruiting volunteers within UCL, the controlled group consisting of healthy individuals with no previous ocular conditions that would affect their muscular functions. The second group will consist of individuals with existing ocular conditions. Both groups will include both sexes across all age and various ethnicities that can understand and follow commands. The purpose of this investigation is to determine the force generated in blinking, maximum and natural eyelid closure. Also to compare and to observe

the correlation between ocular muscles weaknesses in various eye conditions against healthy subjects.

The test for both healthy and diseased group will be the same, and are done in the same way mentioned in section 7.2.3. For the maximum safety of the subjects, and the need of drug administration (anaesthetic eye drop; tetracaine hydrochloride 1%), a clinician should be used as the operator. An ophthalmologist has been trained for this purpose. By using a clinician as the operator, this would provide reassurance to the subject being tested, and advice or consultation on the discomfort (if any) that may occur after the test. There were no reported discomforts from any of the subjects tested.

7.4.1 Hypothesis

It is expected that the weight of eyelid would be similar, or within the normal range (once determined) in the diseased groups. The reason is that weight is not usually affected, but the weakening of the muscles controlling the eyelid movements. However, in certain cases like ptosis, 'over-weight' upper eyelids in older patients are quite common.

Further, it is questionable whether the force of a passive blink would be different in these groups due to the motion of lid closure is generated by the relaxation of LPS, gravity and the elasticity of the tendons and ligaments, whilst the OOM contracts to achieve a full closure. Therefore, initial closure force is essentially the weight and the recoil of tendons and ligaments. Afterwards the OOM contracts to rapidly lower the upper eyelid. The weakness in OOM in diseased patients could produce a slightly lower reading on the force generated

during blinking, but for patients with BSP for example, the force may increase due to constant involuntary pretarsal OOM contraction/ spasm. Weakness in LPS may already have left the upper eyelid in a half closed position and the loss of elasticity of tendons and ligaments in diseased patients should also be considered to impact the force of blinking.

For the measurement of maximum force of lid closure, previous data from Jacobs showed an extremely wide range above and below the mean, so great that the objective of determining the norm became impossible (Jacobs, 1954). With the technology of 21st century, force measurements are now far more accurate and produce less errors. With Jacobs' results as reference, I expect that the results from the control group will provide a range of values that represent the norm of the strength of OOM during maximum closure readings. And that the diseased group would be similar but wider due to weakness and or spastic OOM muscles.

7.4.2 Subject selection and data gathering

We are currently working on obtaining ethical approval to use this device on patients, therefore have only managed to test this on normal subjects. Twelve volunteers (6 males, 6 females) were recruited from UCL. The age ranged between age 22 to 27 (median 26). Due to the manual nature of this apparatus, the same ophthalmologist has been used to avoid variation between operators throughout this experiment.

In addition to name, gender, date of birth, ethnicity, weight of lid, force of natural blink and forced blink force, further data such as any history of ophthalmic condition, whether or not

correction was required and eyelid crease from margin was also documented for future references. Measurements were taken for both left and right eyes.

7.4.3 Data analysis

Multiple measurements (measured in Newton) have been taken and the mean and SEM have been calculated for the categories, weight of upper eyelid, natural blink force and forced blink force. Newton was converted into grams on table 11 & 14 for comparison purposes only. This was calculated by the application of Newton's second law $F = ma$, assuming Earth gravity of 9.80 g.

7.5 Results and discussion

The weight of the eyelids were measured to 14.8 ± 0.9 g (SEM) and the natural blink force is 21.3 ± 1.8 g (SEM). Neither of these were measured in Jacobs's study (Jacobs, 1954). The results appears to be repeatable with a relatively low SEM. Next is the forced closure, which was measured to 85.3 ± 5.2 g (SEM). This value appears to be higher than the previous measures, including the initial prototype and has a higher SEM value of 5.2 g (table 12). This may suggest a possibility of underlying sub-groups, perhaps ethnicity or a male to female differences. Therefore it would be interesting to separate the possible sub-groups and

investigate further, especially Asian oriental to non-Asian oriental to explore how the different anatomy could affect the force dynamics.

	Jacobs' hand-held device (g)	Initial prototype (g)	Current study (g)
Weight of eyelids	Not measured	10.0	14.8 ± 0.9
Blink force	Not measured	11.5	21.3 ± 1.8
Forced closure	60-70 with wide ± of mean	72.5	85.3 ± 5.2
L/R eye variation	No	No	No

Table 12.|Comparison of previous study on forced closure in healthy subjects to current study. Results under current study is displayed here with ± SEM (standard error of the mean).

Scatter plots were generated with error bars to investigate further into the relationships between the different categories. All possible combinations have been plotted against each other; natural blink force (voluntary) to weight of eyelids and forced closure, and forced closure to weight of eyelids (figures 35). The results appear to be well spread over the spaces and showed no distinct differences between the categories. However the error bars were particularly large in the forced blink category.

When comparing Chinese subjects to non-Chinese subjects (figure 37), it seems that the spread of data is much wider for non-Chinese subjects in upper eyelid weight than the Chinese counterpart (figure 37 right panel). Though (voluntary) natural and forced blink force appear to be scattered across for both sub-groups (figure 37 left and bottom panels).

Gender difference was also investigated but found no distinct results (figure 38). However, during forced blink force measurement, female subjects appear to have a more difficult time

getting used to the measuring device and required more encouragement. This could explain the larger error bars (figure 38 right and bottom panels).

Left-right symmetry between each subjects provided no further apparent information. Lines of best fit were plotted and showed positive correlations for all categories (figure 39). This suggested no variation between left and right eyes.

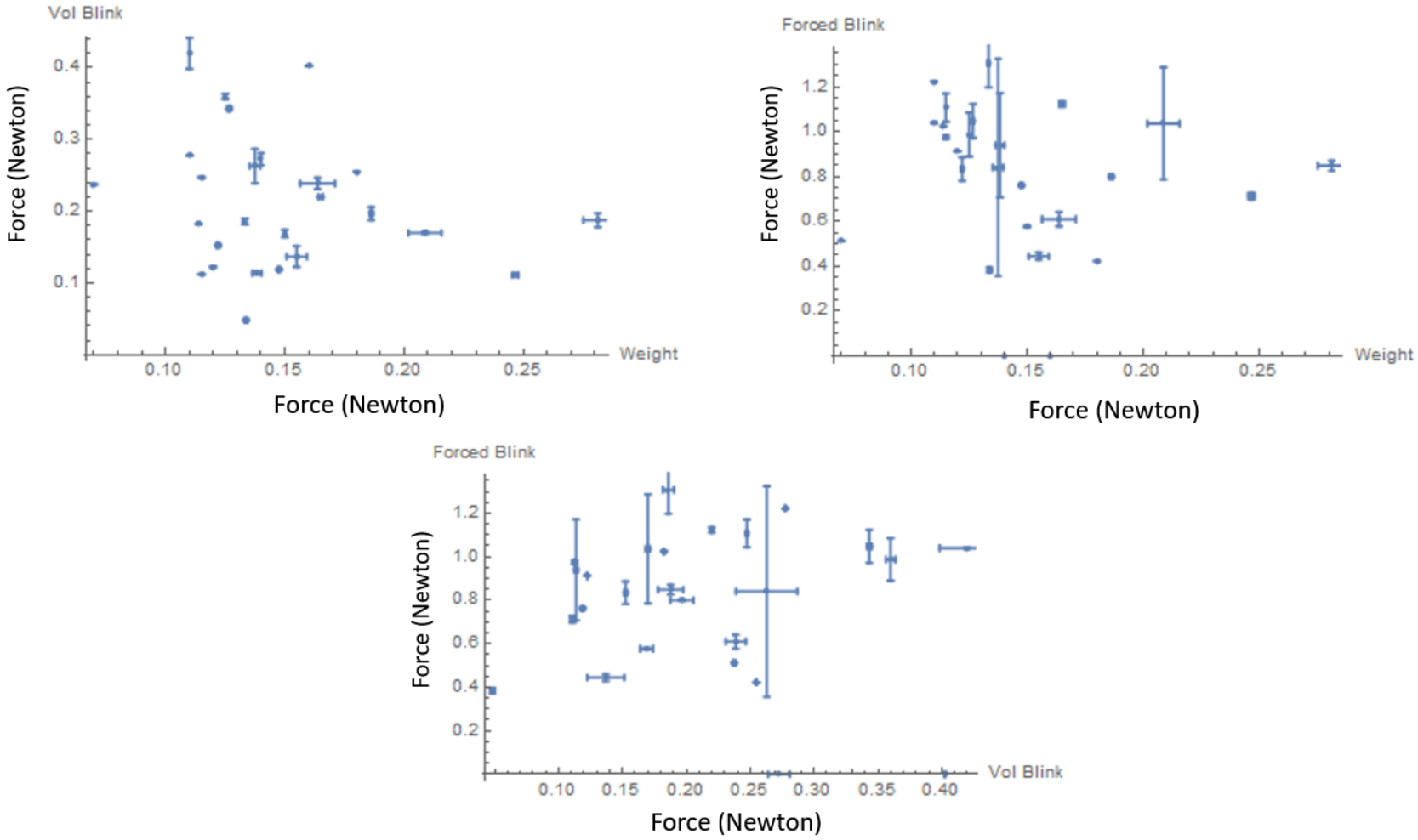

Figure 36.| Overall blink force scatter plots with error bars. Each categories were plotted against each other to investigate the possible relationships between each of them. 'Vol blink' represents natural blinking force (voluntary) and 'weight' represents the weight of eyelids.

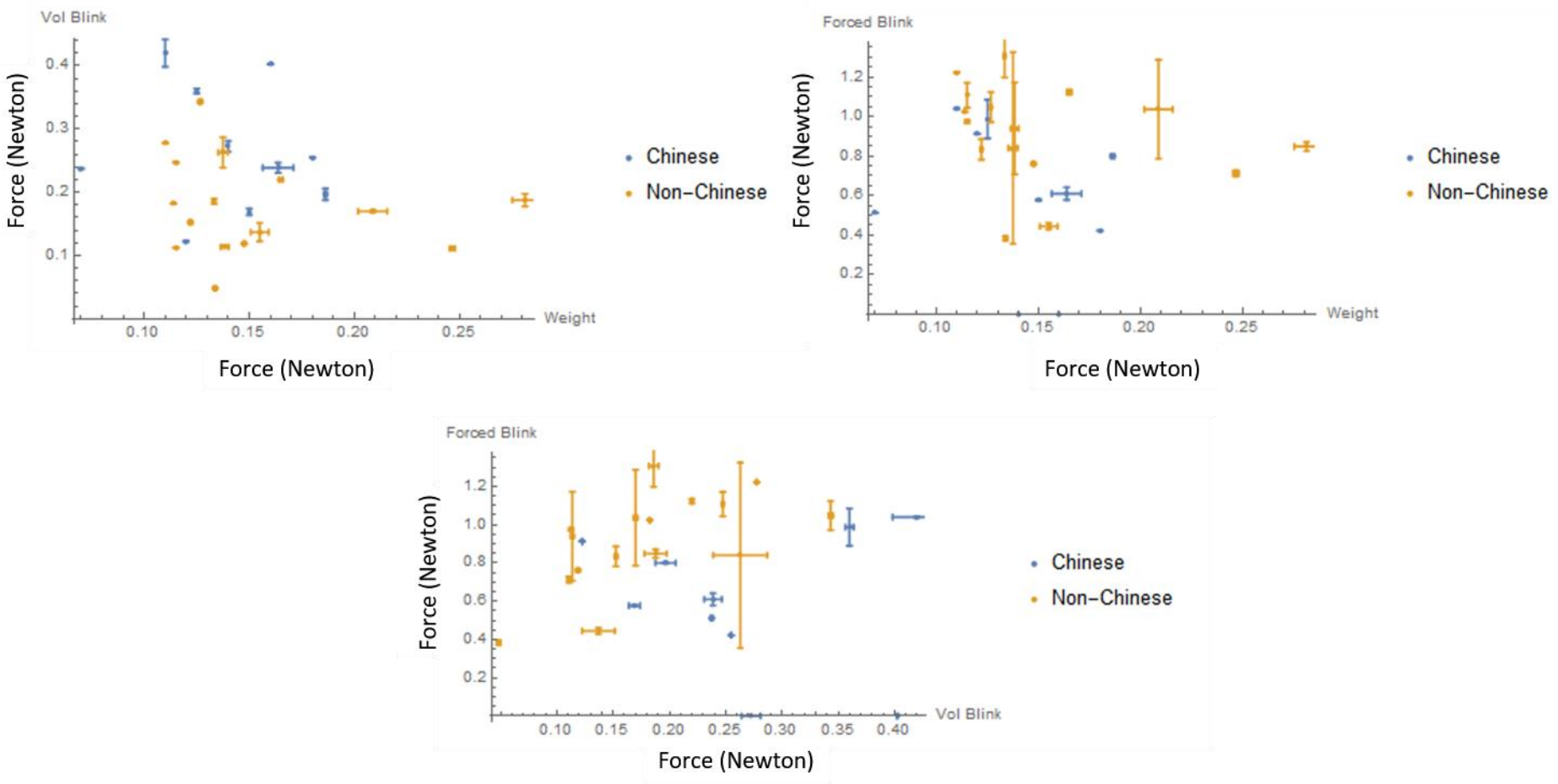

Figure 37.|Overall blink force scatter plots with error bars highlighting Chinese (blue) and non-Chinese subjects (orange). 'Vol blink' represents natural blinking force (voluntary) and 'weight' represents the weight of eyelids.

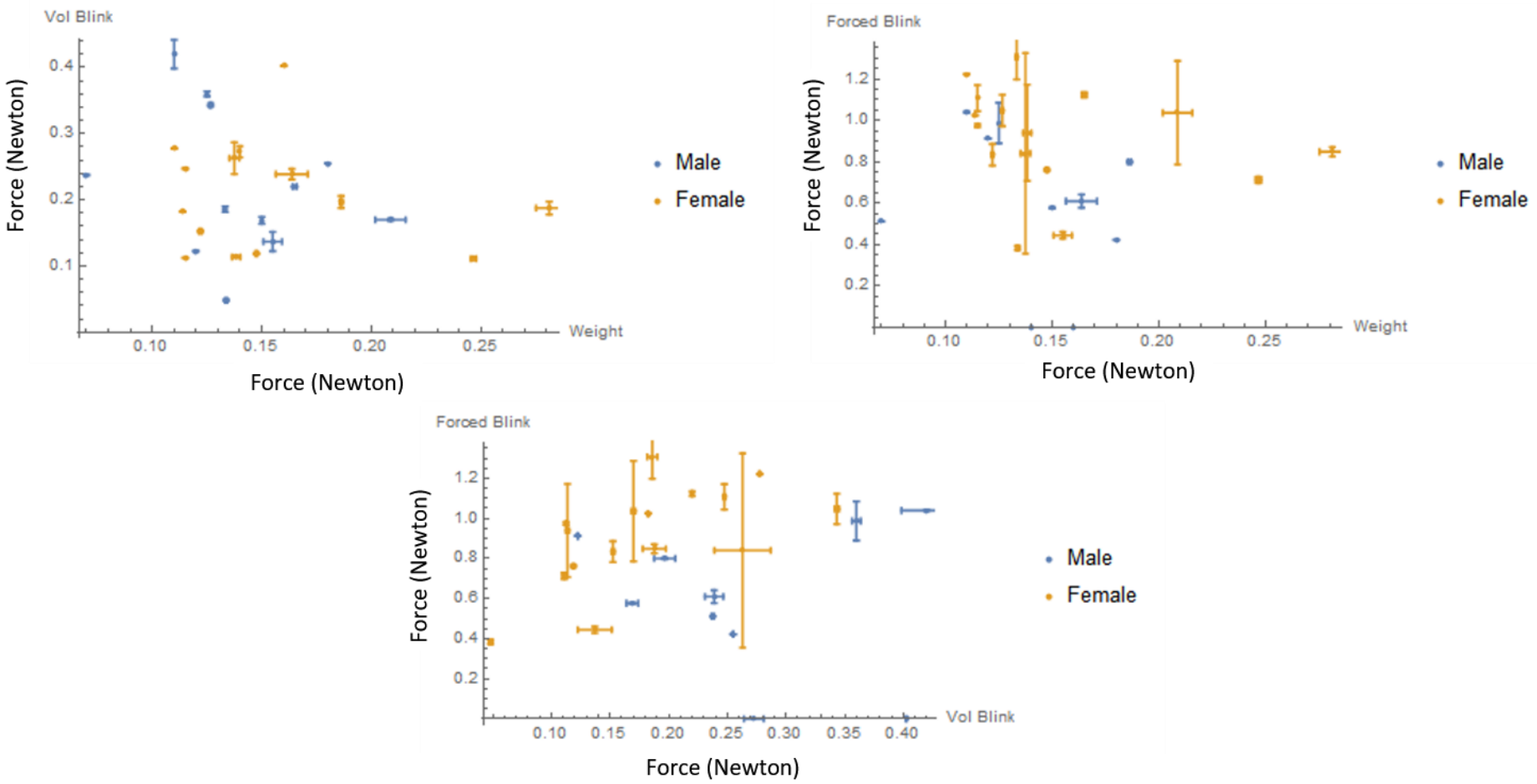

Figure 38.| Overall blink force scatter plots with error bars highlighting male (blue) from female subjects (orange). 'Vol blink' represents natural blinking force (voluntary) and 'weight' represents the weight of eyelids.

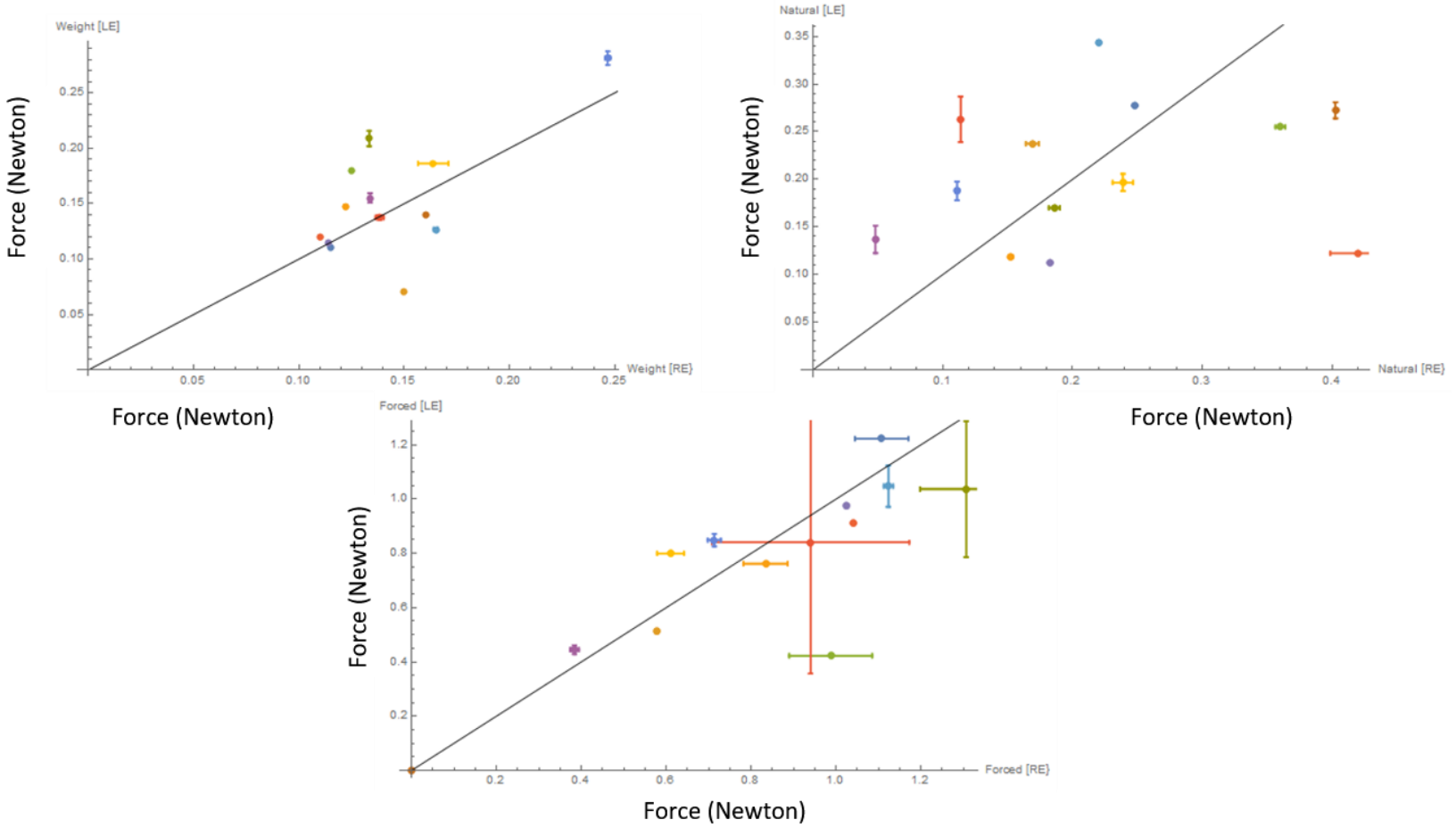

Figure 39.| Scatter plots comparing blink forces of the different categories for left and right eyes. Left panel compares the upper eyelid weight between left and right eyes; right panel compares the (voluntary) natural blink force for left and right eyes; and bottom panel compares the forced blink force between left and right eyes. Each of the single colour represent one subject and a line of best fit was inserted in all plots.

7.4 Summary

A difference in force produced by the upper eyelid during blinking has been implicated in the development of various ophthalmic conditions, compared to normal subjects. In this part of the study, an apparatus for measuring forces involved in blinking was introduced. Various designs have been considered and a prototype was created with the aim to improve previous measuring tool introduced by Jacobs in the 1950s. Despite a few stability issues of the device and troublesome operating methods, our prototype still managed to obtain repeatable values comparable to Jacobs's tool. Achieving 72.5 g of forced closure force compared to the previous measured value of 60-70 g with a wide range on either side of the mean (Jacobs, 1954). This prototype also has the ability to measure the weight of the upper eyelid and the natural blinking force (voluntary), which Jacobs's tool lacks. However, there are other types of blinking that this instrument will not be able to measure. Those include continuous measurements through a complete duration of a blink, spontaneous and reflexive blinks. These types of blinks are more difficult to capture as they involve external stimuli and another dimension; time. A quick test with a very low number of volunteers gave us an average of 10 g for the weight of the upper eyelid and 11.5 g for the natural blinking force (voluntary; table 11).

Due to the basic design of the eyelid engagement, this initial prototype was unable to accommodate various facial contours of different ethical backgrounds. Therefore an improved version have been developed, resolving most of the problems experienced with the initial prototype and minimising errors in this experiment. The result is a more stable table top housing the device and an improved tri-axis positioning unit, and a modified eyelid

engagement unit. These changes also made the measuring task easier with one-man operation and improved subject comfort. We managed to recruit thirteen healthy volunteers from UCL and all three categories; weight of upper eyelids, natural blinking force (voluntary) and maximum blink force was measured for each individual, and we obtained 14.8 ± 0.9 g, 21.3 ±1.8 g and 85.3 ± 5.2 g (SEM) respectively (table 12). We have also made scatter plots to explore possible relationships between each categories (figure 36-38), but were not able to draw much information because of the very small sample size. We believe that with a greater sample size, a more solid conclusion could be formed and determine a norm for each categories. It would be very interesting to compare these results to patients who are suffering from various ophthalmic conditions and perhaps could provide a new method for clinical diagnosis.

CHAPTER 8: CONCLUSIONS AND FUTURE WORK

8.1 Conclusions

In this thesis, blinking dynamics such as PA, blink duration and blink velocity have been explored using a combination of high-speed imaging method and various data analytical techniques. A blinking model based on statistical data has also been generated to discriminate between different diseases from controls. In the latter part of the thesis, a blink force measuring device has been designed and constructed. A small sample of volunteers was tested with this device and the results (i.e. weight of upper eyelid, voluntary natural blink force and the maximum closure force) have been discussed. As a result of this PhD project, one paper has been published in a peer review journal and more are in preparation. A patent has been filed for the force measuring device.

8.1.1 Characteristic blink dynamics in ptosis

A high-speed camera was used to record and characterise voluntary blinking and the blink dynamics of ptosis patients, and were compared to a control group. Twenty-six ptosis patients (of variety of causes) prior to surgery and 45 control subjects were studied and the vertical height of the PA was measured manually at 2 ms intervals during each blink cycle. The PA and blinking speed were plotted with respect to time and a predictive model was

generated to discriminate diseased from healthy subjects. The blink dynamic was first analysed in closing and opening phases, and revealed a reduced speed of the initial opening phase in ptotic patients, suggesting intrinsic muscle function change in ptosis pathogenesis.

The PA versus time curve for each subject was reconstructed using custom-built parameters, and found significant differences between the two groups. Those parameters included the rate of closure, the delay between opening and closing, rate of initial opening, rate of slow opening (non-linear function) and the 'switch point' between those two rates of opening. The 'switch point' of the distinctive two-stage recovery significantly improved the power of the discrimination compared to the beta tests without it. We speculate that the extensive internal connective tissues and the activations of different muscle fibres subtypes in the extraocular muscles contribute to the distinction of ptotic category during the recovery phase.

The parameters of each blink were analysed using LDA and probability-based Gaussian classifier and generated the predictive model. The robustness of this mathematical model was tested against seven additional subjects as a masked control retrospectively, and was able to discriminate ptosis patients from controls with 80% accuracy. The results could potentially improve clinical evaluation and provide a reliable method for the diagnosis and quantification of ptosis. However, at the moment this model appears to be insensitive to the weakness and atrophy of ocular muscles from myopathies or paralysis, contributing the twenty percent mark down. With more sophistication, in terms of introducing more parameters, this model has the potential to predict specific causation of ptosis with a much improved accuracy.

8.1.2 Characterising TED, BEB and ptosis using blink dynamic analysis

A variety of conditions affecting upper eyelid dynamics, including BEB, TED and aponeurotic ptosis patients were investigated by analysing their respective blink dynamic profiles using a high-speed camera image capture. Not only this method is non-invasive, it is also quick and easy to test the patients with a good reproducibility.

Thirteen consecutive BEB, nine consecutive TED and fifteen consecutive ptosis patients were recruited from the oculoplastic service at Moorfields Eye Hospital NHS Foundation Trust. 70 heathy volunteers were also recruited to act as control subjects for this experiment. The same method was employed for this experiment using key features from a standard blink profile, using LDA and multivariate Gaussian probability distributions to generate a predictive model to separate the clinical conditions from controls.

A marked increase of blink duration in BEB and TED was found compared to controls. A reduced maximum speed during the closing phase was also recorded in BEB patients. The predictive model showed significant separation of the mean of the controls from the means of all the diseases, but BEB and TED appear to have more similar blink dynamics. This model was able to distinguish these diseases from controls by analysing the high-speed camera images and achieved accuracy as high as 88.9%.

A detailed analysis of blink dynamics has identified novel characteristics of LPS muscle and OOM function in a variety of disorders affecting the movement of the upper eyelid, as well as describing the clinical phenotype of these conditions. In addition, the modelling has further

confirmed the potential as an additional diagnostic tool, or to monitor clinical progress and outcomes for treatment.

8.1.3 Effects of blepharoplasty surgery for dermatochalasis patients: blink dynamic comparisons between pre-op, post-op and age matched controls using high-speed camera

This study investigates the blinking dynamics of patients suffering from dermatochalasis before and after blepharoplasty surgery and an appropriate control group using a high-speed camera. Voluntary blinking of seven dermatochalasis patients was recorded before and after their corrective surgery, and a group of seven age matched controls. The data gathered were analysed for PA, blink duration and maximum speed of blink during opening and closing phases. A predictive model was generated by calculating the statistics for a number of key parameters extracted from a normal blinking profile to discriminate amongst pre-operation dermatochalasis, post-operation, and controls.

It was found that post-operation patients show improvements in the PA and this measurement in the post-operation group is also significantly greater than controls. Maximum blinking speed is relatively stable across the different groups with post-operation patients showing signs of faster speed during the opening phase. With the multivariable discriminant analysis, it was found that blink duration is essential in classifying the individuals, particularly showing great separation between the pre-operation and the control and post-operation classes.

This study gave us more insight into how successful blepharoplasty surgery is in restoring dermatochalasis patients to normal eye blink performance, and serves as an alternative method to visual appearance for assessing patients post-surgery. The predictive model also achieved 81% accuracy in differentiating across all classes. However, in the future, a power analysis could be employed to determine the minimum sample size required to produce a statistically significant result. This shall improve the accuracy of the model tremendously.

8.1.4 Blink force measurement device

A new apparatus was designed and constructed to allow direct measurement of the force in eyelid closure, particularly the maximum force of contraction and natural force of closure, as well as the weight of eyelids. This study served to define the mechanical characteristics and properties of the muscles involved in blinking.

With a series of concept drawings and CAD 3D drawings, a prototype for measuring forces involved in voluntary blinking was developed. Preliminary testing with a small number of volunteers suggested a few improvements, which was carried out and evolved the current device. Essentially a manual three dimensional positioning unit housing a DFG with a custom build eyelid engagement piece formed the measuring device. A control group of twelve healthy volunteers were recruited from UCL and the instrument measured their weight of the eyelid, natural blinking force (voluntary) and the maximum eyelid closure force with our carefully devised protocol (by collaborating with a qualified ophthalmologist). The operating procedures have markedly improved from the initial prototype and the measured results

appeared to be consistent and repeatable, with the forced closure force comparable to the previous primitive measuring tool by Jacobs from 1950s.

Averaged measurements for each categories were documented and scatter plots were generated with errors bars to investigate the relationships between each categories. The results seems to demonstrate a random spread of information with no distinct separations. However, when Chinese and non-Chinese subjects were highlighted, the scatter plots showed a wider variation of upper eyelid weights for the non-Chinese subjects. Though the (voluntary) natural blink and forced blink forces appear to be well mixed in the data across both subgroups. Gender differences and left-right symmetry provided no further information.

Currently a patent is being filed and we are working towards obtaining ethical approval to test on patients. We can collaborate with MEH to get this device on patient days, e.g. dystonia, blepharospasm and TED patients. This will give us access to a large amount of patients with not-so-common conditions. However, we will first need to increase the subject pool for testing and create a database before starting to gather data from diseased subjects to see whether if there are any correlations between different eye conditions and the force in blinking.

Further improvement of the device could be to develop a strategy or improve the mechanical operation to cater for subjects that may have a hard time cooperating or staying still, such as children and patients with disabilities.

In the future of this project, we hope to gain more information on forces required for blinking, which could also aid on design of new surgical implant materials and improves our understanding of the blinking mechanisms. We may also be able to use such information to

improve clinical diagnoses and implement this procedure as a part of a standard eye examination done regularly at the opticians.

8.2 Recommendations for future work

The work covered by this thesis is essentially two-fold, the high-speed camera work and the force measuring apparatus.

For the high-speed camera work, care must be taken to ensure recruited patients are at the same stage of the disease in question. Diseases that are not primary, have multiple causations, or are on different treatments are more difficult to handle as there will be more to consider during analysis and gathering results. In the present studies, the PA was not strictly the distance between upper and lower eyelid margins but rather the 'opening' or the aperture of the eye. Having said this, it was noticed that in some cases, lower eyelids ascend to narrow the aperture. This may have effects on the speed at which complete closure is achieved. In future studies, it would be interesting to see this effect in a different experimental set up to isolate each eyelid margin and measure the movement of the individual eyelid (upper and lower).

Further in chapter 5, BEB patients were found to have a significantly slower closing phase compared to controls, suggesting slower OOM function in blepharospasm. The reason for such a phenomenon is unclear but indicates the physiology of the closure processes happening behind the scene is likely to be different from the normal blink circuitry, in terms of LPS-OOM coordination. Also, aponeurotic ptosis patients displayed a slower opening phase.

Although insignificant (ptosis speed of opening has an SEM of over 10% of its original value due to a small sample size), a larger sample of aponeurotic ptosis patients may allow more insight on the attenuated PLS maximum velocity, if it was due to an inherent levator myopathy rather than a simple muscular dehiscence as other literature suggested.

In the modelling aspect of the high-speed camera work, it was demonstrated (in chapter 4) in the retrospective test that it might be insensitive to trauma, weakness and atrophy of ocular muscles from myopathies or paralysis. To enhance the power of this model, extra functions (key features) could be designed to capture more features of the PA versus time model curves. It would also be beneficial to add more ptosis and control cases into the learning data set, and also introduce the severity of the ptosis as an extra parameter to improve the outcome of the present model. On the other hand, it is possible that even clinically diagnosed ptosis patients may display some aspect of blinking dynamics that are comparable to controls. This is an area that could be investigated further in the future.

The modelling method covered in chapter 5 has demonstrated its effectiveness to discriminate various conditions, even at the current small sample size. With an increased patient pool, it can improve the learning set of data substantially, and may have potential use as an additional diagnostic tool or to monitor clinical progress and outcomes for treatments. In order to improve the speed at which this modelling process (from camera recording to providing predictions), it is suggested that an automated process be developed, in which the PA can be accurately measured/ detected live, parallel to the high-speed recording. This may be achieved with the combination of eye blink detector using IR light invisible to the human eyes and IR detection unit (Castro, 2008), and a method of eye blink analysis based on eye area approximation, grey scale, brightness and contrasts detection algorithms in the

subsequent recorded images to track eyelid motion automatically (Radlak, et al., 2012). Together with the Mathematica coding and modelling all setup in consequence, it is believed to be possible to generate accurate predictions within seconds after the high-speed camera recording. This would make this process suitable to be employed in clinical practices and even as a part of a standard eye examination at the opticians. This project has great potential to be commercialised once able to determine a norm in the data, and this can be done by testing a large amount of samples (in thousands).

Finally, for the force measuring apparatus, a patent is being filed and as soon as we have obtained ethics approval, the apparatus can then be used to collecting force measurements of a variety of patients. However, the control group must first be expanded greatly to achieve more significant results.

By collecting new blink kinematic information on the muscles involved in blinking, new surgical implant materials can be developed, such as new smart materials for brow-suspension, frontalis sling used in ptosis correction surgeries. Perhaps in the future, material properties that may be suitable for this purpose can be explored; such that they can behave like a muscle, i.e. contract and relax, providing similar blink dynamics as LPS and OOM can be engineered.

a)

ID	blink	start%	toff	min	sharp1	ton	ton-toff	sharp2	tswtch-ton	sharp3	end%	R^2
2C17[LE]		100	33.2221	0.	2.27126	142.476	109.254	0.891468	3.38638×10^{-7}	0.571265	97.8808	0.999623
2C17[RE]		100	43.8741	8.92483	1.68244	149.228	105.354	0.802713	1.13574×10^{-7}	0.446368	94.9334	0.999687
2C4[LE]		97.5162	90.8913	3.48361	1.25145	189.261	98.3694	0.940935	1.6006×10^{-6}	0.505924	100	0.999517
2C4[RE]		100	61.2854	28.8092	0.921826	178.973	117.687	0.637487	0.0036132	0.460459	98.1354	0.999798
2C33[LE]		98.58	54.6811	8.17918	1.78487	150.	95.3189	1.04477	1.88402	0.844755	100	0.99974
2C33[RE]		98.2616	50.5809	0.	2.0516	162.	111.419	0.994389	1.91753	0.825754	100	0.999455
2C1[LE]		100	37.5596	0.	3.1343	151.632	114.072	1.10628	2.24223×10^{-7}	0.480797	98.768	0.999727
2C1[RE]		100	31.8765	0.	3.03873	148.37	116.494	1.00877	0.000450977	0.478152	99.2113	0.999779
2C14[LE]		100	38.6147	0.	3.12388	161.34	122.725	1.1533	4.41675×10^{-7}	2.14341	46.7715	0.708034
2C14[RE]		100	39.8133	0.	3.0232	370.166	330.353	1.49933	-12.1658	1.15636	100	0.800533
2C21[LE]		100	55.1889	0.	1.636	240.	184.811	0.565761	6.38691	0.489616	95.2213	0.995631
2C21[RE]		100	61.7127	0.	1.87946	240.	178.287	0.666018	3.19383	0.486443	100	0.998445
2C25[LE]		100	30.7238	0.	3.26855	141.213	110.49	0.903975	1.24019	0.421698	97.0898	0.99965
2C25[RE]		100	31.3882	0.	3.41929	134.899	103.51	0.964235	0.0685733	0.648443	95.0825	0.999245
2C19[LE]		100	73.9889	0.	1.83591	258.	184.011	1.08525	0.325704	0.650381	100	0.999234
2C19[RE]		100	66.8889	0.	2.50687	286.383	219.494	0.883623	-3.72443	0.617905	98.7569	0.999254
2C23[LE]		100	33.3248	0.	3.58356	160.058	126.733	1.5588	0.866968	0.784379	98.3606	0.999428
2C23[RE]		100	33.4866	0.	3.01685	174.287	140.8	1.12255	-0.0535409	0.488282	99.7782	0.999482
2C43[LE]		100	57.2818	0.	1.42325	201.09	143.809	0.828008	-2.52639×10^{-6}	0.495425	95.4098	0.999666
2C43[RE]		100	59.0504	0.	1.51795	194.175	135.124	0.68507	-34.6442	0.696192	96.0598	0.99987
2C45[LE]		100	46.6449	0.	2.62463	231.15	184.505	0.992585	-6.05824	0.695693	98.3672	0.999603
2C45[RE]		100	52.8357	0.	2.36925	240.627	187.791	0.951203	0.461962	0.608289	98.8019	0.999413
2C6[LE]		98.3098	84.3831	6.51163	1.14438	229.547	145.164	0.638655	3.56948×10^{-6}	0.304058	99.6744	0.999658
2C6[RE]		100	54.0414	0.	1.48616	201.098	147.057	0.719199	1.41229×10^{-8}	0.421515	96.5757	0.999591
2C29[LE]		100	56.9382	0.	1.65816	172.201	115.263	1.12936	0.307515	0.823138	100	0.998426
2C29[RE]		98.2791	49.9313	11.1617	1.62348	160.	110.069	1.02575	1.20728	0.771417	100	0.999038
2C39[LE]		100	53.893	0.	1.68384	314.791	260.898	1.24794	0.00901198	0.577062	97.4634	0.999591
2C39[RE]		100	52.5141	0.	1.77131	305.198	252.683	1.52941	5.52808×10^{-6}	0.489305	96.8735	0.99953
2C7[LE]		100	38.3804	0.	3.27081	221.876	183.496	1.20854	6.06359×10^{-7}	0.828223	97.8826	0.999593
2C7[RE]		100	42.1174	0.	2.70323	229.717	187.6	1.06048	0.0410156	0.641394	100	0.999292
2C11[LE]		100	43.8943	3.51938	1.93051	130.484	86.5893	1.23727	0.216807	0.602812	97.6113	0.999628
2C11[RE]		100	41.9903	0.	2.3819	136.	94.0097	1.00279	0.759684	0.841814	95.6891	0.999539
2C27[LE]		100	65.3627	0.	1.65635	170.	104.637	1.08485	0.848051	0.850493	100	0.999141
2C27[RE]		97.6499	58.2535	0.	1.89224	176.	117.747	1.0902	0.83895	0.746385	100	0.999536
2C31[LE]		100	88.0966	0.	3.07867	223.132	135.035	1.0547	-3.05043	0.804619	100	0.999667
1C17[LE]		100	39.6943	0.	1.67966	243.372	203.678	0.724414	0.543073	0.389829	96.603	0.999329
1C17[RE]		100	33.4965	0.	1.81425	245.236	211.74	0.700388	0.0000132798	0.35635	96.8625	0.999158
1C4[LE]		100	89.9999	0.	1.25	311.16	221.16	0.782197	0.0551384	0.622711	100	0.997566
1C4[RE]		100	84.7593	0.	1.00213	305.	220.241	0.848365	2.96477	0.534057	100	0.997588
1C11[LE]		100	36.4342	0.	2.29251	141.394	104.96	0.629395	10.545	0.586968	96.2694	0.99931
1C11[RE]		100	33.5536	0.	2.58875	145.195	111.641	0.761879	1.60185×10^{-6}	0.515101	97.0299	0.999492
1C3[LE]		100	37.9166	0.	1.75619	241.642	203.725	0.662424	-4.82031×10^{-6}	0.336546	96.551	0.999524

b)

ID	blink	start%	toff	min	sharp1	ton	ton-toff	sharp2	tswtch-ton	sharp3	end%	R^2
2C3[LE]		98.7789	55.7812	18.4312	0.976381	291.966	236.185	0.403157	-66.7096	0.908702	100	0.998883
2C3[RE]		100	60.5286	0.	1.30547	286.	225.471	0.841404	1.46327	0.817869	98.2011	0.999633
2C9[LE]		100	87.1258	0.	0.619471	580.617	493.491	0.498745	-24.0745	1.4658	100	0.983896
2C9[RE]		100	62.6204	2.27962	1.00009	552.	489.38	0.728894	3.53897	1.34438	100	0.979362
1C14[LE]		100	38.8959	0.	1.61895	149.218	110.322	0.934634	8.57101×10^{-8}	0.760007	100	0.999609
1C14[RE]		100	38.7413	0.	1.70884	151.342	112.601	0.929893	1.05234×10^{-6}	0.703858	100	0.999374
1C19[LE]		100	37.1739	0.	1.79365	133.082	95.9084	1.51255	1.1274×10^{-6}	0.46825	93.3907	0.999705
1C19[RE]		100	38.7137	0.	1.90453	137.635	98.9216	1.06242	-1.46246×10^{-6}	0.460048	93.7922	0.99936
1C23[LE]		100	46.5627	0.	1.31611	179.703	133.14	0.702856	3.84566	0.908607	96.8043	0.99963
1C23[RE]		100	40.4948	0.	1.34763	169.307	128.812	0.880262	-3.85497	0.73829	97.9125	0.999245
1C13[LE]		98.1131	33.8215	0.	1.99885	153.824	120.003	1.4396	-2.7175×10^{-7}	0.743258	100	0.999068
1C13[RE]		100	30.2432	0.	1.90724	159.94	129.697	1.19578	0.171968	0.524323	100	0.99968
1C18[LE]		100	34.123	0.	2.22523	145.999	111.876	0.96759	1.13385	0.560937	96.1897	0.999545
1C18[RE]		100	38.4717	0.	2.00128	138.973	100.501	1.15664	0.0000154144	0.632474	96.8227	0.999724
1C26[LE]		100	42.097	0.	1.27146	172.895	130.798	0.961107	1.74531	0.696974	97.8363	0.99957
1C26[RE]		100	45.0411	0.	1.17084	168.8	123.759	1.09411	-32.7178	0.979436	96.6319	0.99953
1C29[LE]		100	33.379	0.	1.61863	166.144	132.765	1.02243	5.19105×10^{-7}	0.61	97.5402	0.999702
1C29[RE]		100	32.9711	0.	1.68499	165.	132.029	0.93273	1.75596	0.577591	98.112	0.999544
1C27[LE]		100	42.2076	0.	1.25778	215.397	173.189	0.697242	-24.4412	0.969226	96.283	0.999612
1C27[RE]		100	43.8912	0.	1.32285	204.551	160.66	0.801544	-16.1862	0.756635	95.256	0.999551
1C33[LE]		100	45.1114	0.	1.56186	147.251	102.139	1.27801	2.14028×10^{-7}	0.500041	97.6648	0.999518
1C33[RE]		100	36.5469	0.	1.83971	145.913	109.367	1.31362	-9.33384	0.641479	97.3577	0.999732
1C22[LE]		100	42.9269	0.	1.41846	179.086	136.159	0.846792	2.96005×10^{-6}	0.368497	97.3816	0.999612
1C22[RE]		100	35.6257	0.	1.35472	172.47	136.845	1.02129	1.18622×10^{-6}	0.342688	97.5292	0.999403
1C6[LE]		100	43.2193	0.	1.98748	163.953	120.734	0.805678	6.85561×10^{-6}	0.409538	93.1493	0.99884
1C6[RE]		100	41.8206	0.	1.83617	151.839	110.018	0.958252	-1.62638×10^{-6}	0.270713	100	0.998207
1C15[LE]		100	41.7726	0.	1.47325	158.62	116.847	1.05586	-1.55792×10^{-6}	0.549295	97.8623	0.999738
1C15[RE]		100	39.1308	0.	1.43614	157.003	117.873	1.14095	1.27203×10^{-6}	0.415841	98.9852	0.999799
1C24[LE]		100	41.8316	0.	1.29006	191.351	149.519	0.849861	8.10975	1.46383	100	0.999109
1C24[RE]		100	41.8344	0.	1.27319	193.951	152.117	0.868174	-22.0629	1.46044	97.4715	0.999266
1C25[LE]		100	38.5226	0.	1.2473	175.102	136.579	1.05957	-40.1015	0.992079	96.4205	0.999395
1C25[RE]		100	36.9686	0.	1.40018	171.735	134.766	1.1179	0.715391	0.598322	96.7475	0.999573
1C32[LE]		100	45.0391	0.	1.05775	184.245	139.206	0.820004	0.0366348	0.893446	100	0.99944
1C32[RE]		100	50.724	0.	1.14964	174.036	123.312	0.979283	3.23329	1.02608	100	0.999449
1C16[LE]		100	39.6214	0.	1.95492	148.294	108.672	0.965934	4.62835×10^{-6}	0.389442	100	0.997368
1C16[RE]		100	42.3248	0.	1.82713	130.978	88.6537	1.44761	0.917278	0.62938	95.407	0.999351
1C9[LE]		100	26.0094	0.	2.60262	144.13	118.121	1.16382	3.15728	1.07914	100	0.998985
1C9[RE]		100	26.1296	0.	2.99499	141.496	115.366	1.21164	1.16588	1.09058	100	0.999089
1C8[LE]		100	37.3607	0.	1.76059	174.848	137.487	1.42648	-2.43325	0.808568	100	0.999533
1C8[RE]		100	35.5805	0.	1.87452	170.	134.42	1.57893	2.05634	0.884057	98.2697	0.99952
1C20[LE]		100	48.0826	0.	1.50689	244.511	196.428	0.720256	0.282954	0.428746	98.506	0.99899
1C20[RE]		100	43.6292	0.	1.39165	253.047	209.418	0.576918	-28.0472	0.834081	97.565	0.999766
1C21[LE]		100	34.191	0.	1.5384	168.842	134.651	1.24646	0.0340954	0.747187	98.2075	0.999498
1C21[RE]		100	33.3826	0.	1.67029	159.106	125.724	1.49692	1.21643×10^{-6}	0.991595	95.7101	0.999373
1C30[LE]		100	33.6227	0.	1.4406	216.962	183.339	0.552403	-22.2092	0.7582	96.371	0.99943
1C30[RE]		100	34.9997	0.	1.33497	229.981	194.981	0.469768	-77.7823	0.704274	92.8435	0.998557

Appendix 1.| Details of subjects a) Control subjects in the ≥40 group. b) Control subjects for the <40 years group. Start% = starting PA (normalised); toff = Time offset at half of closure; min = minimum PA; sharp1 (v_1)= rate of closure; ton = time onset at half initial opening; ton-toff = (t_{off}-t_{on}), time between half closing and half opening; tswitch-ton = (t_4-t_{open}), time delay from half opening to time of switch; sharp2 (v_2)= rate of initial opening; sharp3 (α)= shape parameter of late opening; end% = % of full recovery from start%.

Type	Case		sharp1	sharp2	ton − toff	tswitch − ton	sharp3
"Ptosis"	"2 − 49[RE]"	""	3.368677375978806	1.0273712786544358	141.32391508581355	1.0979057504223704	0.6958563033930171
"Ptosis"	"2 − 24[LE]"	""	2.900216369206696	0.5214602711867842	204.0046854882641	−19.66930493837708	0.3408239000685124 3
"Ptosis"	"2 − 26[LE]"	""	1.0950982608233455	1.0301143850649996	351.35616040 0036	0.5100658307 65484	0.7338379451237389
"Ptosis"	"2 − 14[LE]"	""	1.9315139384408515	0.6032077990873379	194.5102289195452	−56.219636231185234	0.8073599700979737
"Ptosis"	"2 − 59[RE]"	""	1.5668705517423225	0.8265566937486285	129.60068385318476	0.000001009717720990011	0.4692190549366513
"Ptosis"	"2 − 34[LE]"	""	1.9192592174949321	0.7591198579720354	429.29265724906776	0.000008969095006250427	0.5306210565985764
"Ptosis"	"2 − 55[RE]"	""	2.204961166571539	0.8515246444572468	107.70009849715221	1.5226030719531423	0.8104804880505678
"Ptosis"	"2 − 53[RE]"	""	1.6553906409166277	0.3106962918601033	202.9980458592081	$5.713868347356765 \times 10^{-7}$	0.1261026608429714
"Ptosis"	"2 − 46[LE]"	""	2.322047784532598	0.8011178794814411	455.3594609020202	0.8298053336362727	0.7593203913033452
"Ptosis"	"2 − 2[LE]"	""	1.9436779791235468	0.8133690653150573	156.58371162042647	−0.000005572295549427508	0.4127465149249126
"Ptosis"	"2 − 3[LE]"	""	2.1237675833646876	0.8170291938716648	118.952516304 68971	−3.237176741605822	0.4826653611265786
"Ptosis"	"2 − 5[LE]"	""	2.0391375635918845	0.8295507411372246	319.0641780145527	0.07460660035860656	0.5952180819787629
"Ptosis"	"2 − 5[RE]"	""	1.7900617369106564	0.5804612 67639218	289.0179966532667	0.000161854 90892439702	0.6353287382561554
"Ptosis"	"2 − 30[LE]"	""	1.9603675597306762	0.8811325625671573	112.64301189188059	0.000002341264121241693	0.5217198381202035
"Ptosis"	"2 − 42[LE]"	""	2.4959194789426635	0.6528114739185951	165.23455927008783	−34.8222624600 1048	0.8725882638427246
"Ptosis"	"2 − 65[LE]"	""	1.6147597240221472	0.6281092964431323	175.61898117229083	−10.250738588290943	0.4055168009619013
"Ptosis"	"2 − 65[RE]"	""	1.8151823443419983	0.6722278822815031	165.82866106844605	0.000002731822547730189	0.6437431739060031
"Ptosis"	"2 − 13[LE]"	""	3.3364805514672 15	0.656308974017873	234.5095138511998	−2.316693203806551	0.5515784472932435
"Ptosis"	"2 − 13[RE]"	""	3.7046568738213 03	0.7685942661619549	234.92102274150227	1.12878777884805	0.6570514395201754
"Ptosis"	"2 − 9[RE]"	""	2.1247386146053713	1.5820076186056273	110.94916767033016	0.2908840402560599 6	1.025108457915364
"Ptosis"	"2 − 10[LE]"	""	1.3047293302009 83	0.792933671658109	95.42689007350475	$5.309123309871211 \times 10^{-7}$	0.3309765683449008
"Ptosis"	"2 − 10[RE]"	""	1.5119360813522242	0.6006023027745 73	103.37437483149725	1.43595261842961	0.4556877229466043 7
"Ptosis"	"2 − 15[RE]"	""	2.5301480338077873	0.8854940499669689	111.31366996014034	−9.636256523881343	0.6629076619384574
"Ptosis"	"2 − 40[LE]"	""	1.5750285100331192	0.7108719807222778	135.44315476196806	0.2846425728960184 6	0.5985185818777006
"Ptosis"	"2 − 40[RE]"	""	1.6620661079187768	0.7232173394169286	143.03489607116433	−57.4215261916778	0.9049420971351688
"Ptosis"	"2 − 8[LE]"	""	3.913499120765801	1.3192532884866082	124.63721001135761	−12.302618720828775	0.7840184124069054
"Ptosis"	"2 − 6[LE]"	""	3.52179962948167	1.0930414845110603	180.8797591242045	−21.9780041238582	1.0768965174356928
"Ptosis"	"2 − 6[RE]"	""	3.07389763410387	0.8973947152331521	134.69561892501528	0.06584597743997733	0.7743101876501488
"Ptosis"	"2 − 47[LE]"	""	1.1921137061607197	1.0828228759392529	250.6080191880051	$-8.889863352123939 \times 10^{-7}$	0.4478618392034952 6
"Ptosis"	"2 − 51[RE]"	""	2.5920712608565726	0.7952972483609193	123.1369075608118	−0.000002160988543664643	0.27916567650817786
"Normal"	"2C17[LE]"	""	2.2712625450551984	0.8914678228726701	109.25352700157964	$3.386380740266759 \times 10^{-7}$	0.5712652325382578
"Normal"	"2C17[RE]"	""	1.6824374860 96256	0.8027130334067948	105.35428696184144	$1.135744014391093 \times 10^{-7}$	0.4463675944895713
"Normal"	"2C4[LE]"	""	1.2514522221738984	0.9409348292953218	98.36936702718752	0.000001600596078 78793	0.5059236979462699
"Normal"	"2C4[RE]"	""	0.9218263511075157	0.6374872869383892	117.68730990274341	0.0036132040606 27595	0.460458835453785 85
"Normal"	"2C33[LE]"	""	1.7848746868818957	1.0447670939862925	95.31888197501743	1.8840161396143458	0.8447551436914686
"Normal"	"2C33[RE]"	""	2.0516030545284 39	0.9943888228124 38	111.4191212214113	1.9175271422074331	0.825753855975264
"Normal"	"2C1[LE]"	""	3.1343010583692346	1.10628018633748	114.07220690440796	$2.242230436877435 \times 10^{-7}$	0.4807932295390404
"Normal"	"2C1[RE]"	""	3.0387260513907 38	1.0087728141437005	116.49353147086683	0.000450977393 6831607	0.4781521248092253
"Normal"	"2C21[LE]"	""	1.6360002589999634	0.5657606460080972	184.81108180660112	6.386909439815952	0.4896164866473619
"Normal"	"2C21[RE]"	""	1.8794576858259526	0.6660175677 1655	178.28726399991746	3.193829776964293	0.4864431219584003
"Normal"	"2C25[LE]"	""	3.268553063218819	0.9039748201961528	110.48963449432114	1.240194544927192	0.4216979321368702 3
"Normal"	"2C25[RE]"	""	3.419294862698407	0.9642351099140176	103.5104346022311	0.06857330884173507	0.6484432870200165
"Normal"	"2C19[LE]"	""	1.8359124517606606	1.0852465162344258	184.01108103529145	0.3257035729080826	0.650381320645009
"Normal"	"2C19[RE]"	""	2.5068650811193796	0.8836234043341648	219.49380868781958	−3.7244262204764595	0.6179054981784229
"Normal"	"2C23[LE]"	""	3.5835612834380903	1.5588014131211256	126.73346988154208	0.866967543063 2253	0.7843790615629 71
"Normal"	"2C23[RE]"	""	3.0168471121168805	1.1225477735987726	140.80033195984484	−0.053540947896891566	0.4882823197231946 4
"Normal"	"2C43[LE]"	""	1.4232514200075694	0.8280083872997878	143.80856014170467	−0.000002526393132029625	0.4954252902037586 4
"Normal"	"2C43[RE]"	""	1.5179491631535635	0.6850703006038039	135.1241043119386	−34.64419371105518	0.6961916866386257
"Normal"	"2C45[LE]"	""	2.6246264280269327	0.9925853631945898	184.50545635995218	−6.058242872200765	0.6956933811002726
"Normal"	"2C45[RE]"	""	2.3692490329535336	0.9512028968491981	187.7912242289271	0.4619622590265635	0.6082894063258245
"Normal"	"2C6[LE]"	""	1.1443784875401901	0.6386546214833452	145.1639765903745	0.000003569476888287681	0.3040583101168715
"Normal"	"2C6[RE]"	""	1.4861604268688149	0.7191991505241897	147.05664763312302	$1.412286110280547 \times 10^{-8}$	0.4215152235265713 4
"Normal"	"2C29[LE]"	""	1.6581600339863554	1.129355339735196	115.26282659880039	0.3075153491987805 4	0.8231379279733134
"Normal"	"2C29[RE]"	""	1.6234806121294196	1.025752558907707	110.0687346933656	1.2072815159877166	0.7714169633556305
"Normal"	"2C39[LE]"	""	1.6838444131629409	1.2479445985135067	260.898467 86466	0.0090119819424 78542	0.5770618078284132
"Normal"	"2C39[RE]"	""	1.7713120301423588	1.5294147133038416	252.6834670712903	0.000005528078531824576	0.4893053733800427 6
"Normal"	"2C7[LE]"	""	3.270812588351346	1.2085408449683313	183.4955168367344	$6.063594639726944 \times 10^{-7}$	0.8282234809961908
"Normal"	"2C7[RE]"	""	2.7032336493002185	1.0604799964803695	187.5996580318784 2	0.0410155798498 69255	0.641394115469721
"Normal"	"2C11[LE]"	""	1.9305134567547555	1.2372653641224902	86.58930885590499	0.2168073551960 43	0.6028121402348943
"Normal"	"2C11[RE]"	""	2.3818977848209073	1.0027877457125696	94.00969072128709	0.7596844923427568	0.8418136597147221
"Normal"	"2C27[LE]"	""	1.6563492237076893	1.08485031543859	104.63730778170722	0.8480509468983541	0.8504927089629816
"Normal"	"2C27[RE]"	""	1.8922389843940755	1.0902010806953213	117.74651122730839	0.8389495925056565	0.7463850140892423
"Normal"	"2C31[LE]"	""	3.0786650042741317	1.0547030366491739	135.03547358195905	−3.050432911215 7507	0.8046188834096539
"Normal"	"1C17[LE]"	""	4.199157643944056	1.8110359560234228	81.47100592703413	0.2172292463565952 4	0.9745725977080405
"Normal"	"1C17[RE]"	""	4.535630240024286	1.750970556989789	84.69596240614284	0.000001001891845930913	0.8908741617865324
"Normal"	"1C4[LE]"	""	3.124989208773192	1.9554929065141888	88.46413968 50271	0.022055371975355342	1.556778260818234
"Normal"	"1C4[RE]"	""	2.505324085981087	2.1209132335006196	88.09628415 66249	1.185908452962039	1.3351422117976646
"Normal"	"1C11[RE]"	""	6.471869053461678	1.9047138638539378	44.6565999197 00895	$6.131259553399104 \times 10^{-7}$	1.2877284682996095
"Normal"	"1C3[LE]"	""	4.390474095278673	1.6560600291526861	81.490174565643	0.000001073950485874775	0.8413645834774283

Appendix 2.| Details of all subjects involved in this part of the test are included here (age ≥40 ptosis vs Controls). The values of minimum, start and end percentages are neglected as they do not have much influence on the shape: v_1, v_2 and α are shown as sharp1, sharp2 and sharp3 on this table, respectively.

References

Abell K.M. [et al.] Efficacy of Gold Weight Implants in Facial Nerve Palsy: Quantitative Alterations in Blinking [Journal] // Vision Res. - 1998. - 19 : Vol. 38. - pp. 3019-3023.

Agostino R. [et al.] Voluntary, Spontaneous, and Reflex Blinking in Parkinson's Disease [Journal] // Mov Disord.. - 2008. - 5 : Vol. 23. - pp. 669-675.

Anwar A. When is Facial Paralysis Bell Palsy? Current Diagnosis and Treatment [Journal] // Clev Clin J Med. - 2005. - 5 : Vol. 72. - pp. 398-405.

Aramideh M. [et al.] Abnormal Eye Movements in Blepharospasm and Involuntary Levator Palpebrae Inhibition. Clinical and Pathophysiological Considerations [Journal] // Brain. - Dec 1994. - 6 : Vol. 117. - pp. 1457-1474.

Aramideh M. [et al.] Motor Persistence of Orbicularis Oculi Muscle in Eyelid-Opening Disorders [Journal] // Neurology. - 1995. - 5 : Vol. 45. - pp. 897-902.

Arat YO. [et al.] Acute, Unilateral Transient Blepharoptosis of Unknown Etiology: A Review [Journal] // Ophthal Plast Reconstr Surg.. - 2013. - 5 : Vol. 29. - pp. 396-399.

Augusteyn R. [et al.] Human Ocular Biometry [Journal] // Exp Eye Res. - 2012. - 1 : Vol. 102. - pp. 70-75.

Bahn RS. Graves' Ophthalmopathy [Journal] // N Engl J Med. - 2010. - 8 : Vol. 362. - pp. 726-738.

Ballen PH. and Rochkopf L. Congenital Retraction of the Upper Lid [Journal] // Ophthalmic Surg.. - 1987. - 9 : Vol. 18. - pp. 689-690.

Bartalena L., Pinchera A. and Marcocci C. Management of Graves' Ophthalmopathy: Reality and Perspectives [Journal] // Endocr Rev.. - 2000. - 2 : Vol. 21. - pp. 168-199.

Bentivoglio A.R. [et al.] Analysis of Blink Rate in Patients with Blepharospasm [Journal] // Mov Disord.. - 2006. - 8 : Vol. 21. - pp. 1225-1229. - Very interesting read that suggest blink rate is relevant to development of BSP..

Bentivoglio A.R. [et al.] Analysis of Blink Rate Patterns in Normal Subjects [Journal] // Mov Disord.. - November 1997. - 6 : Vol. 12. - pp. 1028-1034.

Bishop CM. Discriminant Functions [Book Section] // Pattern Recognition and Machine Learning. - [s.l.] : Springer Internation Edition, 2006.

Boghen D. Apraxia of Lid Opening: A Review [Journal] // Neurology. - 1997. - 6 : Vol. 48. - pp. 1491-1503.

Bologna M. [et al.] Blinking in Patients with Clinically Probable Multiple System Atrophy [Journal] // Mov Disord.. - 2014. - 3 : Vol. 29. - pp. 415-420.

Bologna M. [et al.] Voluntary, Spontaneous and Reflex Blinking in Patients With Clinically Probable Progressive Supranuclear Palsy [Journal] // Brain. - 2009. - 2 : Vol. 132. - pp. 502-510.

Bullock JD. [et al.] Psychosocial Implications of Blepharoptosis and Dermatochalasis [Journal] // Trans Am Ophthalmo Soc. - 2001. - 1 : Vol. 99. - pp. 65-71.

Burch HB. and Wartofsky L. Graves' Ophthalmopathy: Current Concepts Regarding Pathogenesis and Management [Journal] // Endocr Rev. - 1993. - 6 : Vol. 14. - pp. 747-793.

Carter S.R., Meecham W.J. and Seiff S.R. Silicone Frontalis Slings for the Correction of Blepharoptosis: Indications and Efficacy [Journal] // Ophthalmology. - 1996. - 4 : Vol. 103. - pp. 623-630.

Carter SR. [et al.] Lower Eyelid CO2 Laser Rejuvenation: A Randomized Prospective Clinical Study [Journal] // Ophthalmology. - 2001. - 3 : Vol. 108. - pp. 437-441.

Castro F. L. Class I Infrared Eye Blinking Detector [Journal] // Sensors and Actuators A: Physical. - 2008. - 2 : Vol. 148. - pp. 388-394.

Chakravorty NK. Treatment of Blepharospasm with Levodopa [Journal] // Postgrad Med J. - 1974. - 586 : Vol. 50. - pp. 521-523.

Chand RP. and Park DM. Atypical Blepharospasm Responsive to Sodium Valproate [Letter] [Journal] // Mov Disord. - 1994. - 1 : Vol. 9. - pp. 116-117.

Choi SH. [et al.] Blepharokymographic Analysis of Eyelid Motion in Bell's Palsy [Journal] // Laryngoscope. - 2007. - 2 : Vol. 117. - pp. 308-312.

Choi SH. [et al.] Dynamic and Quantitative Evaluation of Eyelid Motion Using Image Analysis [Journal] // Med. Biol. Eng. Comput.. - 2003. - 2 : Vol. 41. - pp. 146-150.

Chow K., Deva N. and Ng S.G.J. Prolene Frontalis Suspension in Paediatric Ptosis [Journal] // Eye. - 2011. - 6 : Vol. 25. - pp. 735-739.

Chundury RV., Couch SM. and Holds JB. Comparison of Perferences Between OnabotulinumtoxinA (Botox) and IncobotulinumtoxinA (Xeomin) in the Treatment of Benign Essential Blepharospasm [Journal] // Ophthal Plast Reconstr Surg. - 2013. - 3 : Vol. 29. - pp. 205-207.

Collewijn H., vander F. Mark and Jansen T. Precise Recording of Human Eye Movements [Journal] // Vision Res. - 1975. - 3 : Vol. 15. - pp. 447-450.

Cooper DS. Hyperthyroidism [Journal] // Lancet. - 2003. - 9382 : Vol. 343. - pp. 459-468.

Cooper W. On Protrusion of the Eyes, in Connection with Anemia, Palpitation and Goiter [Journal] // Lancet. - 1849. - 1 : Vol. 1. - p. 551.

Costa PG. [et al.] Comparative Study of Botox Injection Treatment for Upper Eyelid Retraction with 6-Month Follow-up in Patients wiht Thyroid Eye Disease in the Congestive or Fibrotic Stage [Journal] // Eye (Lond). - 2009. - 4 : Vol. 23. - pp. 767-773.

Crawford J.S. Repair of Ptosis Using frontalis Muscle and Fascia Lata: A 20-year Review [Journal] // Ophthalmic Surgery. - 1977. - 4 : Vol. 8. - pp. 31-40.

Cruz AAV. [et al.] Graves Upper Eyelid Retraction [Journal] // Surv Ophthalmo. - 2013. - 1 : Vol. 58. - pp. 63-76.

Cruz AAV. [et al.] Supramaximal Levator Resection for Unilateral Congenital Ptosis: Cosimetic and Functional Results [Journal] // Ophthal Plast Reconstr Surg. - 2014. - 5 : Vol. 30. - pp. 366-371.

Davies MJ. and Dolman PJ. Levator Muscle Enlargement in Thyroid Eye Disease-Related Upper Eyelid Retraction [Journal] // Ophthal Plast Reconstr Surg. - 2017. - 1 : Vol. 33. - pp. 35-39.

De Renzi E., Gentilini M. and Bazolli C. Eyelid Movement Disorders and Motor Impersistence in Acute Hemisphere Disease [Journal] // Neurology. - 1986. - 3 : Vol. 36. - pp. 414-418.

DeAngelis DD., Carter SR. and Seiff SR. Dermatochalasis [Journal] // Int Ophthalmo Clin. - 2002. - 2 : Vol. 42. - pp. 89-101.

Defazio G. [et al.] Environmental Risk Factors and Clinical Phenotype in Familial and Sporadic Primary Blepharospasm [Journal] // Neurology. - 2011. - 7 : Vol. 77. - pp. 631-637.

Defazio G. Epidemiology of Primary and Secondary Dystonia. Handbook of Dystonia [Book] / ed. M.E. Stacey. - New York : Informa Healthcare USA, Inc., 2007. - pp. 11-20.

Defazio Giovanni and Livrea Paolo Epidemiology of Primary Blepharospasm [Journal] // Mov Disord.. - [s.l.] : Wiley-Liss, Inc., 2002. - 1 : Vol. 17. - pp. 7-12.

Delgao-Garcia J.M., Gruart A. and Trigo J.A. Physiology of the Eyelid Motor System [Journal] // Ann N Y Acad Sci. - 2003. - 1 : Vol. 1004. - pp. 1-9.

Deuschl G. and Goddemeier C. Spontaneous and Reflex Activity of Facial Muscles in Dystonia, Parkinson's Disease, and in Normal Subjects [Journal] // J Neurol Neurosurg Psychiatry. - 1998. - 3 : Vol. 64. - pp. 320-324.

Dewey RB Jr. and Maraganore DM. Isolated Eyelid-Opening Apraxia: Report of a New Levodopa-Responsive Syndrome [Journal] // Neurology. - 1994. - 9 : Vol. 44. - pp. 1752-1754.

Doane MG. Dynamics of the Human Blink [Journal] // Ber Zusammenkunft Dtsch Ophthalmol Ges.. - 1979. - 1 : Vol. 77. - pp. 13-17.

Dortzbach RK. and Sutula FC. Involutional Blepharoptosis. A Histological Study [Journal] // Arch Ophthalmol. - 1980. - 11 : Vol. 98. - pp. 2045-2049.

Downes R.N. and Collin J.R.O. The Mersilene Mesh Sling - A New Concept in Ptosis Surgery [Journal] // Br J Ophthalmol. - 1989. - 7 : Vol. 73. - pp. 498-501.

Dutton J.J. A Color Atlas of Ptosis: A Practical Guide to Evaluation and Management [Book]. - [s.l.] : P G Publishing Pre Ltd., 1989.

Eckstein AK. [et al.] Euthyroid and Primarily Hypothyroid Patients Develop Milder and Significantly More Asymmetrical Graves Ophthalmopathy [Journal] // Br J Ophthalmol. - Aug 2009. - 8 : Vol. 93. - pp. 1052-1056.

Eden K. and Trotter W. Lid Retraction in Toxic Diffuse Goitre [Journal] // Lancet. - 1942. - pp. 385-387.

Edmonson B.C. and Wulc A.E. Ptosis Evaluation and Management [Journal] // Otolaryngol Clin North Am.. - 2005. - 5 : Vol. 38. - p. 921.

El-Toukhy E. [et al.] Mersilene Mesh Sling as an Alternative to Autogenous Fascia Lata in the Management of Ptosis [Journal] // Eye. - 2001. - 2 : Vol. 15. - pp. 178-182.

Estcourt S. [et al.] The Patient Experience of Service for Thyroid Eye Disease in the United Kingdom: Results of a Nationwide Survey [Journal] // Eur J Endocrinol. - 2009. - 3 : Vol. 161. - pp. 483-487.

Esteban A. and Gimenez-Roldan S. Involuntary Closure of Eyelids in Parkinsonism. Electrophysiological Evidence for Prolonged Inhibition of the Levator Palpebrae Muscles [Journal] // J Neurol Sci.. - Jul 1988. - 3 : Vol. 85. - pp. 333-345.

Esteban A. and Gimenez-Roldan S. Nociceptive Reflex of the Orbicularis Oculi. Study in Normal Subjects and in Peripheral Facial Lesions [Journal] // Arch Neurobiol (Madr). - 1973. - 4 : Vol. 36. - pp. 283-294.

Etgen T. [et al.] Bilateral Grey Matter Increase in the Putamen in Primary Blepharospasm [Journal] // J. Neurol Neurosurg Psychiatry. - 2006. - 9 : Vol. 77. - pp. 1017-1020.

Evinger C. [et al.] Blinking and Associated Eye Movements in Humans, Guinea Pigs, and Rabbits. [Journal] // J Neurophysiol.. - 1984. - 2 : Vol. 52. - pp. 323-339.

Evinger C., Manning KA. and Sibony PA. Eyelid Movements: Mechanisms and Normal Data [Journal] // Invest Ophthalmol Vis Sci. - Feb 1991. - 2 : Vol. 32. - pp. 384-400.

Falcao MF. [et al.] The Relationship Between Two Types of Upper Eyelid Movements: Saccades and Pursuit [Journal] // Invest Ophthalmol Vis Sci.. - 2008. - 6 : Vol. 49. - pp. 2444-2448.

Farooqui AA. [et al.] Oculomotor Palsy Following Varicella in an Immunocompetent Adult [Journal] // South Med J. - 2009. - 4 : Vol. 102. - p. 445.

Finsterer J. Ptosis: Causes, Presentation and Management [Journal] // Aesthetic Plast Surg.. - 2003. - 3 : Vol. 27. - pp. 193-204.

Flanagan J.C. and Campbell C.B. The Use of Autogenous Fascia Lata to Correct Lid and Orbital Deformities [Journal] // Transactions of the American Ophthalmology Society. - 1981. - 1 : Vol. 79. - pp. 227-242.

Forget R. [et al.] Botulinum Toxin Improves Lid Opening Delays in Blepharospasm-Associated Apraxia of Lid Opening [Journal] // Neurology. - 2002. - 12 : Vol. 58. - pp. 1843-1846.

Fox S.A. Ophthalmic Plastic Surgery. [Book]. - New York : Grune & Stratton, 1976. - 5th.

Fox S.A. Surgery of Ptosis [Book]. - Baltimore, USA : The Williams & Wilkins Company, 1980.

Fox S.A. The Palpebral Fissure [Journal] // Am. J. Ophthalmol.. - 1966. - 1 : Vol. 62. - pp. 73-78.

Frueh B.R. and Musch D.C. Evaluation of Levator Muscle Integrity in Ptosis with Levator Force Measurement [Journal] // Ophthalmology. - 1996. - 2 : Vol. 103. - pp. 244-250.

Frueh B.R. and Musch D.C. Levator Force Generation in Normal Subjects [Journal] // Trans Am Ophthalmol Soc.. - 1990. - Discussion 120-1 : Vol. 88. - pp. 109-121.

Fuchs AF. [et al.] Discharge Patterns of Levator Palpebrae Superioris Motoneurons During Vertical Lid and Eye Movements in the Monkey. [Journal] // J. Neurophysiol.. - 1992. - 1 : Vol. 68. - pp. 233-243.

Fuchs AF. and Robinson DA. A Method for Measuring Horizontal and Vertical Eye Movement Chronically in the Monkey [Journal] // J Appl Physiol. - 1966. - 3 : Vol. 21. - pp. 1068-1070.

Fujiwara T. [et al.] Etiology and Pathogenesis of Aponeurotic Blepharoptosis [Journal] // Ann Plast Surg.. - 2001. - 1 : Vol. 46. - pp. 29-35.

Garcia D. [et al.] Spontaneous Interblink Time Distributions in Patients with Graves' Orbitopathy and Normal Subjects [Journal] // Invest Ophthalmol Vis Sci. - 2011. - 6 : Vol. 52. - pp. 3419-3424.

Garcia DM. [et al.] Spontaneous Blinking in Patients with Graves' Upper Eyelid Retraction [Journal] // Curr Eye Res. - 2010. - 6 : Vol. 35. - pp. 459-465.

Garrity JA. [et al.] Results of Transantral Orbital Decompression in 428 Patients with Severe Graves' Ophthalmopathy [Journal] // Am J Ophthalmol. - 1993. - 5 : Vol. 116. - pp. 533-547.

Gay AJ. and Wolkstein MA. Topical Guanethidine Therapy for Endocrine Lid Retraction [Journal] // Arch Ophthalmol. - 1966. - 3 : Vol. 76. - pp. 364-367.

Georgescu D. [et al.] Upper Eyelid Myectomy in Blepharospasm with Associated Apraxia of Lid Opening [Journal] // Am J Ophthalmol.. - 2008. - 3 : Vol. 145. - pp. 541-547.

Goldstein JE. and Cogan DG. Apraxia of Lid Opening [Journal] // Arch Ophthalmol. - 1965. - 1 : Vol. 73. - pp. 155-159.

Gosain AK. [et al.] Surgical Anatomy of the SMAS: A Reinvestigation [Journal] // Plast Resconstr Surg. - 1993. - 7 : Vol. 92. - pp. 1254-1263.

Graves RJ. Clinical Lecture [Journal] // London Medical and Surgical Journal. - 1835. - 164 : Vol. 7. - pp. 225-232.

Gruart A., Blazquez P. and Delgado-Garcia JM. Kinematics of Spontaneous, Reflex and Conditioned Eyelid Movements in the Alert Cat [Journal] // J Neurophysiol. - 1995. - 1 : Vol. 74. - pp. 226-248.

Guinot C. [et al.] Relative Contribution of Intrisics vs Extrinsic Factors to Skin Aging as Determined by a Validated Skin Age Score [Journal] // Arch Dermatol. - 2002. - 11 : Vol. 138. - pp. 1454-1460.

Guitton D., Simard R. and Codere F. Upper Eyelid Movements Measured With a Search Coil During Blinks and Vertical Saccades [Journal] // Invest Ophthalmol Vis Sci. - 1991. - 13 : Vol. 32. - pp. 3298-3305.

Hakkanen H. [et al.] Blink Duration as an Indicator of Driver Sleepiness in Professional Bus Drivers [Journal] // Sleep. - 1999. - 6 : Vol. 22. - pp. 798-802.

Hallett M. [et al.] Update on Blepharospasm: Report From the BEBRF International Workshop [Journal] // Neurology. - 2008. - 16 : Vol. 71. - pp. 1275-1282.

Hallett M. Blepharospasm: Recent Advances [Journal] // Neurology. - 2002. - 9 : Vol. 59. - pp. 1306-1312.

Han MH. and Kwon ST. A Statistical Study of Upper Eyelids of Korean Young Women [Journal] // Korean J Plast Surg.. - 1992. - 6 : Vol. 19. - pp. 930-935.

Harrison AR. [et al.] Myofiber Length and Three-Dimensional Localization of NMJs in Normal and Botulinum Toxin Treated Adult Extraocular Muscles [Journal] // Invest Ophthalmol Vis Sci. - 2007. - 8 : Vol. 48. - pp. 3594-601.

Hayashi T. T. Mechanisms of Contact Lens Motion [Report] : Thesis / Berkeley: University of California. - California : Berkeley, 1977.

Hazin R., Azizzadeh B. and Tariq-Bhatti M. Medical and Surgical Management of Facial Nerve Palsy [Journal] // Curr Opin Ophthalmol.. - 2009. - 6 : Vol. 20. - pp. 440-450.

Hertenstein JR., Sarnat HB. and O'Connor DM. Acute Unilateral Oculomotor Palsy Associated with Echo 9 Viral Infection [Journal] // J Pediatr. - 1976. - 1 : Vol. 89. - pp. 79-81.

Hintschich C.R. and Haritoglou C. Full Thickness Eyelid Transection (Blepharotomy) for Upper Eyelid Lengthening in Lid Retraction Associated with Graves' Disease [Journal] // Br J Ophthalmol. - 2005. - 4 : Vol. 89. - pp. 413-416.

Hintschich C.R., Zurcher M. and Collin J.R.O. Mersilene Mesh Brow Suspension: Efficiency and Complications [Journal] // Br J Ophthalmol. - 1995. - 4 : Vol. 79. - pp. 358-361.

Horie C. [et al.] Decreased Dopasmine D2 Receptor Binding in Essential Blepharospasm [Journal] // Acta Neurol Scand. - 2009. - 1 : Vol. 119. - pp. 49-54.

Huang T. Reduction of Lower Palpebral Bulge by Plicating Attenuated Orbital Septa: A Technical Modification in Cosmetic Blepharoplasty [Journal] // Plast Resconstr Surg. - 2000. - 7 : Vol. 105. - pp. 2552-2558.

Hung G., Hsu F. and Stark L. Dynamics of the Human Blink [Journal] // Am J Optom Physiol Opt.. - 1977. - 10 : Vol. 54. - p. 678.

Ishibashi A. [et al.] MR Findings in Isolated Oculomotor Nerve Palsy Associated with Infectious Mononucleosis Caused by Epstein-Barr Virus Infection [Journal] // J. Comput Assist Tomogr. - 1998. - 6 : Vol. 22. - pp. 995-997.

Iwasaki M. [et al.] Effects of Eyelid Closure, Blinks, and Eye Movements on the Electroencephalogram [Journal] // Clin Neurophysiol. - 2005. - 4 : Vol. 116. - pp. 878-885.

Jacobs H. B. Strength of the Orbicularis Oculi [Journal] // Brit. J. Ophthal.. - 1954. - 9 : Vol. 38. - pp. 560-566.

Jacobs LC. [et al.] Intrinsic and Extrinsic Risk Factors for Sagging Eyelids [Journal] // Arch Dermatol.. - 2014. - 8 : Vol. 150. - pp. 836-843.

Jankovic J. Disease-Oriented Approach to Botulinum Toxin Use [Journal] // Toxicon. - 2009. - 5 : Vol. 54. - pp. 614-23.

Jankovic J., Havins W. E. and Wilkins R. B. Blinking and Blepharospasm: Mechanism, Diagnosis and Management [Journal] // JAMA. - 1982. - 23 : Vol. 248. - pp. 3160-3164.

Jeong S. [et al.] The Asian Upper Eyelid: An Anatomical Study With Comparison to the Caucasian Eyelid [Journal] // Arch Ophthalmol.. - 1999. - 7 : Vol. 117. - pp. 907-912.

Jinnah H. A. and Hallett M. In the Wink of an Eye - Nature and Nurture in Blepharospasm [Journal] // Neurology. - 2011. - 7 : Vol. 77. - pp. 616-617.

Jones LT. An Anatomical Approach to Problems of the Eyelids and Lacrimal Apparatus [Journal] // Arch Ophthalmol.. - 1961. - 1 : Vol. 66. - pp. 111-124..

Jost WH. and Kohl A. Botulinum Toxin: Evidence-Based Medicine Criteria in Blepharospasm and Hemifacial Spasm [Journal] // J Neurol. - 2001. - 1 : Vol. 248. - pp. 21-24.

Kakizaki H., Malhotra R. and Selva D. Upper Eyelid Anatomy – An Update [Journal] // Ann. Plast Surg.. - 2009. - 3 : Vol. 63. - pp. 336-343.

Kakizaki H., Zako M. and Nakano T. The Levator Aponeurosis Consists of Two Layers That Include Smooth Muscles [Journal] // Ophthal Plast Reconstr Surg. - 2005. - 4 : Vol. 21. - pp. 379-382.

Karson CN. [et al.] Blink rates and disorders of movement [Journal] // Neurology. - 1984. - Vol. 34. - pp. 677-678.

Karson CN. Spontaneous Eye Blink Rates and Dopaminergic Systems. [Journal] // Brain. - 1983. - Vol. 106. - pp. 643-653.

Katowitz J.A. Frontalis Suspension in Congenital Ptosis Using a Polyfilament, Cable-Type Suture [Journal] // Archives of Ophthalmology. - 1979. - 9 : Vol. 97. - pp. 1659-1663.

Kazim M. and Gold KG. A Review of Surgical Techniques to Correct Upper Eyelid Retraction Associated with Thyroid Eye Disease [Journal] // Curr Opin Ophthalmol. - 2011. - 5 : Vol. 22. - pp. 391-393.

Kenyon RV. A Soft Contact Lens Search Coil for Measuring Eye Movements [Journal] // Vision Res. - 1985. - 11 : Vol. 25. - pp. 1629-1633.

Kerty E. and Eidal K. Apraxia of Eyelid Opening: Clinical Features and Therapy [Journal] // Eur J Ophthalmol.. - 2006. - 2 : Vol. 16. - pp. 204-208.

Ketelsen UP., Buchholz G. and Schmidt D. Light and Electron Microscopic Appearances of the Orbicularis Oculi Muscle in Patients with Chronic Progressive Ocular Muscular Dystrophy and in Normal Persons [German] [Journal] // Klin Monbl Augenheikd. - 1978. - 3 : Vol. 173. - pp. 317-328.

Khoo DH. [et al.] Graves' Ophthalmopathy in the Absence of Elevated Free Thyroxine and Triiodothyronine Levels: Prevalence, Natural History, and Thyrotropin Receptor Antibody Levels [Journal] // Thyroid. - Dec 2000. - 12 : Vol. 10. - pp. 1093-1100.

Klawans HL. and Goodwin JA. Reversal of Glabellar Refelx in Parkinsonism by L-Dopa [Journal] // J Neurol Neurosurg Psychiatry. - 1969. - 5 : Vol. 32. - pp. 423-7.

Klostermann W., Vieregge P. and Kompf D. Apraxia of Eyelid Opening After Bilateral Stereotaxic Subthalamotomy [Journal] // J Neuroophthalmol. - Jun 1997. - 2 : Vol. 17. - pp. 122-123.

Kook K.H. [et al.] Scanning Electron Microscopic Studies of Supramid Extra From the Patients Displaying Recurrent Ptosis After Frontalis Suspension [Journal] // American Journal of Ophthalmology. - 2004. - 5 : Vol. 138. - pp. 756-763.

Korošec M. [et al.] Eyelid Movements During Blinking in Patients with Parkinson's Disease [Journal] // Mov Disord.. - 2006. - 8 : Vol. 21. - pp. 1248-51.

Kowal L. Pretarsal Injections of Botulinum Toxin Improve Blephospasm in Previously Unresponsive Patients [Journal] // J Neurol Neurosurg Psychiatry. - 1997. - 4 : Vol. 63. - p. 556.

Kuki I. [et al.] Successful Steroid Pulse Therapy for Acute Unilateral Oculomotor Nerve Palsy Associated with Norovirus Infection [Journal] // No To Hattatsu. - Japan : [s.n.], 2008. - 4 : Vol. 40. - pp. 324-327.

Kwon K. A. [et al.] High-Speed Camera Characterization of Voluntary Eye Blinking Kinematics [Journal] // J. R. Soc. Interface. - 12 06 2013. - 85 : Vol. 10.

Le TT [et al.] Proportionality in Asian and North American Caucasian Faces Using Neoclassical Facial Canons as Criteria [Journal] // Aesthetic Plast Surg.. - Jan-Feb 2002. - 1 : Vol. 26. - pp. 64-9.

Lee M.J. [et al.] Frontalis Sling Operation Using Silicone Rod Compared with Preserved Fascia Lata for Congenital Ptosis: A Three-Year Follow-up Study [Journal] // Ophthalmology. - 2009. - 1 : Vol. 116. - pp. 123-129.

Lelli Jr GJ., Duong JK. and Kazim M. Levator Excursion as a Predictor of Both Eyelid Lag and Lagophthalmos in Thyroid Eye Disease [Journal] // Ophthal Plast Resconstr Surg. - 2010. - 1 : Vol. 26. - pp. 7-10.

Lenskiy A. A. and Lee JS. Driver's Eye Blinking Detection Using Novel Color and Texture Segmentation Algorithms [Journal] // IJCAS. - 2012. - 2 : Vol. 10. - pp. 317-327.

Leone Jr C.R., Shore J.W. and Van Gemert J.V. Silicone Rod Frontalis Sling for the Correction of Blepharoptosis [Journal] // Ophthalmic Surgery. - 1981. - 12 : Vol. 12. - pp. 881-887.

Liu D. and Hsu WM. Oriental Eyelids: Anatomic Differences and Surgical Consideration [Journal] // Ophthal Plast Reconstr Surg.. - 1986. - 2 : Vol. 2. - pp. 59-64.

Mackie IA. Riolan's Muscle: Action and Indications for Botulinum Toxin Injection [Journal] // Eye (Lond). - 2000. - 3A : Vol. 14. - pp. 347-352.

Madroszkiewicz M. Pomiary Okulomiodynamometryczne Dzwigaczy Powiek Gornych [Oculomyodynamometric Measurements of Levator Muscles of the Upper Eyelids (Author's Transl)] [Journal] // Klin Oxzna. - 1980. - 1 : Vol. 82. - pp. 43-44.

Mak FHW. [et al.] Analysis of Blink Dynamics in Patients with Blepharoptosis [Journal] // Journal of the Royal Society Interface. - 2016. - 9 : Vol. 13.

Manners R.M., Tyers A.G. and Morris R.J. The Use of Prolene as a Termporary Suspensory Material for Brow Suspension in Young Children [Journal] // Eye. - 1994. - 3 : Vol. 8. - pp. 346-348.

Marsden C. D. Blepharospasm-Oromandibular Dystonia Syndrome (Brueghel's Syndrome).A Variant of Adult-Onset Torsion Dystonia? [Journal] // J neurol Neurosurg Psychiatry. - 1976. - 12 : Vol. 39. - pp. 1204-1209.

Ma'touq J. [et al.] Eye Blinking-Based Method for Detecting Driver Drowsiness [Journal] // J Med Eng Techmol. - 2014. - 8 : Vol. 38. - pp. 416-419.

Mcelligott J.G., Loughnane M.H. and Mays L.E. The Use of Synchronous Demodulation for the Measurement of Eye Movements by Means of an Ocular Magnetic Search Coil [Journal] // IEEE Trans Biomed Eng.. - 1979. - 6 : Vol. 26. - pp. 370-374.

McNaught K. St. P. [et al.] Brainstem Pathology in DYT1 Primary Torsion Dystonia [Journal] // Ann Neurol. - 2004. - 4 : Vol. 56. - pp. 540-547.

Mehta P., Patel P. and Olver J.M. Functional Results and Complications of Mersilene Mesh Use for Frontalis Suspension Ptosis Surgery [Journal] // Br J Ophthalmol. - 2004. - 3 : Vol. 88. - pp. 361-364.

Micheli F. [et al.] Blepharospasm and apraxia of eyelid opening in lithium intoxication [Journal] // Clin Neuropharmacol.. - 1999. - 3 : Vol. 22. - pp. 176-179.

Mitra S. [et al.] Curtis Laxa: a Report of Two Interesting Cases [Journal] // Indian J Dermatol. - 2013. - 4 : Vol. 58. - p. 328.

Nakauchi K., Mito H. and Mimura O. Frontal Suspension for Congenital Ptosis Using an Expanded Polytetrafluoroethylene (Gore-Tex) Sheet: One-Year Follow-Up [Journal] // Clin Ophthalmol. - 2013. - 1 : Vol. 7. - pp. 131-136.

Naumann M. [et al.] Imaging the Pre and Postsynaptic Side of Striatal Dopaminergic Synapses in Idiopathic Cervical Dystonia: a SPECT Study Using [123I]Epidepride and [123I]Beta-CIT [Journal] // Mov Disord.. - 1998. - 2 : Vol. 13. - pp. 319-323.

Nerad J.A. Techniques in Ophthalmologic Plastic Surgery [Book]. - Cincinnati : Saunders Elsevier, 2010. - 1st.

Nunery WR. [et al.] The Risk of Diplopia Following Orbital Floor and Medial Wall Decompression in Subtypes of Ophthalmic Graves' Disease [Journal] // Ophthal Plast Reconstr Surg. - 1997. - 3 : Vol. 13. - pp. 153-160.

Obermann M. [et al.] Morphometric Changes of Sensorimotor Structures in Focal Dystonia [Journal] // Mov Disord.. - 2007. - 8 : Vol. 22. - pp. 1117-1123.

Older JJ. Eyelid Tumours: Clinical Diagnosis and Surgical treatment [Book]. - [s.l.] : Manson Publishing, 2003. - 2nd : p. 66.

Onizuka T. and Masaki I. Blepharoplasty in Japan [Journal] // Aesthetic Plast Surg.. - 1984. - 2 : Vol. 8. - pp. 97-100.

Optican L.M. [et al.] An Amplitude and Phase Regulating Magnetic Field Generator for an Eye Movement Monitor [Journal] // IEEE Trans Biomed Eng.. - 1982. - 3 : Vol. 29. - pp. 206-209.

Orchard L. N. and Stern J. A. Blinks as an Index of Cognitive Activity During Reading [Journal] // Integrative Physiology and Behavioural Science. - April-June 1991. - 2 : Vol. 26. - pp. 108-116.

Pandya S., King WM. and Tawil R. Facioscapulohumeral Dystrophy [Journal] // Phys Ther. - 2008. - 1 : Vol. 88. - pp. 105-113.

Paris GL. and Quickert MH. Disinsertion of the Aponeurosis of the Levator Palpebrae Superioris Muscle After Cataract Extraction [Journal] // Am J Ophthalmol.. - 1976. - 3 : Vol. 81. - pp. 337-340.

Pariseau B., Worley M. W. and Anderson R. L. Myectomy for Blepharospasm 2013 [Journal] // Curr opin in Ophthalmol. - September 2013. - 5 : Vol. 24. - pp. 488-493.

Perkins SW., Dyer WKT. and SImo F. Transconjunctival Approach to Lower Eyelid Blepharoplasty. Experience, Indications, and Technique in 300 Patients [Journal] // Arch Otolaryngol Head Neck Surg. - 1994. - 2 : Vol. 120. - pp. 172-177.

Perlmutter JS. [et al.] Decreased [18F]Spiperone Binding in Putamen in Idiopathic Focal Dystonia [Journal] // J Neurosci. - 1997. - 2 : Vol. 17. - pp. 843-850.

Perros P. [et al.] A Questionnaire Survey on the Management of Graves' Orbitopathy in Europe [Journal] // Eur J Endocrinol. - 2006. - 2 : Vol. 155. - pp. 207-211.

Peshori KR. [et al.] Aging of the Trigeminal Blink System [Journal] // Exp Brain Res.. - 2001. - 3 : Vol. 136. - pp. 351-363.

Pochin EE. The Mechanism of Lid Retraction in Graves Diseases [Journal] // Clin Sci. - 1939. - 1 : Vol. 4. - pp. 91-101.

Porter JD., Burns LA. and May PJ. Morphological Substrate for Eyelid Movements: Innervation and Structure of Primate Levator Palpebrae Superioris and Orbicularis Oculi Muscles [Journal] // Journal of Comparative Neurology. - 1989. - 1 : Vol. 287. - pp. 64-81.

Porter JD., May PJ. and Burns LA. The Anatomical Substrate of Blink Movements: Structure and Innervations of Primate Levator Palpebrae Superioris and Orbicularis Oculi Muscles [Journal] // Society for Neuroscience Abstracts. - 1988. - Vol. 14. - p. 960.

Prabhakar BS., Bahn RS. and Smith TJ. Current Perspective on the Pathogenesis of Graves' Disease and Ophthalmopathy [Journal] // Endocr Rev. - 2003. - 6 : Vol. 24. - pp. 802-835.

Prummel MF. and Wiersinga WM. Smoking and Risk of Graves' Disease [Journal] // JAMA. - 1993. - 4 : Vol. 269. - pp. 479-782.

Purwanto D., Mardiyanto R. and Arai K. Electric Wheelchair Control with Gaze Direction and Eye Blinking [Journal] // Artif Life Robotics. - 2009. - 1 : Vol. 14. - pp. 397-400.

Putterman AM. Thyroid ophthalmopathy: surgical management [Book Section] // Current Therapy in Endocrinology and Metabolism / ed. Bardin CW.. - Mosby, St. Louis : [s.n.], 1997. - 6th.

Quan T. and Fisher GJ. Role of Age-Associated Alterations of the Dermal Extracellular Matrix Microenvironment in Human Skin Aging: A Mini-Review [Journal] // Gerontology. - 2015. - 5 : Vol. 61. - pp. 427-437.

Radlak K. and Smolka B. A novel approach to the eye movement analysis using a high speed camera [Journal] // 2nd International Confernce on Advances in computational tools for engineering applications (ACTEA). - Gliwice, Poland : [s.n.], 2012. - pp. 145-150.

Remmel R.S. An Inexpensive Eye Movement Monitor Using the Scleral Search Coil Technique [Journal] // IEEE Trans Biomed Eng. . - 1984. - 4 : Vol. 31. - pp. 388-390.

Reulen J.P.H. and Bakker L. The Measurement of Eye Movement Using Double Magnetic Induction [Journal] // IEEE Trans Biomed Eng. . - 1982. - 11 : Vol. 29. - pp. 740-744.

Robinson D.A. A Method of Measuring Eye Movement Using a Scleral Search Coil in a Magnetic Field [Journal] // IEEE Trans Biomed Eng.. - 1963. - 1 : Vol. 10. - pp. 137-145.

Rowan R.J. and Hayes G.S. Silicone Sling for Ptosis [Journal] // South Med J.. - 1977. - 1 : Vol. 70. - pp. 68-69.

Ruban J.M. [et al.] A New Material in Ptosis Surgery With Brow Suspension: Wide Porous Expanded Polytetrafluoroethylene: Analysis of Our First 75 Cases [Journal] // Orbit. - 1996. - 2 : Vol. 15. - pp. 67-79.

Saad J. and Gourdeau A. A Direct Comparison of Onabotulinumtoxina (Botox) and IncobotulinumtoxinA (Xeomin) in the Treatment of Benign Essential Blepharospasm: A Split-Face Technique [Journal] // J Neuroophthalmol.. - Sept 2014. - 3 : Vol. 34. - pp. 233-236.

Saeki N. [et al.] Isolated Superior Division Oculomotor Palsy in a Child with Spontaneous Recovery [Journal] // J Clin Neurosci. - 2000. - 1 : Vol. 7. - pp. 62-64.

Salouti R. [et al.] Comparison of Horizontal Corneal Diameter Measurements Using Galilei, EyeSys and Orbscan II Systerms [Journal] // Clin Exp Optom. - 2009. - 5 : Vol. 92. - pp. 429-33.

Saonanin P. Update on Asian Eyelid Anatomy and Clinical Relevance [Journal] // Curr Opin Ophthalmol.. - 2014. - 5 : Vol. 25. - pp. 436-442.

Saunders R.A. and Grice C.M. Early Correction of Severe Congenital Ptosis [Journal] // J Pediatr Ophthalmol Strabismus.. - 1991. - 5 : Vol. 28. - pp. 271-273.

Schwaber MK. [et al.] Gadolinium-Enhanced Magnetic Resonance Imaging in Bell's Palsy [Journal] // Laryngoscope. - 1990. - 12 : Vol. 100. - pp. 1264-1269.

Sharma T.K. and Willshaw H. Long-Term Follow-Up of Ptosis Correction Using Mersilene Mesh [Journal] // Eye. - 2003. - 6 : Vol. 17. - pp. 759-761.

Shih MJ., Liao SL. and Lu HY. A Single Transcutaneous Injection with Botox for Dysthyroid Lid Retraction [Journal] // Eye (Lond). - 2004. - 5 : Vol. 18. - pp. 466-469.

Skarf B. Normal and Abnormal Eyelid Function [Book Section] // Walsh and Hoyt's Clinical Neuro-Ophthalmology / ed. Miller NR. [et al.]. - Philadelphia : Lippincott Williams and Wilkins, 2005. - 6th : Vol. 2.

Smith D. [et al.] Lid Opening Apraxia is Associated with Medial Frontal Hypometabolism [Journal] // Mov Disord.. - 1995. - 3 : Vol. 10. - pp. 341-344.

Sprenger A. [et al.] Long-Term Eye Movement Recordings with a Scleral Search Coil-Eyelid Protection Device Allows New Applications [Journal] // J Neurosci Methods. - 2008. - 2 : Vol. 170. - pp. 305-309.

Stava M.W. [et al.] Conjugacy of Spontaneous Blinks in Man: Eyelid Kinematics Exhibit Bilateral Symmetry [Journal] // Invest Ophthalmol Vis Sci. - 1994. - 11 : Vol. 35. - pp. 3966-3971.

Steinkogler F.J. [et al.] Gore-Tex Soft-Tissue Patch Frontalis Suspension Technique in Congenital Ptosis and in Blepharophimosis-Ptosis Syndrome [Journal] // Plast Reconstr Surg. - 1993. - 6 : Vol. 92. - pp. 1057-1060.

Sudhakar P. Upper Eyelid Ptosis Revisited [Journal] // Am J Clin Med. - 2009. - 3 : Vol. 6. - pp. 5-14.

Sun WS. [et al.] Age-Related Changes in Human Blinks: Passive and Active Changes in Eyelid Kinematics [Journal] // Invest Ophthalmol Vis Sci. - 1997. - 1 : Vol. 38. - pp. 92-99.

Suzuki Y. [et al.] Glucose Hypometabolism in Medial Frontal Cortex of Patients with Apraxia of Lid Opening [Journal] // Graefes Arch Clin Exp Ophthalmol.. - 2003. - 7 : Vol. 241. - pp. 529-534.

Tabatabaie S. Z. [et al.] Frontalis Sling Operation Using Silicone Rods in Comparison to Ptose-Up for Congenital Ptosis with Poor Levator Function [Journal] // Iranian J Ophthalmol. - 2012. - 1 : Vol. 24. - pp. 3-10.

Takagi M. [et al.] Reconsideration of Bell's Phenomenon Using a Magnetic Search Coil Method [Journal] // Doc Ophthalmol. - 1992. - 4 : Vol. 80. - pp. 343-352.

Takahashi Y., Leibovitch I. and Kakizaki H. Frontalis Suspension Surgery in Upper Eyelid Blepharoptosis [Journal] // Open Ophthalmol J. - 2010. - 4 : Vol. 4. - pp. 91-97.

Tenzel RR. and Stewart WB. Blepharo-Confusion - Blepharochalasis or Dermatochalasis? [Journal] // Arch Ophthalmol. - 1978. - 5 : Vol. 96. - pp. 911-912.

Traisk F., Bolzani R. and Ygge J. A Comparison Between the Magnetic Scleral Search Coil and Infrared Reflection Methods for Saccadic Eye Movement Analysis [Journal] // Arch Clin Exp Ophthalmol. - 2005. - 8 : Vol. 243. - pp. 791-797.

Trokel S., Kazim M. and Moore S. Orbital Fat Removal. Decompression for Graves' Orbitopathy [Journal] // Ophthalmol. - 1993. - 5 : Vol. 100. - pp. 674-682.

Tsuji S. [et al.] Meige Syndrome with Apraxia of Lid Opening After the Discontinuation of Sulpiride Treatment [Journal] // Pharmacopsychiatry. - 2002. - 4 : Vol. 35. - pp. 155-156.

Uddin JM. and Davies PD. Treatment of Upper Eyelid Retraction Associated with Thyroid Eye Disease with Subconjunctival Botulinum Toxin Injection [Journal] // Ophthalmol. - 2002. - 6 : Vol. 109. - pp. 1189-1187.

Ugarte Marta and Teimory Masoud Apraxia of Lid Opening [Journal] // Br J Ophthalmol. - 2007. - 7 : Vol. 91. - p. 854.

van Harten P. N., Hoek H. W. and Kahn R. S. Acute Dystonia Induced by Drug Treatement [Journal] // BMJ. - 1999. - 7210 : Vol. 319. - pp. 623-626.

VanderWerf F. [et al.] Eyelid Movements: Behavioral Studies of Blinking in Humans Under Different Stimulus Conditions [Journal] // J Neurophysiol. - May 2003. - 5 : Vol. 89. - pp. 2784-2796.

Wambier SPF. [et al.] Two-Dimensional Video Analysis of the Upper Eyelid Motion During Spontaneous Blinking [Journal] // Ophthal Plast Reconstr Surg. - 2014. - 2 : Vol. 30. - pp. 146-151.

Watanabe A. The Impact of Levator Aponeurosis Advancement On Spontaneous Blinks and Tear Volume in Blepharoptosis [Conference] // Poster presentation at: AAO Annual meeting. - Chicago : [s.n.], 2012.

Weetman A. and Wiersinga WM. Current Management of Thyroid-Associated Ophthalmopathy in Europe. Results of an International Survey [Journal] // Clin Endocrinol (Oxf). - 1998. - 1 : Vol. 49. - pp. 21-28.

Wheatcroft SM., Vardy SJ. and Tyers AG. Complications of Fascia Lata Harvesting for Ptosis Surgery [Journal] // Br J Ophthalmol. - 1997. - 7 : Vol. 81. - pp. 581-583.

Wouters RJ. [et al.] Upper Eyelid Motility in Blepharoptosis and in the Aging Eyelid [Journal] // Invest Ophthalmol Vis Sci. - March 2001. - 3 : Vol. 42. - pp. 620-625.

Yamashita S. [et al.] Acute Ophthalmoparesis Accompanied with Influenza A Infection [Journal] // Intern Med. - 2008. - 18 : Vol. 47. - pp. 1627-1629. - Epub.